MICROCOPY RESOLUTION TEST CHART

NATIONAL BUREAU OF STANDARDS-1963-A

REPORT DOCUMENTATION PAGE		READ INSTRUCTIONS BEFORE COMPLETING FORM
1. REPORT NUMBER Technical Report HL-83-2	2. GOVT ACCESSION NO. AD A12-9444	3. RECIPIENT'S CATALOG NUMBER
4. TITLE (and Subtitle) FIXED-CONE VALVE PROTOTYPE TESTS, NEW MELONES DAM, CALIFORNIA		5. TYPE OF REPORT & PERIOD COVERED
		6. PERFORMING ORG. REPORT NUMBER Final report
7. AUTHOR(s) Timothy L. Fagerburg		8. CONTRACT OR GRANT NUMBER(s)
9. PERFORMING ORGANIZATION NAME AND ADDRESS U. S. Army Engineer Waterways Experiment Station Hydraulics Laboratory P. O. Box 631, Vicksburg, Miss. 39180		10. PROGRAM ELEMENT, PROJECT, TASK AREA & WORK UNIT NUMBERS
11. CONTROLLING OFFICE NAME AND ADDRESS U. S. Army Engineer District, Sacramento 650 Capitol Mall Sacramento, Calif. 95814		12. REPORT DATE February 1983
		13. NUMBER OF PAGES 97
14. MONITORING AGENCY NAME & ADDRESS(if different from Controlling Office)		15. SECURITY CLASS. (of this report) Unclassified
		15a. DECLASSIFICATION/DOWNGRADING SCHEDULE

16. DISTRIBUTION STATEMENT (of this Report)

Approved for public release; distribution unlimited.

17. DISTRIBUTION STATEMENT (of the abstract entered in Block 20, if different from Report)

18. SUPPLEMENTARY NOTES

Available from National Technical Information Service, 5285 Port Royal Road, Springfield, Va. 22151

19. KEY WORDS (Continue on reverse side if necessary and identify by block number)

Flow control
New Melones Dam
Pressure measurement
Valves
Water pressure

20. ABSTRACT (Continue on reverse side if necessary and identify by block number)

Prototype measurements include static and dynamic values of pressures due to flow in the 66- and 78-in.-diam Howell-Bunger valves and hoods and strain on one vane of each valve. Transverse, vertical, and peripheral accelerations were measured at the downstream end of the valve cone. Vertical accelerations were also measured on the upstream end of the hood of each valve. Data were recorded on analog magnetic tape and played back on oscillograph charts to verify the recording.

(Continued)

DD FORM 1473 EDITION OF 1 NOV 65 IS OBSOLETE

20. ABSTRACT (Continued).

> Results of the data reduction include information on discharge character-
istics of the New Melones valves, evaluation of the pressure fluctuations for
flows in the valves and hoods, evaluation of the vibration of the valve and
hood structures, and evaluation of the strain measurements on the test vanes.

The significant amplitudes of accelerations on the FC&I valve were due
to the dynamic flow control shift which was not evident in vibrations of the
LL valve. The pressure fluctuations revealed that buffeting was more evident
in the fully developed turbulent flow of the LL valve than that resulting
from the upstream bifurcations in the FC&I conduit.

PREFACE

The prototype tests described in this report were conducted during April-June 1979 by the U. S. Army Engineer Waterways Experiment Station (WES) under the sponsorship of the U. S. Army Engineer District, Sacramento.

Tests were conducted under the general supervision of Messrs. H. B. Simmons, *Chief of the Hydraulics Laboratory*, and M. B. Boyd, *Chief of the Hydraulic Analysis Division*, by T. L. Fagerburg with the assistance of E. D. Hart. This report was prepared by Mr. Fagerburg under the supervision of Mr. Hart, Chief of the Prototype Evaluation Branch, with assistance from Dr. F. M. Neilson, Hydraulic Engineering Information Analysis Center. Instrumentation support was obtained from Messrs. L. M. Duke, H. C. Greer, R. Hammack, and J. L. Pickens.

Acknowledgment is made to individuals of the Sacramento District for their assistance in the investigation.

Commanders and Directors of WES during the investigation and the preparation and publication of this report were COL John L. Cannon, CE, COL Nelson P. Conover, CE, and COL Tilford C. Creel, CE. Technical Director was Mr. F. R. Brown.

1

CONTENTS

CONVERSION FACTORS, U. S. CUSTOMARY TO METRIC (SI)
UNITS OF MEASUREMENT

U. S. customary units of measurement used in this report can be converted to metric (SI) units as follows:

Multiply	By	To Obtain
cubic feet per second	0.02831685	cubic metres per second
Fahrenheit degrees	*	Celsius degrees or Kelvins
feet	0.3048	metres
feet per second per second	0.3048	metres per second per second
inches	25.4	millimetres
inches per second	25.4	millimetres per second
microinches per inch	0.001	microns per millimetre
miles (U. S. statute)	1.609344	kilometres
pounds (force) per square inch	6894.757	pascals
pounds (mass)	0.4535924	kilograms
pounds (mass) per square foot	4.882428	kilograms per square metre
slugs (mass) per cubic foot	515.3788	kilograms per cubic metre
square feet	0.09290304	square metres

---

* To obtain Celsius (C) temperature readings from Fahrenheit (F) readings, use the following formula: $C = (5/9)(F - 32)$. To obtain Kelvin (K) readings, use: $K = (5/9)(F - 32) + 273.15$.

Figure 1. New Melones Dam and Reservoir

4

FIXED-CONE VALVE PROTOTYPE TESTS
NEW MELONES DAM, CALIFORNIA

PART I: INTRODUCTION

Pertinent Features of the Project

1.   The multipurpose New Melones Dam and Reservoir (Figure 1) is
located in central California on the Stanislaus River approximately
40 miles* east of the city of Stockton (Figure 2).   The rock-fill dam
with earth-fill core is 625.5 ft high and 1,560 ft long.   The ungated,
unlined remote spillway is 6,000 ft long and is located approximately
1.5 miles northwest of the damsite.   The 150,000-kw powerhouse is
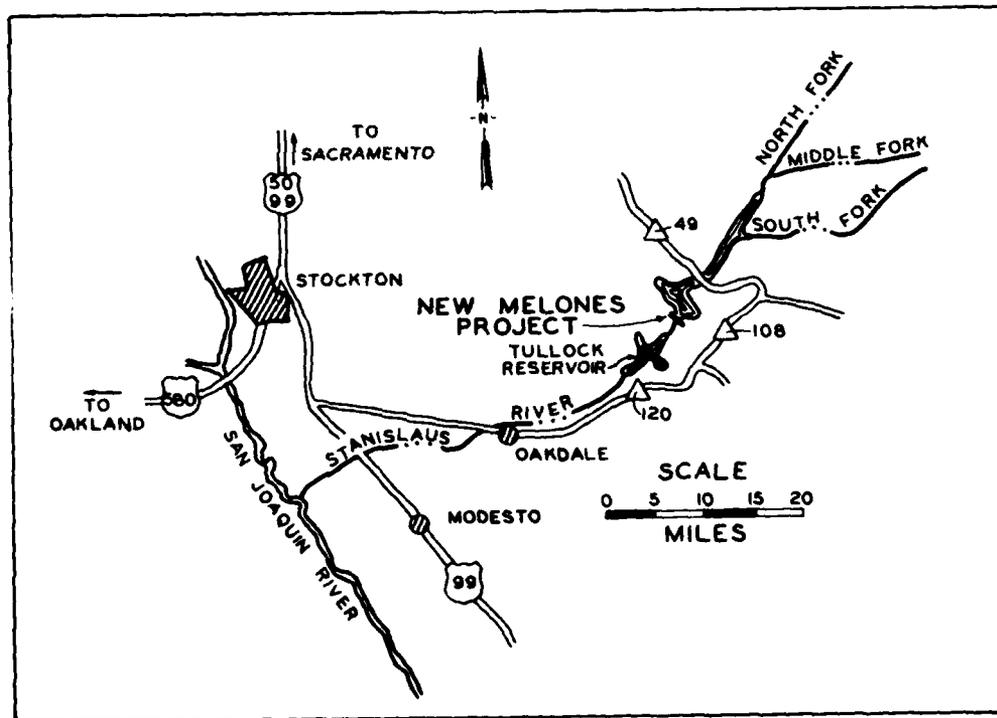
Figure 2.   Vicinity map

---

*   A table of factors for converting U. S. customary units of measure-
ments to metric (SI) units is presented on page 3.

located on the right bank of the river about 500 ft downstream of the toe of the dam.

Outlet works

2. The outlet works, as shown in Plate 1, consist of a 23-ft-diam multipurpose tunnel with a low-level intake for diversion and a high-level intake for flood control, power, irrigation, and other purposes. Two 17-ft-diam spur tunnels serve the turbines in the powerhouse. The third spur tunnel is 13 ft in diameter and bifurcates at the downstream end to accommodate two 96-in. ring follower gates and two 78-in.-diam fixed-cone valves with 18-ft-diam hoods. These valves regulate flood and irrigation flows (FC&I). The right valve (looking downstream) was used for the FC&I tests.

3. The diversion tunnel was later plugged just downstream of the spur tunnels. Diversion flow is now provided by two 6-ft-diam conduits which bypass the plug and are equipped with two 72-in. ring follower gates and two 66-in. fixed-cone valves with 15.5-ft-diam hoods. These were designated the low-level (LL) valves. The right valve was used for the LL tests.

Howell-Bunger valve

4. Background information on the Howell-Bunger valve is presented in detail elsewhere (Neilson 1971, Elder and Dougherty 1953). Figure 3 presents the basic components of the New Melones valves. The stationary valve body is composed of a cylindrical shell, a system of eight equally spaced vanes, and the cone. The vanes are attached to the shell and cone. The cylindrical sleeve is opened and closed by means of a pair of hydraulic pistons. During closing operations, the sleeve is moved in a downstream direction over the valve shell. Conversely, during an opening operation, the sleeve moves upstream, exposing a series of discharge ports formed by the vanes and cone. The valve is fully opened when the sleeve has been withdrawn to the extent that flow is controlled by the shell lip or until it meets the stops. Pertinent dimensions of the FC&I and LL test valves are listed below:

6

ELEVATION
(LOOKING DOWNSTREAM)

SECTION A-A
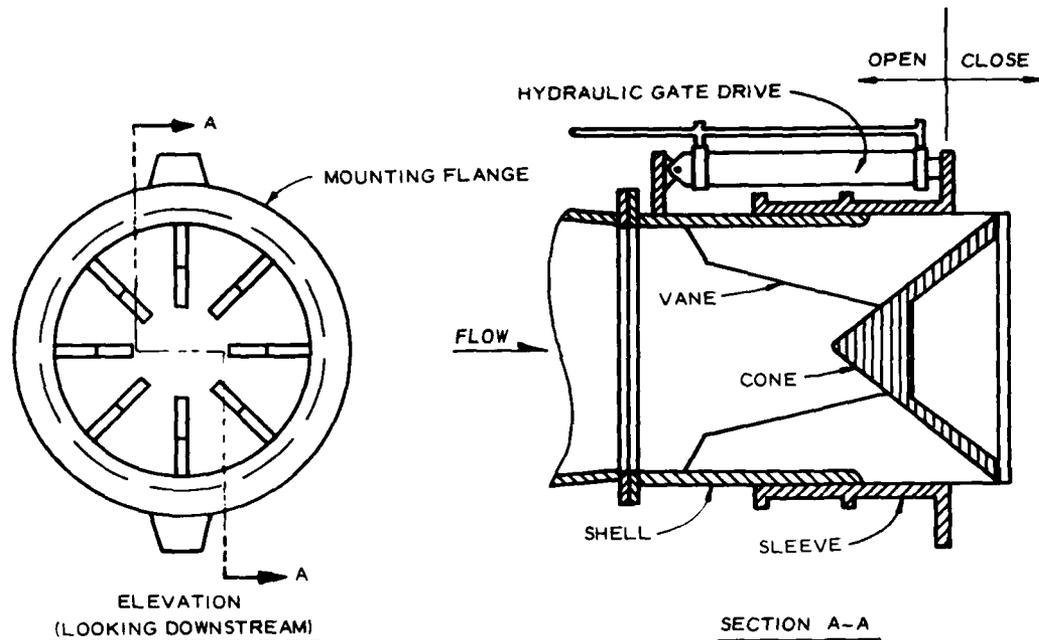
Figure 3. Eight-vane Howell-Bunger valve

Item	Dimensions of Valve	
	LL	FC&I
Number of vanes	8	8
Vane thickness, in.	1.75	2.25
Valve inside diameter, in.	66	78
Shell thickness, in.	1.875	2.375
Sleeve thickness, in.	1.75	2.25
Overall length of valve, in.	96.25	107.50
Estimated weight of valve, including sleeve, lb	33,000	50,000
Estimated weight of drive mechanism each valve, lb	2,000	2,000

Model Studies

5. In January 1976, at the request of the U. S. Army Engineer District, Sacramento, model studies were authorized by the U. S. Army Engineer Division, South Pacific. The model studies were conducted in the Hydraulics Laboratory of the U. S. Army Engineer Waterways Experiment Station (WES). The final report of findings (Maynord and Grace 1981) has been published.

7

6. The primary purpose of the model study was to determine the pressures and associated frequencies acting on the valve vanes. Because of the vane design (no hub), unusual approach flow conditions (upstream bifurcations), and high head at New Melones Dam (up to 530 ft and 516 ft at the FC&I and LL valves, respectively), the vane pressures were needed for use in a structural analysis. Secondary purposes included determining discharge characteristics, pressure conditions in the approach conduits, and hood performance.

Purpose and Scope of Prototype Tests

7. In December 1977, the Sacramento District requested that WES prepare a proposed prototype test program; the proposal was submitted to the District in February 1978. A meeting of personnel from the Office, Chief of Engineers, South Pacific Division, Sacramento District, and WES was held in January 1978 at WES to discuss New Melones Dam design matters, model test results, and prototype instrumentation and testing. At that time the prototype instrumentation facilities which should be installed and the field data desired were specified.

Purpose

8. Howell-Bunger or fixed-cone valves, regulating high head reservoirs, have been subjected to severe damage at other projects (Campbell 1961, Mercer 1970, Neilson 1971, Neilson and Pickett 1980). Because of the potentially high heads at New Melones (given in paragraph 6), the Sacramento District desired that valve stresses and vibrations be monitored in the prototype LL and FC&I valves. Specifically, the prototype tests were requested to (a) determine the dynamic response of the vanes, valves, and hoods, (b) determine the probability of a fatigue-type failure under prolonged operation, and (c) compare the prototype results with the model data. If any adverse trends were indicated, further testing could be requested.

Scope

9. Two sets of tests were conducted at different pool elevations. The first tests were conducted on the LL valve only at a reservoir

elevation of 750.0 ft NGVD*. The second series was made on the LL and FC&I valves at reservoir elevations of 805.5 and 804.1, respectively. Measurements consisted of the following:

a. Static and fluctuating pressures in the conduit upstream of the test valves.

b. Axial and bending vane strain at the calculated point of maximum stress.

c. Static and fluctuating pressures on both sides of a vane at two locations on the vane. This information would be used to determine the net fluctuating loads as a function of time.

d. Valve vibrations in the vertical, transverse, and torsional directions.

e. Jet pressures on the valve hood.

f. Hood backsplash plate pressures and vibrations.

10. These measurements were made at each valve for the conditions listed in Table 1 during a continuously opening and closing valve and at set valve openings of 25, 40, 50, 60, 70, 85, and 100 percent. These values of valve openings are used to maintain a consistency with the notation used in the model study (Maynord and Grace 1981).

---

* All elevations (el) cited herein are in feet referred to the National Geodetic Vertical Datum (NGVD).

9

PART II: TEST FACILITIES, EQUIPMENT, AND PROCEDURES

Test Facilities

11.   Locations of the instrumentation described herein are shown
in Plates 2 and 3.   Specifications for the transducers are listed in
Table 2.

Conduit pressures

12.   During construction of the project, a ring of four pressure
transducer boxes was embedded in both the LL and FC&I test valve con-
duits just upstream of the valves.   A 3/4-in. electrical conduit was
also embedded connecting the boxes and a manifold located topside.
Wires were installed in these conduits for pulling through the cables
for pressure transducers PC1-PC4.

13.   The surface cover plate of each of these boxes, as well as
all others described herein, was installed flush with the exterior sur-
face.   Two interchangeable cover plates were fabricated for each mount-
ing box, one for a permanent cover and the other for WES to use as a
guide in fabricating special adapters for the transducers to install
just prior to the tests.   The special adapters are shown in Figure 4.

Vane pressures

14.   The valve manufacturer drilled the 6:00- and 10:30-o'clock
vane (looking downstream) of the FC&I and LL test valves, respectively,
to accommodate pressure transducers at two locations on each side of the
vanes (PUD, PLD, PUB, and PLB).   The notation used for the vane pressure
transducers is (a) U and L designate the upper and lower vane surfaces,
respectively, (b) B and D designate the downstream and upstream location,
respectively, and (c) P designates pressure transducer.   The transducers
were housed in special adapters, one of which is shown in Figure 4.   A
transducer and adapter are shown being installed in the test vane in
Figure 5.   These were fabricated at WES to conform to the holes drilled
in the vanes and to provide a waterproof housing for the transducers.
The electrical cables passed through holes drilled in the vane which
exited at the valve shells as shown in Plates 2 and 3.   To permit

10
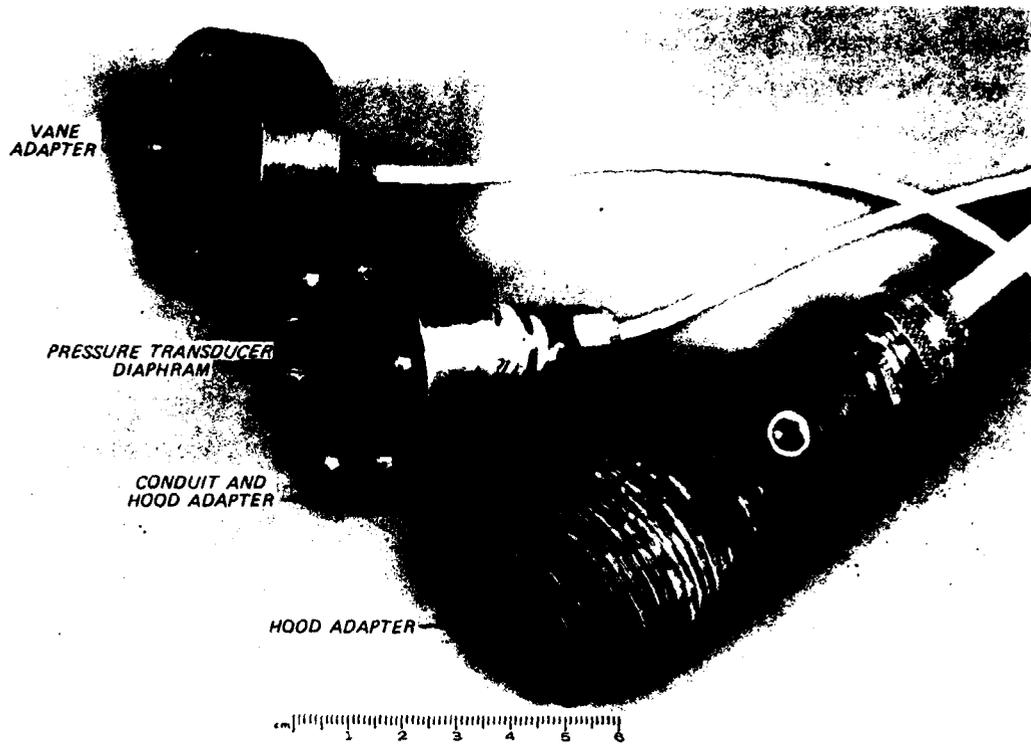
Figure 4. Waterproof pressure transducer adapters
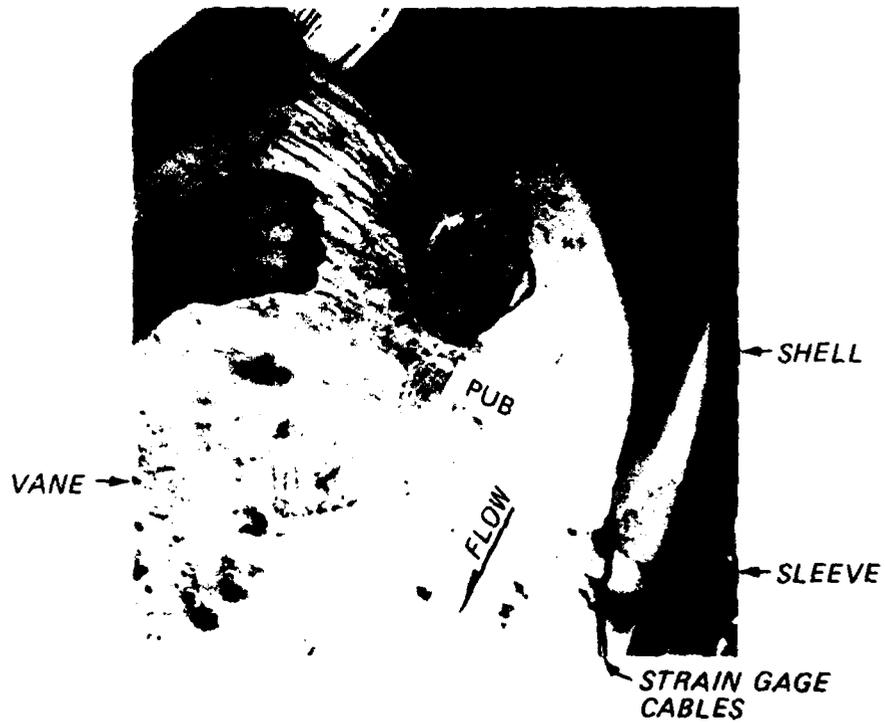
Figure 5. Installation of vane pressure transducer PUB (in adapter)

model-prototype comparisons, these transducers were located in positions comparable to those used in the model studies conducted at WES (Maynord and Grace 1981).

Hood pressures

15. Pressure transducers were installed in the test valve hoods and backsplash plates as shown in Plates 2 and 3. Electrical cables from some of these transducers passed through conduit to the afore-mentioned terminal boxes (PHC in the LL and PH11, PH12, and PH13 in the FC&I). Their transducer adapters were identical with those used in the conduit and are also shown in Figure 4. The remaining transducer cables were exposed and led directly from the transducer to the recording room (PHB in the LL and PH6-PH10 in the FC&I). These last five transducers were housed in 1-3/8-in. threaded adapters that were screwed in from the back side of the hood (Figures 4 and 6).

Vibrations

16. Three accelerometers were mounted on the back side of the test valve cones as shown in Plates 2 and 3. Accelerometers for measuring vertical (AVC) and transverse (ATC) acceleration were mounted in the special cannister shown in Figure 7. For torsional valve oscillations, an accelerometer was mounted on the periphery (AVP) of the cone to measure vertical movement. Simultaneous data then from AVC and AVP were reduced and processed for determining the torsional vibrations. The electrical leads from these transducers passed from the back side of the cone, through a vane, and out the valve shell also shown in Plates 2 and 3.

17. Backsplash plate vibrations were measured with accelerometer AHA whose location is also shown in Plates 2 and 3. The transducers were bolted to special steel plates which were in turn welded to the backsplash plates. The electrical cables passed directly from the transducers to the recording room.

Vane stress

18. Model studies at WES indicated that the 6:00-o'clock FC&I vane (looking downstream) and the 10:30-o'clock LL vane would be subjected to the most severe range of pressure fluctuations. Therefore,

12
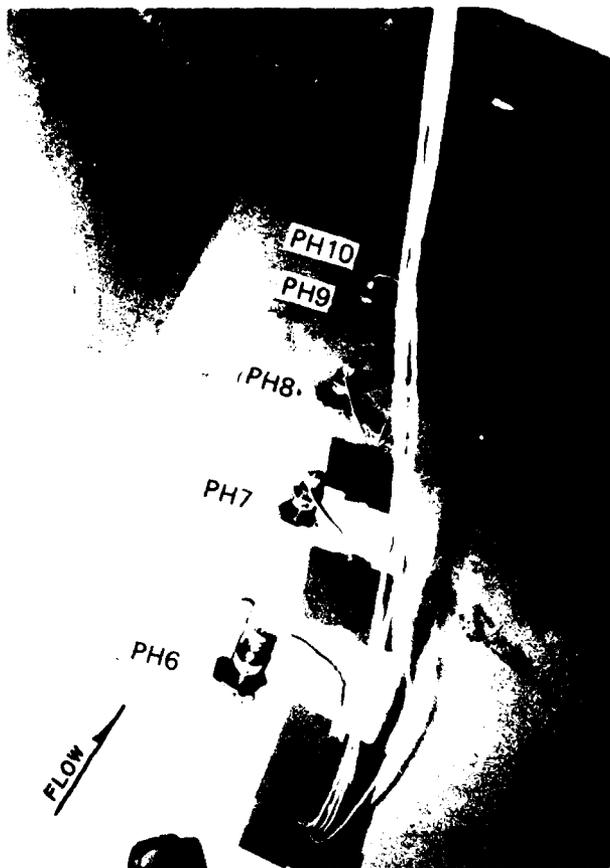
Figure 6. Transducers installed in the
hood of the FC&I valve

strain gages were attached at the calculated locations of maximum stress
on each of these vanes. Their locations and electrical cable holes
which pass through the shell are shown in Plates 2 and 3 and Figure 5.

19. The strain gages were connected electrically in a manner that
used four gages to measure flexural strain and four others to measure
axial strain. Each set of four leads was attached to a Wheatstone
bridge so that each measured one type of strain only; that is, for the
case of axial strain, the arrangement was such that any accompanying
flexural strain canceled out. Likewise, for flexural strain measure-
ments, the accompanying axial strain canceled out. A hydraulic jack
was used to apply a bending and axial load to the test vane to relate
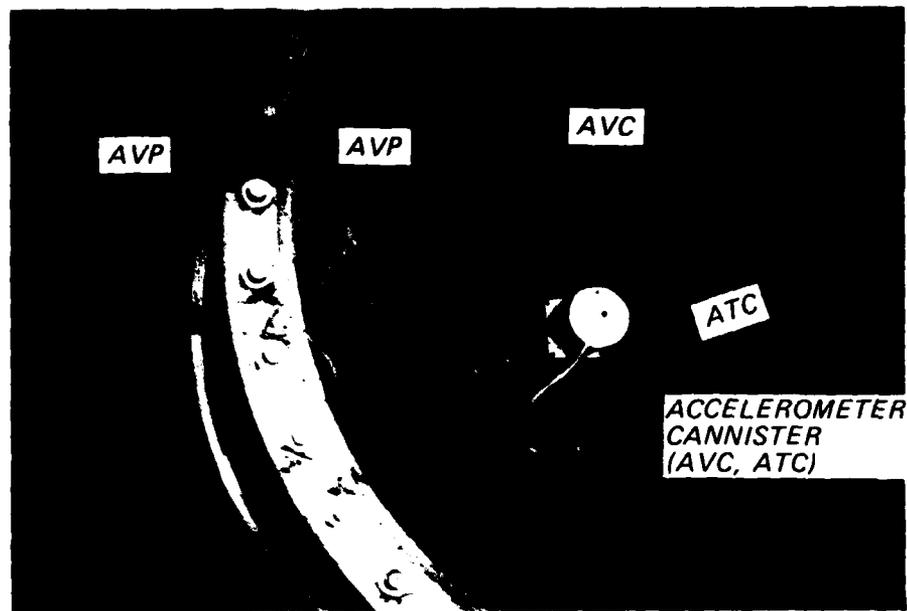
Figure 7. Accelerometers installed on the outside
of the LL valve

the recorded data to the direction of net instantaneous vane loading.
No magnitude could be given to these applied loads; therefore, the
laboratory calibration values were used.

Recording equipment

20. The recording equipment consisted of (a) WES-fabricated ampli-
fiers to condition the instrument output signal, (b) a Sabre III model,
32-channel magnetic-tape recorder, (c) a galvanometer driver to supply
higher current to the high frequency galvanometers, and (d) a 12-in.
chart oscillograph capable of reproducing 14 channels at a time at paper
speeds from 0.25 to 160 ips. Figure 8 shows the equipment setup at
the recording station. Tape recording speed was 7.5 ips. Oscillogram
recordings were made at speeds of 0.25 and 1.0 ips.

Test Procedures

21. Tests were conducted in the following sequence: (a) LL
valve tests at pool elevations ranging from 750.1 to 750.5, (b) LL

14
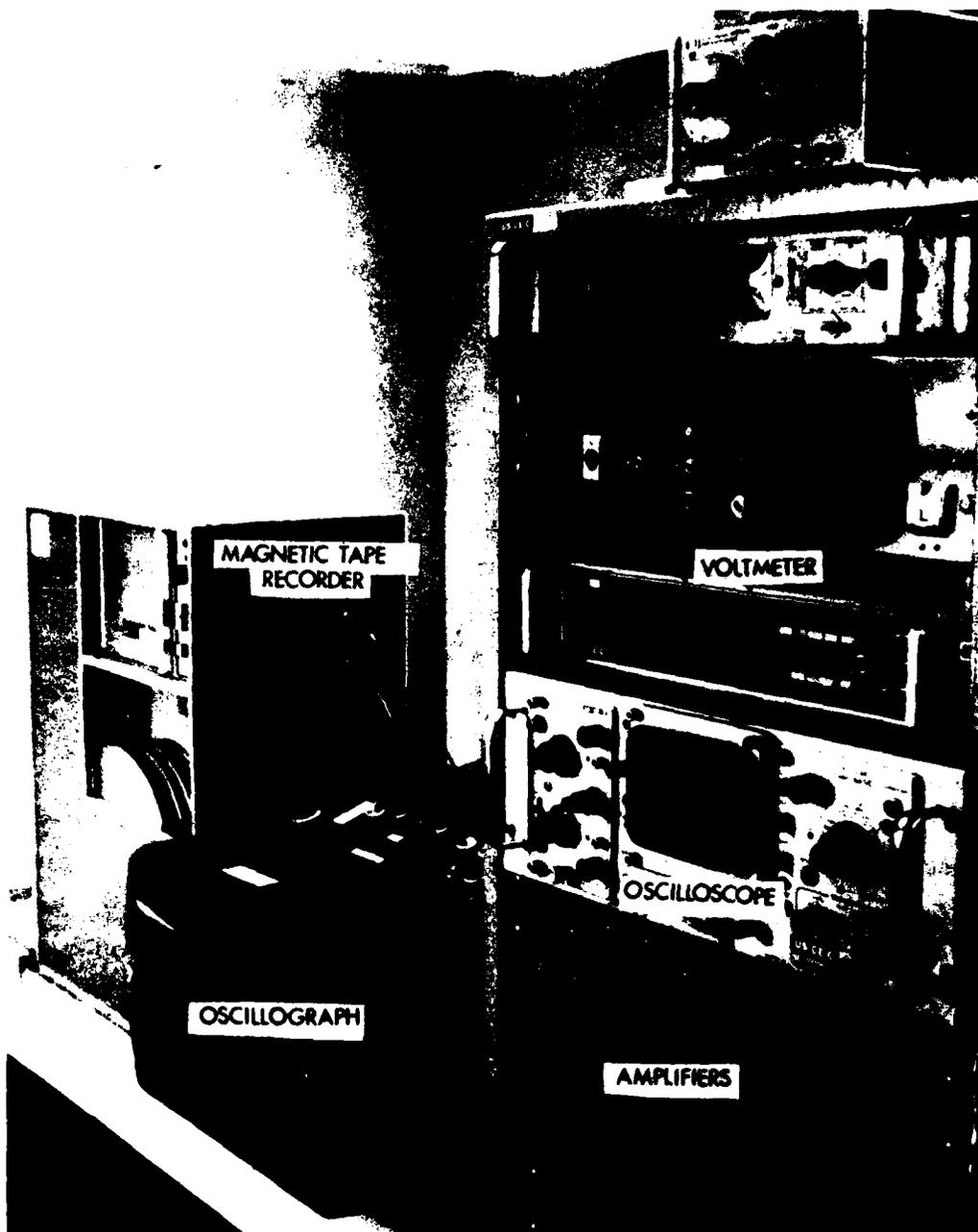
Figure 8. Equipment utilized for recording test data

valve tests at pool el 805.5, and (c) FC&I valve tests at pool el 804.1. All the tests were recorded on magnetic tape. During each individual test, a portion of the test data was transferred to the oscillogram to confirm that the data were being recorded and to make a visual check on the results. The initial tests on the first LL valve test series consisted of a continuous valve opening and closing procedure for monitoring the static pressure changes. The remaining tests consisted of monitoring the dynamic responses at a much higher gain setting while the valve was held at individual openings for 3 to 4 min. In the initial phase of the second series of LL valve tests, the valve was stopped at the predetermined valve openings for 10 to 20 sec before continuing on to the next setting. This was done to allow for any lag in pressure buildup, as shown in Plate 4, that may have resulted due to the length of the approach conduit. The remaining LL tests were similar to the first series for monitoring the dynamic responses at individual settings.

22. The FC&I valve tests generally followed the same procedures as the second series of LL valve tests. The initial tests monitored the changes of static conditions and the remaining tests monitored the dynamic responses at each valve opening.

23. The test procedure was generally the same for all three test series (Table 1) and consisted of the following: (a) record test number, date, and time, (b) record water temperature and air temperature, (c) record pool elevation, (d) zero level of instruments, (e) record step calibrations, (f) open the ring follower to flood the valve and record static conditions, (g) open the valve according to the desired valve operation, and (h) record data on magnetic tape and oscillogram.

PART III: TEST RESULTS

Pressure-Discharge Relationships

Average pressure values

24. These measurements are concerned with average pressures at all pressure transducer locations in the valves and conduits as a function of gate opening and head. Results are indicators of general valve performance and of the general validity of the valve rating curve. Note that discharge was not measured and a precise rating cannot be obtained uniquely from these data. Three series of tests are presented:

   a. Series I (LL valve). Average values are from recordings made while the gate is opened continuously from fully closed to fully opened. Average values are not available for these tests for the condition in which the gate is held in a fixed position, such as in b below.

   b. Series II (LL valve). The gate is opened to a specific setting and held in position until steady flow is attained; the complete transducer output (i.e., the mean and fluctuating components are retained in the data) is recorded during the steady-state condition.

   c. Series III (FC&I valve). These tests are identical with b above but are performed on the FC&I valve.

Test conditions are listed in Table 1 and measured average pressures in Table 3. Accuracy of these pressures (scaled from oscillographs) is ±2.5 ft. Adjusted discharge values, listed in Table 1, are obtained using the model (Maynord and Grace 1981) discharge coefficients and prototype average-pressure data. The "adjusted" values are derived in the following paragraphs (25-27) and are used thereafter in this report.

Discharge equations

25. The following six equations assume steady-state flow through either the LL or FC&I conduits.

   a. Valve rating curve (Neilson 1971)

$$Q = CA\sqrt{2gH_{net}} \tag{1}$$

   in which

17

Q = discharge, cfs, through one valve*

C = valve discharge coefficient

A = cross-sectional area of flow passage at valve intake; $A = 23.8 \text{ ft}^2$ for the 66-in. LL valve and $A = 33.2 \text{ ft}^2$ for the 78-in. FC&I valve

g = acceleration due to gravity (32.2 ft/sec^2)

H_{net} = net total head, ft, at valve intake referenced to datum at the valve center line

<u>b</u>. Definition of H_{net} (Neilson 1971)

$$H_{net} = h_R + \frac{Q^2}{2gA_R^2} \qquad (2)$$

in which

h_R = piezometric head, ft, in the conduit immediately upstream from the valve at the piezometer ring (referenced to datum at the valve center line)

A_R = flow-passage cross-sectional area at the station corresponding to h_R ($A_R = 27.0 \text{ ft}^2$ for the LL valve and 39.0 ft^2 for the FC&I valve at transducer ring PC1 - PC2 - PC3 - PC4).

<u>c</u>. Combining Equations 1 and 2

$$Q = CA \sqrt{\frac{2gh_R}{1 - \left(\frac{CA}{A_R}\right)^2}} \qquad (3)$$

<u>d</u>. Head loss in the upstream conduit

$$H_L = H_T - H_{net} \qquad (4)$$

---

* For convenience, symbols and unusual abbreviations are listed and defined in the Notation (Appendix A).

in which

H_L = head loss, ft

H_T = total head at conduit intake, ft; i.e. pool
elevation minus the elevation of the valve
center line

e. Upstream conduit loss coefficient (definition)

$$k = \frac{H_L}{\dfrac{Q^2}{2gA^2}}$$ (5)

in which k equals loss coefficient (form plus hydraulic
friction) for the upstream conduit.

f. Transducer PC4 rating curve

$$Q = C_{EU}\sqrt{\Delta h_4} = C_{ED}\sqrt{h_4}$$ (6)

in which

C_{EU} = flow coefficient for the flow passage upstream
of PC4 (i.e. independent of valve opening),
$ft^{5/2}$/sec

Δh_4 = piezometric head drop, ft, between pool and
transducer PC4

C_{ED} = flow coefficient for the flow passage down-
stream from PC4 (i.e., essentially independent
of flow acceleration but dependent on valve
opening), $ft^{5/2}$/sec

h_4 = piezometric head, ft, at transducer PC4

Calibration of transducer PC4

26. In order to have consistent accuracy in discharge measure-
ment, model test C values at one valve opening (50 percent) are used to
calibrate pressure transducer PC4 (see Table 3, tests 17 and 26) as a
discharge measurement device as follows:

19

Valve/Series	C	h_4 ft	Δh_4* ft	Eqn 3 Q cfs	Eqn 2 H_{net} ft	Eqn 4 H_L ft	Eqn 5 k	Eqn 6 C_{EU} $ft^{5/2}/sec$
LL/II	0.47	114.8	158.7	1,057	138.6	134.9	4.41**	84
FC&I/III	0.49	236.5	49.6	2,207	286.1	0.0	0.00†	313

* $\Delta h_4 = H_T - h_4$ where H_T = pool el - el of PC4.

** By equating Equation 5 and the Darcy-Weisbach equation, the k value relative to 3,400 ft of 6-ft-diam LL upstream conduit is found to be equivalent to an $f = [(4.41)(6)/3,400] \times (6.0/5.5)^4 = 0.011$

† This k value suggests negligible upstream loss for the FC&I conduit.

Discharges

27. The above rating corresponds to the following values (see Tables 1 and 3).

    <u>a</u>. LL valve (Series II), H_T = 273.5 ft.

Valve Opening %	S/D*	h_4 ft	Δh_4 ft	$Q = 84\sqrt{\Delta h_4}$ cfs	$Q^2/2gA^2$ ft	$C_{ED} = Q/\sqrt{h_4}$ $ft^{5/2}/sec$	C** Equation 3	
25	0.148	195	78	740	15.0	53.0	0.270	(0.27)†
40	0.217	139	134	970	25.8	82.3	0.403	(0.40)
50	0.262	115	158	1,060	30.8	98.8	0.470	(0.47)
60	0.308	90	183	1,140	35.6	120.0	0.554	(0.56)
70	0.353	76	197	1,180	38.2	135.5	0.604	(0.64)
85	0.421	49	224	1,260	43.5	180.0	0.732	(0.74)
100	0.450	41	232	1,280	44.9	198.0	0.774	(0.75)

* S/D = ratio of sleeve travel to valve diameter (see sketch below for fixed-cone valve dimensions).

** Using the known and computed values, find C with Equation 3.

† Model values are in parentheses; note that the prototype C value is <u>set</u> equal to the model value at 50 percent opening (S/D = 0.262) as shown in Figure 9.
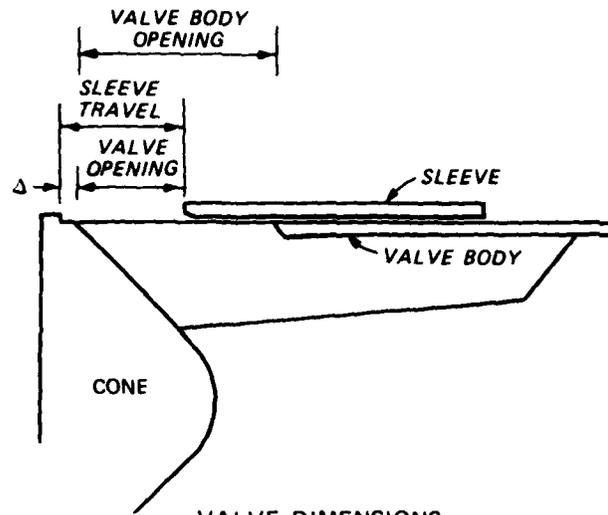
VALVE DIMENSIONS

	FC&I, IN.	S/D*	LOW LEVEL, IN.	S/D*
VALVE DIAMETER	78	1.00	66	1.00
VALVE BODY OPENING	39.62	0.508	33.44	0.507
Δ	2.48	0.032	2.20	0.035
MAXIMUM SLEEVE TRAVEL	35.00	0.450	29.70	0.450

* S = SLEEVE TRAVEL, IN.
  D = VALVE DIAMETER, IN.

b. FC&I valve (Series III), H_T = 286.1 ft

Valve Opening %	S/D*	h_4 ft	Δh_4 ft	Q = $313\sqrt{\Delta h_4}$ cfs	$Q^2/2gA^2$ ft	$C_{ED} = Q/\sqrt{h_4}$ $ft^{5/2}/sec$	C Equation 3
25	0.145	272	14	1,170	19.3	70.9	0.260 (0.26)**
40	0.213	250	36	1,880	50.0	118.9	0.417 (0.41)
50	0.258	236	50	2,210	68.8	143.9	0.49 (0.49)
60	0.303	222	64	2,500	88.0	167.8	0.555 (0.57)
70	0.349	200	86	2,900	118.5	205.1	0.644 (0.66)
85	0.415	172	114	3,340	157.2	254.7	0.741 (0.77)
100	0.449	172	114	3,340	157.2	254.7	0.741 (0.77)

* See sketch of valve dimensions above.
** Model values are in parentheses; note that the prototype C value is set equal to the model value at 50 percent opening (S/D = 0.258) as shown in Figure 9.
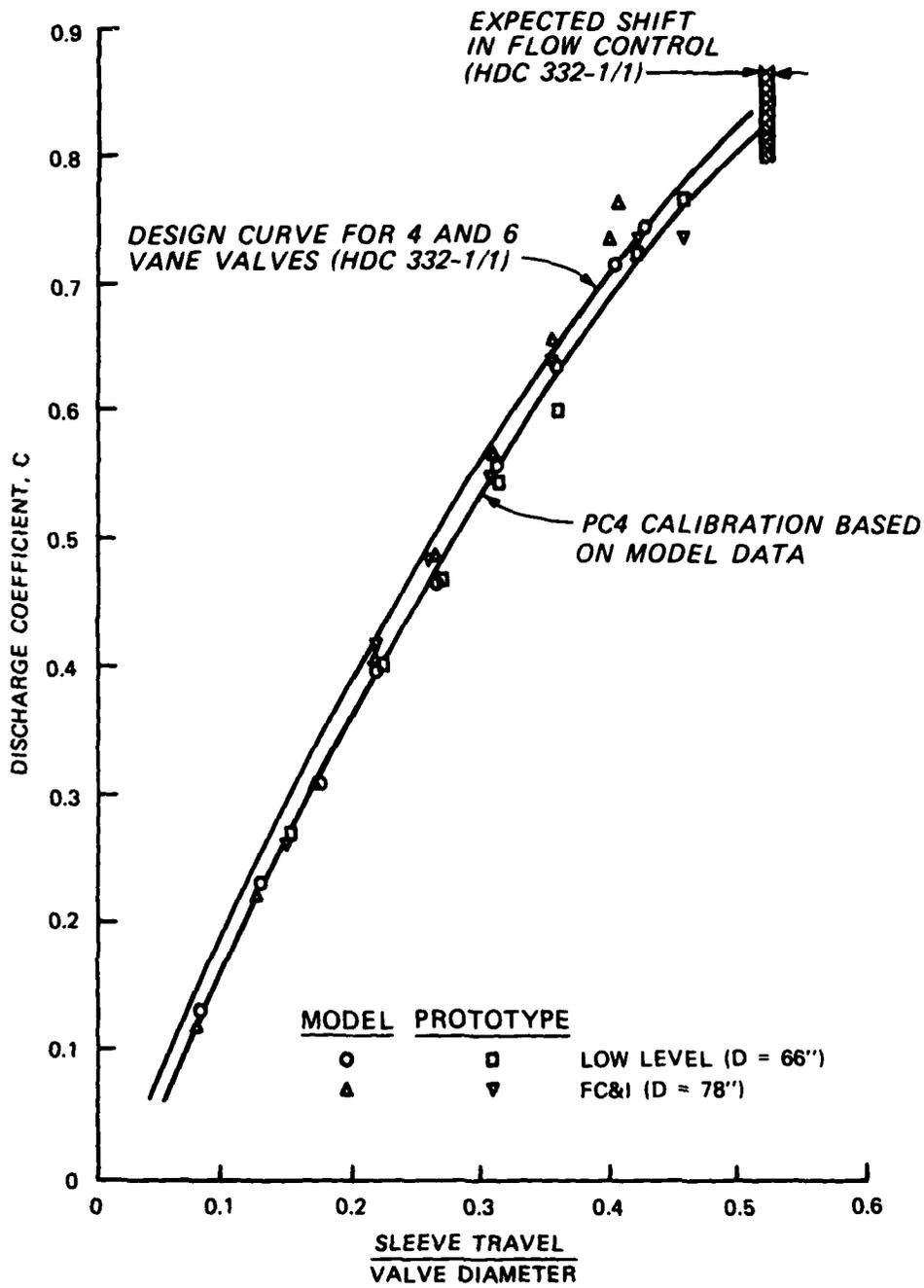
Figure 9. Comparison of model and prototype discharge coefficients

22

28. The PC4 rating is shown in Figures 10a and b for the LL valve (Series II) and the FC&I valve (Series III), respectively. Data from transducers PC1 and PC3 and project rating curve (Maynord and Grace 1981) values are also shown. The "adjusted" discharge values listed in Table 1 are from the PC4 rating. Remarks concerning the rating and the values shown in Figure 10 (a and b) are:

a. The absolute accuracy is dependent first, on the accuracy of the 50 percent model C values in the prototype and second, on the accuracy of Equation 2 using solely PC4 data.

b. The accuracy of the model C values cannot be absolutely determined from these data, although the reasonableness of the upstream loss coefficients (f values in paragraph 26) is supportive.

c. For the LL valve, the entering flow appears essentially uniform (Figure 10a; PC1 data match the PC4 rating); therefore, the PC4 rating (Equation 6 with C_{EU} = 84) should be satisfactory. Note that the 1979 project rating probably underestimates the discharge by about 10 percent.

d. For the FC&I valve, the entering flow appears nonuniform at gate openings less than about 70 percent (S/D = 0.349) as shown in Figure 10b. However, the data (PC1 and PC3 compared with the PC4 rating) at high discharges are supportive of a tendency toward more uniform flow at large gate openings. The PC4 rating (which is in excellent agreement with the 1979 project rating) is accepted herein, i.e. Equation 6 with C_{EU} = 313 .

e. The discharge coefficient, C in Equation 1, is shown in Figure 9 for the LL and FC&I valve in both model and prototype. As noted previously, the prototype is set equal to the model at 50 percent open; the maximum departures occur for openings above 50 percent. The largest difference is for the LL valve at 70 percent (S/D = 0.349) (0.64 in the model versus 0.61 in the prototype). The constant value (0.74) for the 85 percent and 100 percent (S/D = 0.415 and 0.449, respectively) prototype FC&I valve indicates that the valve shell rather than the valve sleeve is the flow control for these openings.

Unsteady flows (continuous opening)

29. The flow characteristics (as determined from PC4 and the downstream rating coefficient) for the LL valve (Series I tests) are as follows (see Tables 1 and 3):

23

LL VALVE 6/1/79
UPPER POOL AT 805.5 FT MSL

FC&I VALVE 6/29/79
UPPER POOL AT 804.1 FT MSL

Δh, FT

400
200
100
80
60
40
20

$PC4\ (\Delta h_4)\ RATING$

$Q(cfs) = 84\sqrt{\Delta h_4}$

a. LL VALVE - SERIES II TEST

Δh, FT

200
100
80
60
40
20
10

85 & 100 %
70 %
60 %
50 %
40 %

$PC4\ (\Delta h_4)\ RATING$

25% OPEN

$Q(cfs) = 313\sqrt{\Delta h_4}$

b. FC&I VALVE - SERIES III TEST

Δh, FT

400
200
100
80
60
40
20

LL VALVE
UPPER POOL 750.5

EXPECTED RATING PC4 (Δh_4)

$Q(cfs) = 84\sqrt{\Delta h_4}$

c. LL VALVE - SERIES I TEST

LEGEND

O   PROJECT RATING Q AT Δh_4
■   PROJECT RATING Q AT Δh_4
     (CONTINUOUS OPENING)
▼   PC1 (Δh_1) AT ADJUSTED Q
▲   PC3 (Δh_3) AT ADJUSTED Q
□   MODEL RATING
●   CALCULATED STEADY STATE

Figure 10.   Data scatter; piezometric head on transducer
at valve reducer

Valve Opening %	S/D	C_{ED}	Continuous Opening Values				Computed Steady-Flow Conditions	
			h_4 ft	Δh_4^* ft	$Q = C_{ED}\sqrt{h_4}$ cfs	$Q^2/2gA^2$ ft	Q, cfs Eqn 5, 1	Δh_4 ft $(Q/84)^2$
25	0.148	53.0	108	110	550	8.3	660	62
40	0.217	82.3	90	129	780	16.7	870	107
50	0.262	98.8	78	140	870	20.8	950	128
60	0.308	120.0	64	155	960	25.3	1,020	147
70	0.353	135.5	51	168	970	25.8	1,060	159
85	0.421	180.0	35	184	1,070	31.4	1,130	181
100	0.450	198.0	30	189	1,090	32.6	1,140	184

$*$ $\Delta h_4 = H_T - h_4$ where $H_T = 219$ ft.

30. The PC4 rating is shown in Figure 10c for the LL valve for the Series I data. The pressure data (PC1 and PC4) do not match the rating curve at low discharges. Since steady-flow conditions were not attained as a result of the continuous sleeve opening, the divergence of the data from the rating curve is expected. The Series I calculated steady-state flow conditions listed above are also shown in Figure 10c.

Pressure Distribution in the Valve

31. The average measured pressures at the four locations (PUB, PUD, PLB, PLD) in each of the tested valves are listed in Table 3. As expected, the trend is toward lower pressures at larger gate openings. Remarks concerning the listed values are as follows:

a. As observed in the model tests, the opposing mean pressures (PUD versus PLD and PUB versus PLB) are not equal. The consequence is an average-pressure loading on the vanes due, conceptually, to misalignmemt of the vanes relative to the direction of the flow at the leading edge of the vanes.

b. Negative average pressures occur at transducer location PUB for both the LL and FC&I valves at 85 and 100 percent open values during the higher head tests. The magnitudes of these extreme average values (-24.6 ft for the LL valve at 100 percent open (S/D = 0.450) and -31.4 ft for

the FC&I valve at both 85 and 100 percent (S/D = 0.415 and 0.449, respectively) are near enough to vapor pressure (about -33 ft) that some level of form cavitation is likely to be occurring.

32. The relationship used for model-prototype comparisons and for extrapolation to higher pool evalations for confined steady-flow circumstances is

$$E = \frac{\Delta h}{\dfrac{Q^2}{2gA^2}} \tag{7}$$

in which E , Euler number, is expected to be influenced by geometric changes (such as valve opening and cavitation in the valve body for the vane transducers), and Δh is a piezometric head differential (transducer PC4 minus the particular vane transducer of interest). Values of E are shown in Plate 5 (a-f); the following remarks pertain to these data.

a. The scaling accuracy of E is dependent on the accuracy of two pressure measurements--PC4 and a vane transducer. The consequent extreme error in E due to scaling errors is about +30, +20, and +15 percent for the Series I, II, and III test data, respectively, at a valve opening of 70 percent. For smaller valve openings, the possible scaling error is substantially larger because of much smaller Δh values.

b. The physical reproducibility of E is influenced by changes in flow geometry due first to valve opening changes and second, to the elastic response of the valve to changes in internal pressure loading. The prototype, for example, is relatively more flexible than the model.

c. The apparent variation in E with valve opening as shown in Plate 5(a-f) is likely to be attributable to scaling errors (a, above) and to physical causes (b, above). The reasonably long distance between sleeve lip and vane transducers, as shown in Plate 6 for both valves, suggests that the nearly constant FC&I prototype value is the more reasonable (but not assured) trend.

d. Values of E at 70 percent open, S/D = 0.353 for LL valve and 0.349 for the FC&I valve, are summarized below. Plots c and d and e and f, respectively, of Plate 5 show that the prototype extreme differential between vane surfaces is 0.9 for the LL valve (i.e., 1.8-0.9) and 0.3 for the FC&I valve (i.e., 0.7-0.4); the upper surface pressure

26

is higher for both valves. The values of Œ are summarized below:

| Valve/Series | Model (M) or Prototype (P) | Table of Values of $\Delta h/(Q^2/2gA^2)$ at 70% Open (Œ) | | | |
| | | U-Surface | | L-Surface | |
		D-Value	B-Value	D-Value	B-Value
LL/I	P	0.7	0.8	0.3	0.5
	M	0.7	0.7	0.2	0.5
LL/II	P	0.6	1.8	0.9	1.0
	M	--	0.7	0.3	0.5
FC&I/III	P	--	0.7	0.4	0.5
	M	0.9	1.1	0.8	1.0

Flow Control

33. A change of the location at which the flow is controlled occurs in most fixed-cone valves. At small openings, the flow is controlled along the sleeve lip; at large openings, a point is reached where the control shifts to the downstream edge of the fixed shell as illustrated below. Intense vibrations and pressure fluctuations can

SLEEVE

SHELL

CONTROL POINTS (SHELL LIP AND SLEEVE LIP)

VANE
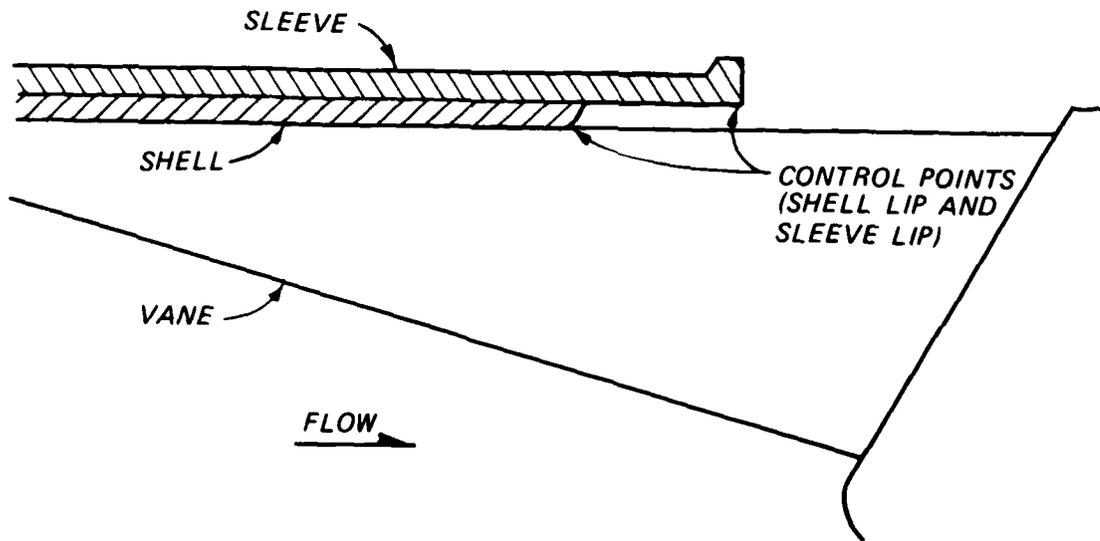
FLOW

occur for operation within a rather narrow range of openings that separate these two flow-control situations. Consequently, a preliminary step during the reduction of dynamic (vibration related) data was the identification of the largest opening at which the sleeve controls (and the smallest opening at which the shell controls) the flow. This was done by visual inspection of expanded oscillograph time-history recordings taken as the sleeve was moved between the test values listed in Table 1. Recordings of pressure, strain, and acceleration were scanned and compared with the model information concerning control shift. Occurrences were as follows.

a. LL valve

Sleeve Travel		%	
S, in.	S/D	Open	Comment
All	All	All	The Series I continuous opening data do not contain a defined small range of intense vibration near valve full open (no flow control shift)
29.0	0.439	89	Series II accelerometer data contain a narrow range of increased acceleration resulting from control shift
29.0	0.439	89	Series II strain gage data (vanes) show an abrupt change (spike) during opening resulting from control shift
29.0	0.439	89	Model (opening) flow control shift
27.8	0.421	85	Model (closing) flow control shift

b. FC&I valve

		%	
S, in.	S/D	Open	Comment
31.0	0.397	81	Series III (opening) vibration increases
31.7	0.406	83	Series III (closing) vibration increases

(Continued)

28

S, in.	S/D	% Open	Comment
34.2	0.438	90	Model (opening) flow control shift during preliminary tests
31.2	0.400	82	Model (closing) flow control shift
30.68	0.393	80	Model (closing) flow control shift (duplicate test)
31.0 (est)	0.397	81	Model (opening) pressure, about 5 in. upstream from sleeve lip, changes from above to below atmospheric

34. Deflection of a flow, as occurs in a fixed-cone valve, involves a change in linear momentum and, therefore, also involves pressure forces. Deflection along the cone corresponds to high pressures along the cone surface and a pressure gradient decreasing into the flow. The abruptness of the expansion at the shell lip probably causes a separation zone to exist along the sleeve for some distance downstream from the shell. Deflection along the separation surface corresponds to low pressures in the separation zone and a pressure gradient increasing into the flow. Geometric characteristics that enter into the separation, flow-control, and transducer response are shown in Plates 6 and 7. The following features, taken from Plates 6 and 7, are of interest.

a. Transducers PUD and PLD are well upstream from the shell lip and are not at geometrically similar locations in the LL and FC&I valves (Plate 6).

b. The minimum flow passage area is at the sleeve lip (A_2 in Plate 7) and equals the minimum area in the valve body (A_r in Plate 7) at S/D values of 0.412 and 0.425 for the FC&I and the LL valves, respectively (Plate 7).

c. At common S/D ratios, the ratio of the thickness of the shell (t_s) to the sleeve extension (ℓ_g) is greater in the FC&I valve than in the LL valve, implying the shift should occur later in the LL than the FC&I valves which agrees with paragraph 33.

35. The significance of cavitation in the flow-control problem is nullified by assuring a positive pressure along the sleeve between the

29

shell and sleeve lips (downstream from the separation zone). For example, if A_2 is limited to 0.95A_r for the FC&I valve then S/D is limited to 0.39 as shown in Plate 7. This value is less than any of the experimental (model and prototype FC&I valve) critical S/D values listed above. Similarly, if A_2 is limited to 0.95A_r for the LL valve then S/D is limited to 0.40 for the LL valve which is also less than the critical S/D values listed above. Note that the value of t_s/ℓ_g for the LL valve example given above at S/D equal 0.400 is 0.200 and for the FC&I valve example at S/D equal 0.39 is also 0.200 indicating that the relative sizes of the separation zones should be similar.

Dynamic Pressure Measurements

Overview

36. These measurements are concerned with pressure fluctuations from three transducers (PC1, PC3, PC4) in the conduit and four transducers (PUB, PUD, PLB, PLD) on the test vane in the FC&I valve, and from two transducers (PC1, PC4) in the conduit and four transducers (PUB, PUD, PLB, PLD) on the test vane in the LL valve. Hood pressure fluctuations were measured from two transducers (PHB, PHC) in the LL hood and from eight transducers (PH6-PH13) in the FC&I hood. The reduction and analysis of the pressure data included digitizing the data from the magnetic tape, producing time-history plots, and transforming the data from the time to frequency domain. The frequency transformation is a mathematical Fourier Transform (or Fast Fourier Transform, abbreviated FFT) of the digitized data. The high, low, and peak-to-peak instantaneous pressures were obtained by means of a computer scan from the digital time-history data for each transducer recording. Figure 11 is an example of the 1-sec digital time-history, which contains the maximum peak-to-peak fluctuation as determined from a preliminary computer scan of the test record, and the FFT plot, which gives a "dominant" frequency, f_D, that is defined as the frequency at which the maximum Fourier coefficient is obtained. The dominant frequencies (Tables 4-6) were generally low (0 to 15 Hz) with the exception of pressure transducer PC4 (located in the wall of the reducer). This transducer

30
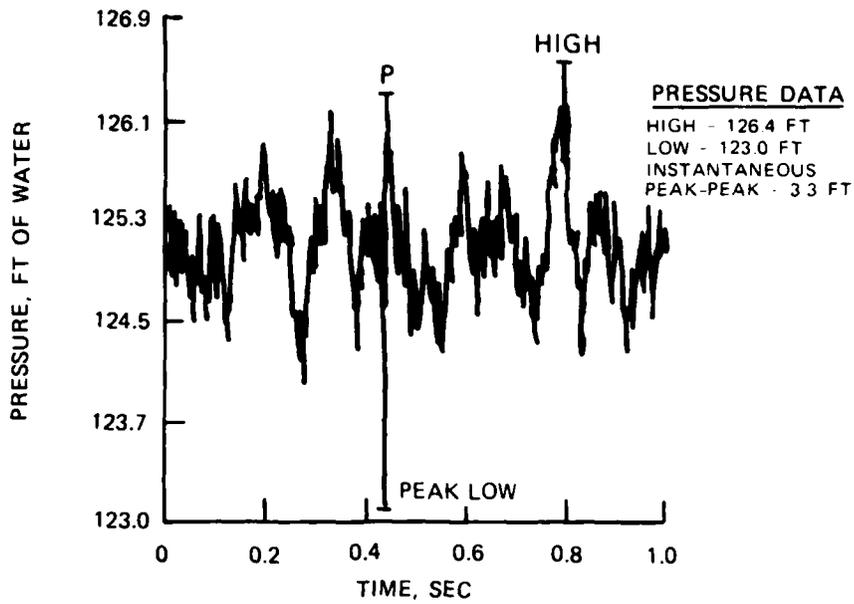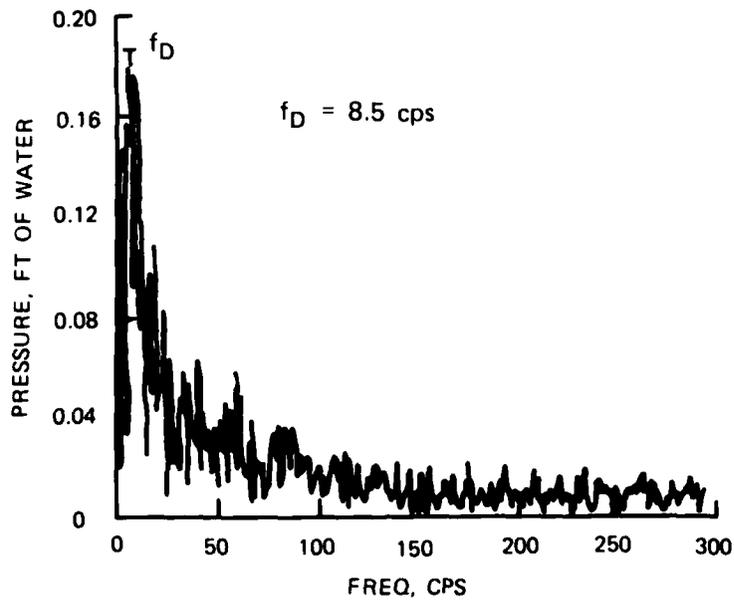
a. TIME-HISTORY PLOT

b. FFT PLOT

Figure 11. Example of the 1-sec digital time-history and FFT plot
(LL test Series II, 40 percent valve opening)

31

experienced the highest dominant frequencies (ranging from 60 to 180 Hz) for both series of LL valve tests and for the FC&I valve tests.

37. During the FFT data analysis, the amplitudes of the low-frequency components of pressure fluctuations were determined to be much greater than the amplitudes of the high-frequency components. Despite the lower amplitudes, the higher frequencies may be of more significance as far as valve structural vibration is concerned. Consequently, where noted in the text, high band-pass digital filters were sometimes used to eliminate frequencies below 5 Hz. Plate 8 illustrates the consequence of the filtering procedure. The example (which is not test data) is a pure harmonic at a frequency of 1 Hz and of large amplitude that is combined with another pure harmonic at a frequency of 60 Hz and of small amplitude.

38. The dynamic pressure data obtained as described above are listed in Tables 4, 5, and 6 and discussed in the following paragraphs. The listed pressure data are from the following transducers:

  a. Reducer. Transducers PC1 and PC4 for Series I and II (LL valve) and PC1, PC3, and PC4 for Series III (FC&I valve).

  b. Vanes. Transducers PUB, PUD, PLB, and PLD for Series I and II and PUB, PLB, and PLD for Series III.

  c. Hood. Transducers PHC and PHB for Series I and II and PH6-PH13 for Series III (Figure 6).

Note that Tables 4-6 list the magnitude and dominant frequency of the valve reducer and vane pressure fluctuations while the measured mean values for these transducers are listed in Table 3. On the other hand, mean values are available for the hood transducers for Series III tests and are shown in Table 6.

Pressure Fluctuations

Frequency analysis

39. Pressure fluctuation data listed in Tables 4-6 are from magnetic tape analog records digitized at the rate of 1,000 samples/second. Series I data (Table 4) are not filtered, whereas Series II and III data (Tables 5 and 6, respectively) are filtered by the procedure described

previously. A 1-sec digital time-history and FFT plot (0 to 500 Hz for Series I and 0 to 300 Hz for Series II and III) were made for each listed channel (Figure 11). The 1-sec sample was chosen so that it contained the maximum peak-to-peak fluctuation determined from a preliminary computer scan of 15 to 20 sec of the test record. The plots are not included herein; however, a qualitative evaluation of the FFT plots is presented in Table 7. The descriptive symbols referred to as "Nature" in the table are described below.

a. Because of the dominance of low-frequency turbulence and limited sample length most plots contain large amplitude components in the range 0 to 20 Hz. This is denoted by "<20 Hz."

b. The hood-transducer FFT's normally show large variations in frequency component amplitude; the overall trend of amplitude is to become less at higher frequency and is denoted by "Irr."

c. Plots showing apparent electrical noise are denoted as "Noise (e)."

d. Plots showing a general trend toward constant or increasing-with-frequency amplitudes are denoted as "Noise (u)."

e. Distinct peaks at frequencies greater than 20 Hz are included only when they are clearly discernible in the record and are obviously not electrical noise. The symbol "+" denotes FFT's that contain multiple separate peaks of significant amplitudes (i.e., about 40 percent greater than that of the maximum component amplitude in the 0- to 20-Hz range).

40. The FFT overview, as listed in Table 7, shows only one consistent (and apparently flow-dependent) peak at frequencies greater than 20 Hz--this peak is from transducer PLD. Electrical noise (60 Hz and harmonics thereof) is significant only for transducer PC4 and only during Series I tests. The isolated 120-Hz spike indicated for PC4 during Tests 20 and 21 is as likely to be due to mechanical vibration as to electrical causes. Overall:

a. The piezometer ring FFT data (PC1, PC3, and PC4) tend to contain several peaks that extend to high frequencies and that are probably caused by mechanical vibration and reverberation; the highest peaks are commonly in the "<20 Hz" range as shown in Table 7.

33

<u>b</u>. The vane FFT data (PLB, PLD, PUB, and PUD) contain the least number of isolated peaks and the larger peaks are always in the "<20 Hz" range.

   <u>c</u>. The hood FFT data (PHB, PHC, and PH6-13) are dominated by isolated peaks extending to high frequencies; these are probably caused by mechanical vibration and reverberation of the hood and backsplash deflector.

41. Except for the FC&I amplitudes, the flow-dependent peaks in the LL valve PLD FFT data tend to decrease (rather than increase as would be anticipated from solely velocity considerations) with increasing valve openings. Peak amplitudes and frequencies are shown in Figure 12. Tests at higher heads are required to determine whether or not the increase in amplitude appearing in the FC&I valve which appears to be related to a vane vortex-shedding phenomenon (i.e. Strouhal, S_t , number dependent), as indicated in Figure 12, also occurs for the LL valve.

42. The maximum amplitudes of the pressure fluctuations are listed in Tables 4-6. The hood pressures are discussed in a subsequent section--this discussion pertains only to the reducer and vane pressures. These latter values are presented in Plates 9 and 10 and listed in Tables 8 and 9 in the form $\left(P_{max} - P_{min}\right)\Big/\left(V^2/2g\right)$ where P_{max} and P_{min} are the maximum and minimum peak amplitudes expressed in feet of water and the velocity, V , equals Q/A where A is the cross-sectional area of the valve. Because of the random nature of turbulent flow and the generally small scale of the pressure fluctuations (as compared with the overall change in pressure from closed to valve full open operation) the values presented in Plates 9 and 10 and Tables 8 and 9 are not expected to be strictly reproducible in the field.

43. The following listing considers particular groupings of the transducers. The data are vane and reducer pressure fluctuations in the 50, 60, and 70 percent open circumstance (i.e., for the higher velocity tests but preceding tests at openings near, at, or greater than the flow-control circumstance discussed previously). Listed values are the maximum amplitude (from Tables 8 and 9) rounded to the nearest 10 percentile; values in parentheses are average values for 50 to 100 percent open (from Plates 9 and 10).

34

PEAK FFT COMPONENT, FT

0.4

0.2

0

0.2   0.4
S/D

0.4

0.2

0

0.2   0.4
S/D

PEAK FREQUENCY, Hz

300

200

100

$f \approx \dfrac{S_t Q}{t_v A}$

$t_v = 1.75''$
$S_t = 0.4$

0   0.2   0.4
S/D

300

200

100

$f \approx \dfrac{S_t Q}{t_v A}$

$t_v = 2.25''$
$S_t = 0.4$

0   0.2   0.4
S/D
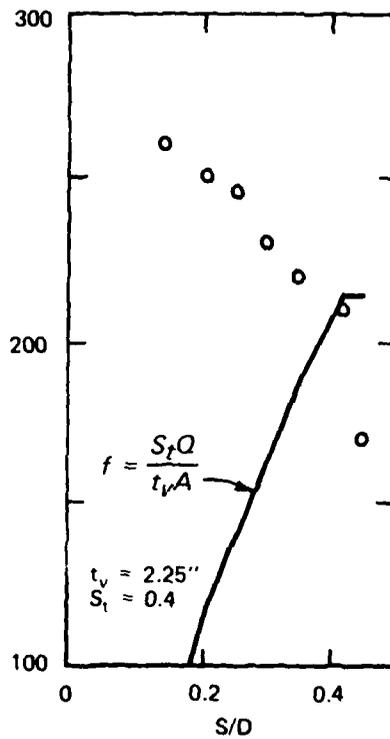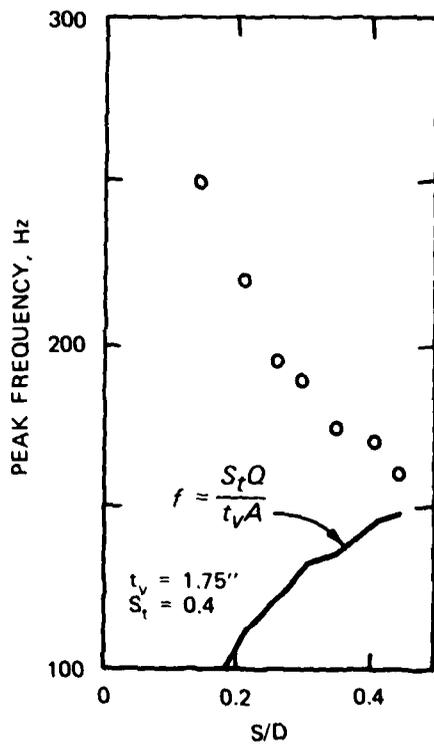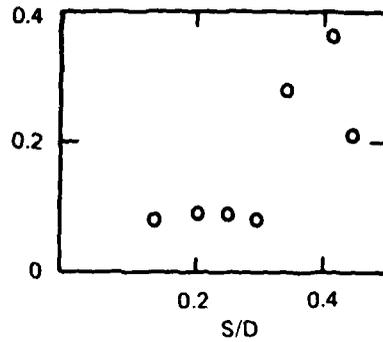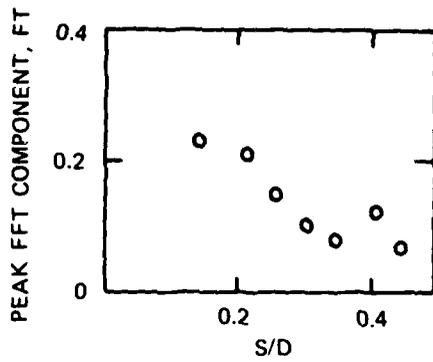
a. SERIES II (LL VALVE)   b. SERIES III (FC&I VALVE)

Figure 12.   Transducer PLD (persistent FFT peak at 160 to 260 Hz)

Transducer Group	Values of $(P_{max} - P_{min})/(Q^2/2gA^2)$		
	Series I	Series II	Series III
Reducer	0.3 (0.16)	0.2 (0.14)	0.2 (0.12)
Vanes (D, upstream)	0.4	0.3	0.1
(B, downstream)	0.3 $\bigg\}$ (0.18)	0.3 $\bigg\}$ (0.18)	0.1 $\bigg\}$ (0.06)
Vanes (U, surface*)	0.4	0.3	0.1
(L, surface*)	0.4	0.3	0.1

* U = upper surface for LL valve; left surface for FC&I
   valve.
  L = lower surface for LL valve; right surface for FC&I
   valve.

44. The above group values indicate:

   a. Extreme fluctuation amplitudes are not measurably dif-
      ferent at upstream or downstream, or U or L surface,
      locations on the vanes.

   b. Amplitudes, when considered as a percentage of the valve
      velocity head, in the LL valve reducer and in the FC&I
      valve reducer are not significantly different.

   c. Amplitudes, when considered as a percentage of the
      valve velocity head, along the vanes in the LL valve are
      substantially greater than those in the FC&I valve; this
      difference indicates that buffeting, due to the upstream
      bifurcations in the FC&I conduit, is smaller than that
      occurring in a fully developed turbulent flow (such as in
      the LL conduit).

Pressure Loading on the Vanes

Vane pressures

45. Vane pressures, designated by PUB, PUD, PLB, and PLD, are
listed in Tables 4-6. Location of each transducer is shown in Plates 2
and 3. Upstream and downstream pressure transducer locations are des-
ignated by the letters D and B, respectively. Upper surface and lower
surface of the LL vanes are designated by the letters U and L, respec-
tively. In the case of the FC&I valve, the test vane is oriented
vertically; therefore, the left and right surfaces of the vane (looking
in a downstream direction) are designated by the letters U and L,
respectively.

36

46. Digitized data at each valve opening test were scanned to find the maximum instantaneous pressure for each vane pressure transducer. The largest of these maximum pressures was then used as the point for net vane pressure determination as illustrated in Figure 13.
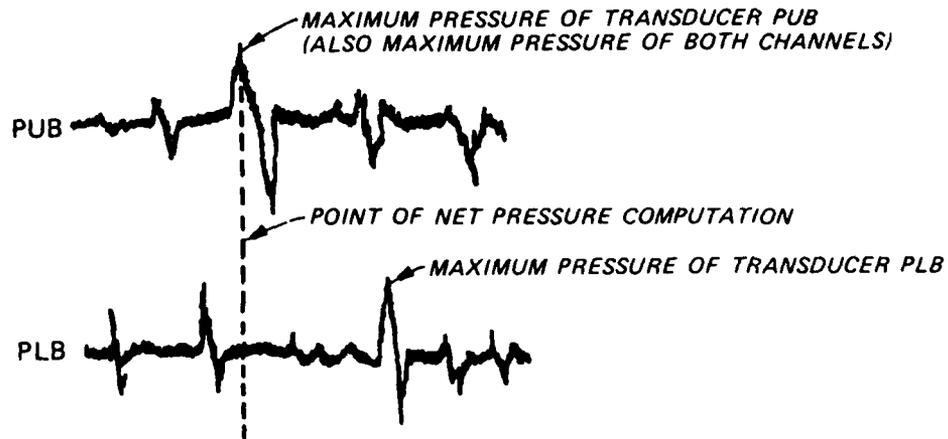
Figure 13. Determination of net pressures

Pressures from the lower vane surface (PLB, PLD) were subtracted from those of the upper vane surface (PUB, PUD) to give the net pressure (Plate 11). Table 10 lists the maximum instantaneous net vane pressures determined for each test in the series of LL and FC&I valve tests. A comparison was made between the maximum net vane pressures obtained from the model study and those from the prototype tests as shown in Plates 12 and 13. The primary direction of the differential vane pressure is also illustrated in these plates. The apparent variation between the model and prototype data can be attributed to the differences in the elastic response of the valves to changes in internal pressures. As stated previously, the prototype valve is considered to be more flexible than the model valve.

47. Pressure loadings on the vanes of the valves are expressed in terms of a differential pressure existing over the entire vane. Design differential pressures given for the LL and FC&I valves were 134 ft and 129 ft, respectively. Therefore, maximum instantaneous net vane pressures were used as a form of expressing the existing pressure loading conditions on the vanes. Comparison of the design pressures with

the values given in Table 10 revealed that the existing pressure conditions are well below the design loading values. For example, the maximum differential vane pressure recorded was 66.6 ft at 100 percent valve opening (S/D = 0.449) during the FC&I tests.

Backsplash plate and hood pressure

48. Pressure fluctuations on the backsplash plate and hood of the LL valve were measured using pressure transducers PHB and PHC, respectively (Plate 2). The FC&I valve had no distinct backsplash plate per se, and fluctuations were measured using pressure transducers PH6-PH13 as shown in Plate 3. Tables 4-6 list the pressures and fluctuations at the backsplash plate and hood of the valve for the three series of tests. In the LL valve tests, the impingement point was estimated using results from the one pressure transducer located in the valve hood. The backsplash resulting from the flow jet in the hood of the LL valve was minimal as reflected by the pressures for transducer PHB in Tables 4 and 5. The largest mean backsplash pressure that could possibly be recorded would have been equal to the velocity head of the jet. However, this did not occur, indicating that the backsplash from the issuing jet was not directed near the location of transducer PHB.

49. In the FC&I tests, the mean pressures listed in Table 6 for the eight pressure transducers (PH6-PH13) installed in the hood were used to determine where the impingment point occurred. It was assumed that the impingement point would occur at the transducer which recorded a maximum mean pressure equal to the velocity head of the issuing jet.

50. In order to determine the course of the jet and impingement on the hood, a method of conformal mapping was used. Although this method has been developed for two-dimensional flow only, it has been shown that the results can be applied with good accuracy to the corresponding three-dimensional flows (Elder and Dougherty 1953). Figure 14 is a sketch of the comparable two-dimensional flow of the New Melones valves where c is the final flow width, β equals the angle of deflection, R is the radius of the fixed-cone valve, and S is the sleeve travel. All of the dimensions have been expressed as a ratio to the approaching flow width. Therefore, in relating this method to the

38

corresponding three-dimensional flow, the following relationship was used:

$$\frac{c}{S} = \frac{(w2\pi r)}{S(2\pi R)}$$

(8)
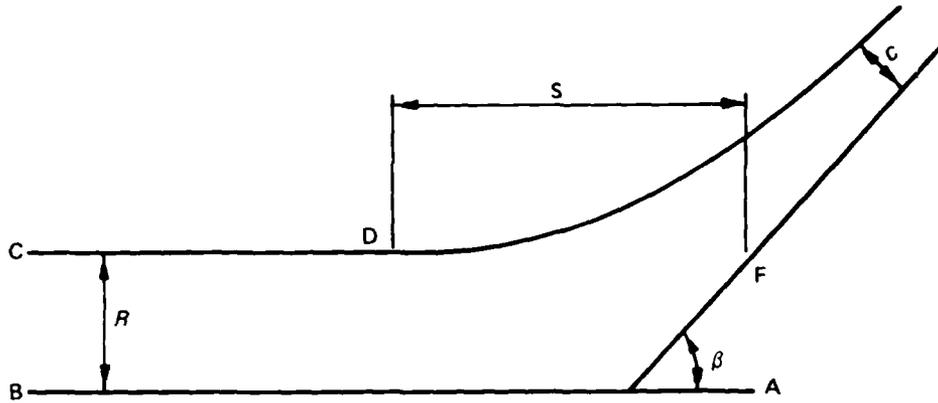
Figure 14.   Sketch of a two-dimensional jet

where r is the distance from the center line of the valve to the jet impingement point on the hood, and w is the thickness of the three-dimensional jet. Since the values of c and S are two-dimensional, it is necessary to multiply by the radius of the valve to get w in feet. Solving for w , the equation then becomes

$$w = \frac{cR^2}{r}$$

(9)

Using the maximum sleeve opening for each valve, c is equal to 0.4680. The value of r is determined by the angle of deflection β which for the two-dimensional jet is between 39.19 deg and 42.04 deg for all possible sleeve travels. Even though it is impossible to predict the exact value of β for the cone, the range is likely to be approximately the same (Elder and Dougherty 1953). Using the extreme angle of 42.04 deg for β , which is approximately the same as the angle of the cone for both valves, the most upstream impingment on the hood and the thickness of the issuing jet were determined and are shown in Figures 15 and 16. However, since the mean hood pressures were not equal to the velocity

39
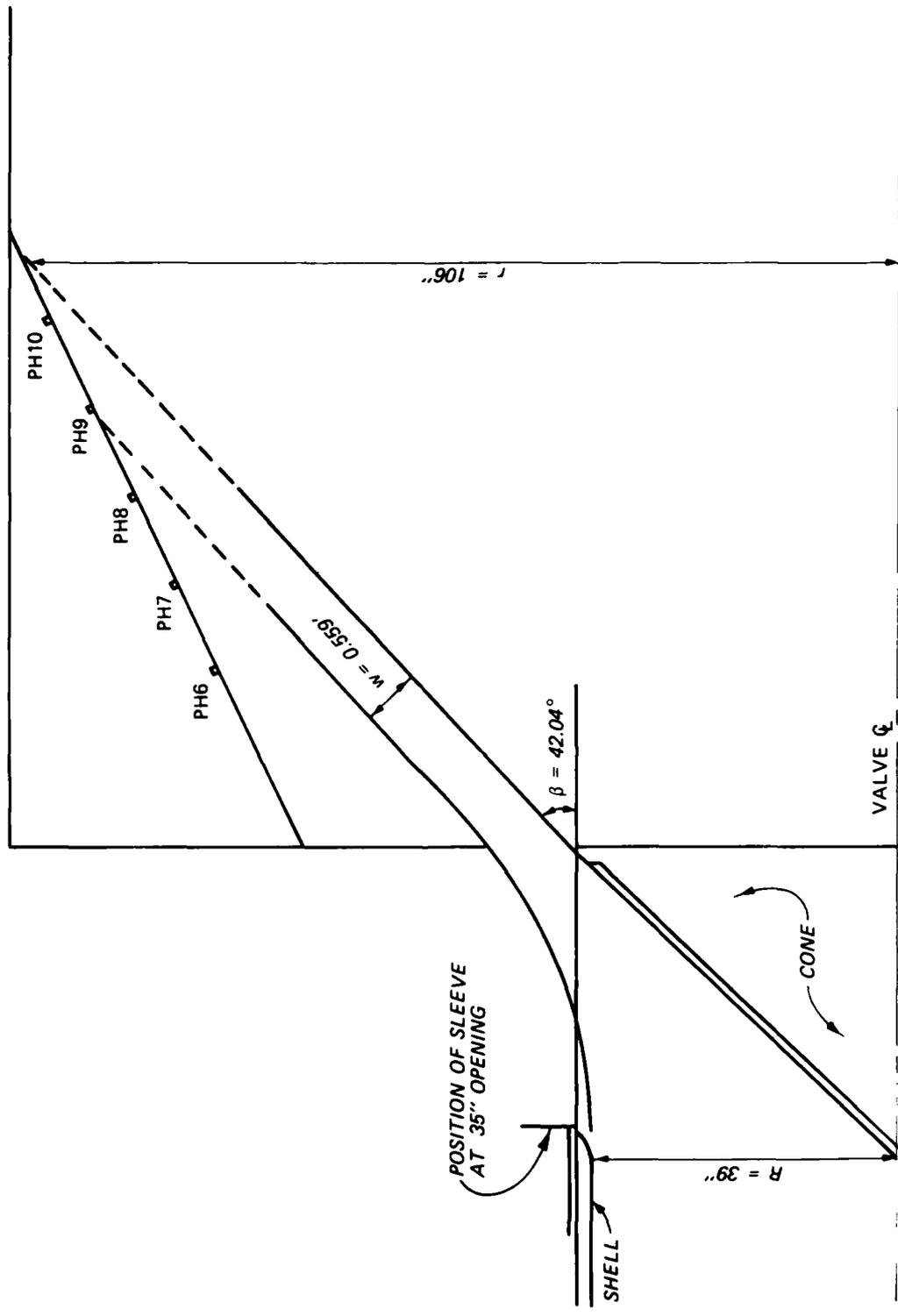
Figure 15. FC&I valve jet impingement point determination
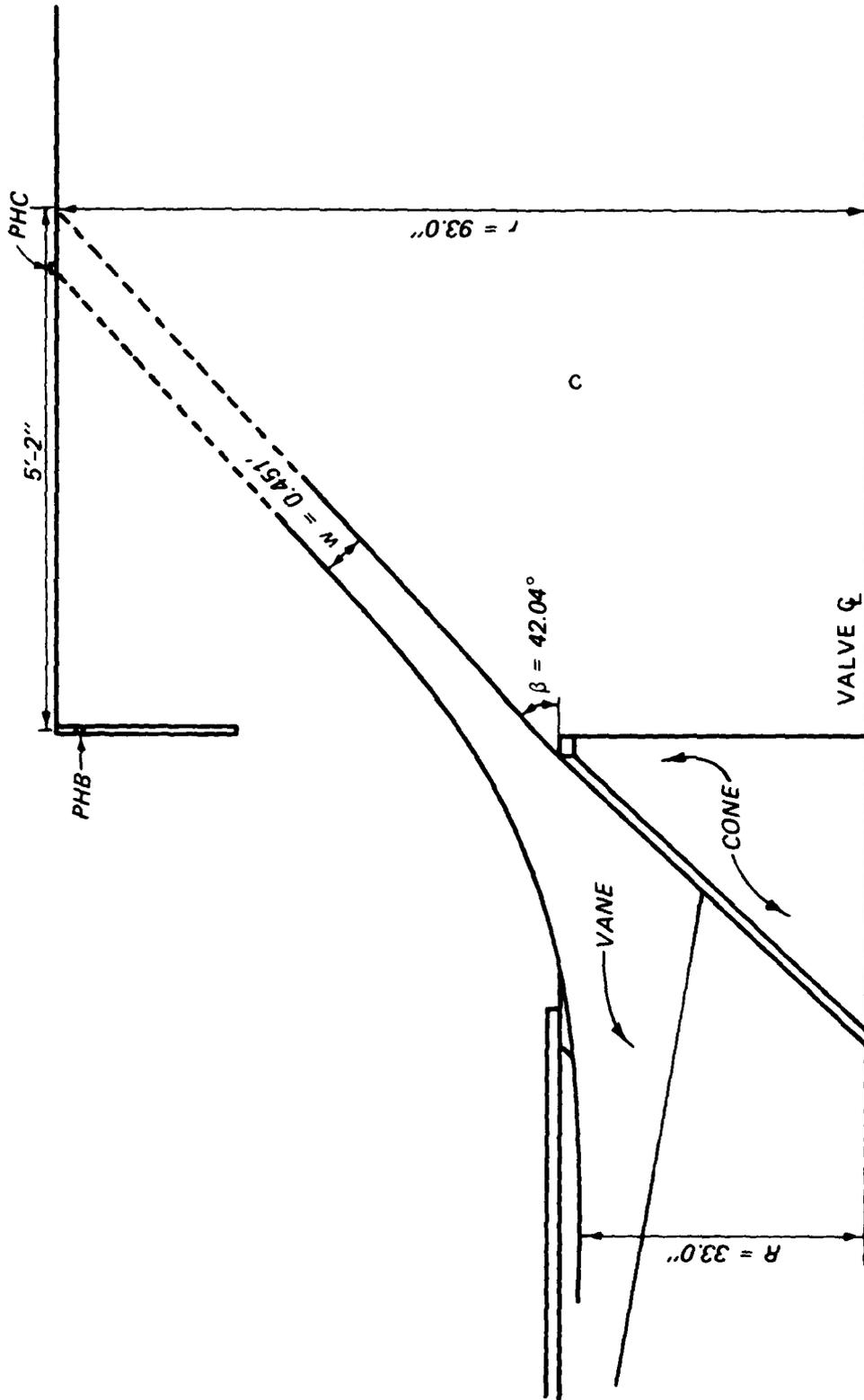
Figure 16. LL valve jet impingement point determination

41

head of the issuing jet, it is assumed that the angle of the jet was between the two extremes and did not impinge directly on any of the pressure transducers located in the respective hoods. Variation of mean hood pressures listed in Table 6 for the different valve openings is probably due to the flow curvature at the surface of the hood and not the jet impingement.

Acceleration

51. The natural frequency of the fundamental mode of vibration for the LL and FC&I valves was first determined by means of an analytical study which was performed by the valve manufacturer. Results of the study indicated that the natural frequency for the LL valve was 55 Hz; it was assumed that the natural frequency of the FC&I valve would be similar. An attempt was made to confirm this value in the field at the time of testing by performing a "ring" test; i.e., striking the valve at various places at various intensities to determine the combination that recorded the best accelerometer signal. The signal was continuously monitored and the recording equipment adjusted to accommodate the resulting magnitude. From the oscillograph recordings of this test, it was determined that the apparent natural frequency of the valve was between 50 and 55 Hz.

52. Acceleration data which were taken from the magnetic tape analog records and digitized at a rate of 1,000 samples/sec are listed in Table 11. A 1-sec digital time-history and an FFT (0 to 500 Hz) were made for each test in each series. Each 1-sec sample was chosen so that it contained the maximum peak-to-peak amplitude of acceleration in the manner described for pressure fluctuations in paragraph 39. Plates 14 and 15 are representative examples of the 1-sec digital time-histories and corresponding FFT's. An evaluation of the data listed in Table 11 was made to determine the significant acceleration information for each test series. Remarks concerning the information presented in Table 11 are:

a. In general, maximum acceleration amplitudes and associated displacement values of the Series II, LL valve and hood test data are relatively small but indicate a substantial increase overall as compared with the Series I data. These differences are probably caused by the increase in pool elevation and the subsequent increase in flow velocities. Frequencies of the LL valve accelerations, in general, experienced very little change as a result of the increase in flow and on the average remained slightly below the computed natural frequency of the valve (55 Hz).

b. The FC&I valve and hood maximum acceleration amplitudes and displacements listed in Table 11 were considerably greater that those of the LL valve. Larger dimensions and higher flow velocities of the FC&I valve are most likely the cause for this large difference in data. Frequency components of the accelerations were generally greater than the assumed natural frequency of the valve except for ATC, with an average frequency slightly below 55 Hz. Higher frequencies displayed by accelerometer AVP (135 to 188 Hz), from Table 11, are likely caused by a "ringing" of the valve cone that may have resulted from the increase in flow as the valve opening increased.

53. Using the FFT results described above, an attempt was made to determine a specific frequency or range of frequencies at which the valves and hoods vibrated and if any significant trends in the peak frequency data would indicate some type of flow dependence. A qualitative evaluation of the plots was performed and is summarized in Table 12. The descriptive symbols used in this table are described below.

- Distinct peaks are denoted by a (+) in Table 12 when they are clearly discernible and not the result of electrical noise.

- FFT's showing a general trend toward constant or increasing-with-frequency amplitudes are denoted by "Noise (u)."

- Plots having large variations in amplitude but with a general trend toward becoming less at higher frequencies are denoted by "Irr."

The FFT evaluation (summarized in Table 12) of accelerometers AVC, AVP, and AHA illustrates a specific range of frequencies at which the valves and hoods vibrated. In general:

43

a. Series I and II, LL valve vibrations were found to have a mean frequency of 45 Hz which is slightly less than the computed natural frequency of 55 Hz. Higher frequency peaks were present but of relatively small amplitudes and are therefore relatively insignificant. No significant increase in the LL valve frequency response occurred as a result of increasing flow rates at the heads tested.

b. Hood vibrations for the Series I, LL valve tests had a frequency range of 67 to 492 Hz. Series II, LL hood vibrations experienced a substantial increase in frequency, ranging from 89 to 426 Hz, which is in response to the increased magnitude of the issuing flow jet velocity head. However, in both series of tests the noise level was extremely high with very few distinct peaks occurring on the FFT.

c. FC&I valve vibration frequencies, though not always distinct peaks, were found to average 70 Hz which is significantly higher than the assumed natural frequency of the valve (55 Hz). Vibration frequencies of the FC&I hood ranged from 145 to 159 Hz. Tests at higher heads would be required to determine what significant changes would occur in the peak vibration frequencies of the FC&I valve and hood.

54. Valve vibration frequency data listed in Table 12 for the LL and FC&I valves are considered a reasonably accurate representation of the natural frequency and harmonics thereof. Since these valves are elastic structures, in which many resonant frequencies exist, any one of a number of frequencies could be indicative of the natural frequency of vibration. However, it is generally the lower frequencies that receive the driving power more frequently due to the ease at which they are excited. Vibration data of Table 11 are the result of the pressure forces and flow conditions in the valves and hoods which are the main constituents of the excitation forces. The higher frequency values of Table 12 are listed to show that there are a number of frequencies that exist as a result of the vibration of such an elastic structure. However, it is believed that most of the energy is directed toward the excitation of the lower frequency values.

Torsional vibration

55. Torsional vibration data were computed using the vertical accelerometers in the center and on the periphery of the valve (AVC

44

and AVP, respectively). Instantaneous net torsional accelerations (AVP-AVC), relative to the valve center line, were determined by the same method as that used for the instantaneous net vane pressure determination described in paragraph 46. Table 13 lists the torsional acceleration data for the LL and FC&I valve tests. A negative value indicates a clockwise torque (when looking at the valve in the downstream direction), and a positive value implies a counterclockwise torque acting on the valve. Although the data imply that no general trend of torque direction exists on either valve, the direction of the maximum net torsional accelerations for a particular valve opening is indicated. Net displacements associated with net torsional accelerations were computed using the dominant frequencies from Table 11, for accelerometer AVP, and are listed in Table 13. These values were relatively small with the maximum displacement of the LL valve and the FC&I valve being 0.0039 in. and 0.0042 in., respectively.

Valve failure criteria

56. Both theoretical and experimental studies have been conducted to determine safety parameters for operation of Howell-Bunger valves. These studies have confirmed that valve failure is closely associated with a critical velocity (or a critical discharge) during the vibration period (Mercer 1970, Wang 1973). The equation used for determining a parametric value ($\pi/4$ S/D) which was related to valve failures is:

$$\left(\frac{\pi}{4}\frac{S}{D}\right) = \frac{Q}{C_v t_v D} \div \sqrt{\frac{E}{\rho}} \qquad (10)$$

where

$\frac{S}{D}$ = dimensionless distance traveled by the flow

Q = discharge, cfs (using the maximum discharge experienced)

C_v = dimensionless valve coefficient dependent upon the ratio of the shell thickness to vane thickness (t_s/t_v) and the number of vanes

t_v = thickness of the vane, ft

D = diameter of the valve, ft

E = Young's modulus of elasticity, 29×10^6 psi (4.176×10^9 psf)

45

ρ = mass per unit volume, 15.22 $lb\text{-}sec^2/ft^4$ for A-514 steel

t_s = thickness of the shell, ft

57. Mercer (1970) states that valves with a parametric value below 0.115 have operated successfully and all valves with values greater than 0.130 have failed. These critical values were drawn from over 20 examples in which some valve failures did occur.

58. The values of C_v for various thickness ratios were only given for valves having four or six vanes. Since the valves at New Melones dam have eight vanes, a C_v value had to be determined for this condition. Using a table of values for C_v for four- and six-vane valves with identical thickness ratios, a value of 2.74 was extrapolated for a valve with eight vanes (Figure 17).
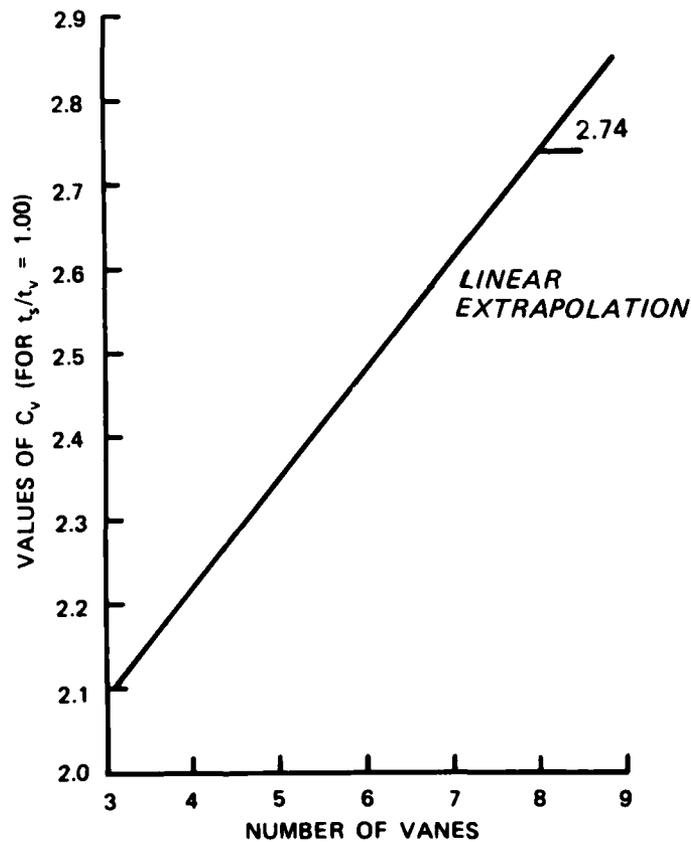
Figure 17. Determination of C_v values for valve failure criteria

59. Letting $Q = 1,280$ cfs (maximum discharge, see Table 1), $C_v = 2.74$, $D = 5.5$ ft, $\rho = 15.22$ lb-sec^2/ft^4, and $t_v = 0.15$ ft, the parametric value of the LL valve was found to be 0.034. For the FC&I valve, letting $Q = 3,340$ cfs, $C_v = 2.74$, $D = 6.5$ ft, $\rho = 15.22$ lb-sec^2/ft^4, and $t_v = 0.19$ ft, the parametric value was found to be 0.060. The above values are well below the limit (0.115) for those valves which have not failed. This implies that even at the highest tested discharges, the valves are operating under conditions at which no failures have been recorded.

Acceleration response
to flow-control changes

60. During the stepped-valve-opening tests of the FC&I valve, excessive acceleration fluctuations occurred when the valve opening approached 81 percent (S/D = 0.397). This same situation was observed during the LL stepped-valve opening tests at 89 percent (S/D = 0.439) valve opening but the acceleration fluctuations were considerably smaller than those of the FC&I valve as noted in paragraph 33a. The increase in acceleration intensities is the result of a change in the location at which flow is controlled as discussed in paragraph 33. Plate 16 represents a typical oscillogram recording of the acceleration responses at the time of the flow-control change (note changes in pressures also).

61. The effect of the flow-control shift is further illustrated by results from the time-history playbacks of the magnetic tape data. Plate 17 presents a typical comparison of the acceleration responses prior to and during the flow-control change. These data are from transducer AVC and AVP which were mounted in the center and on the periphery, respectively, of the FC&I valve and responded to vertical movements of the valve. Note the differences in the vertical scales of the two plots for AVC. The amplitudes of acceleration for AVC were greater during the flow-control change and increased by a factor of about 2.0. The acceleration amplitudes of AVP increased during the flow-control change by a factor of about 3.0. The probability density plots shown in Plate 18 indicate that the probability of a specific magnitude of acceleration

47

occurring is much greater within the period of the flow-control change. For example, the probability of accelerometer AVC experiencing an acceleration of +0.4 g during the control change is about 8.4 percent. Prior to the occurrence of the control change, the probability of AVC experiencing an acceleration of this same magnitude is about 2.7 percent.

62. The probability that acceleration fluctuations, resulting from the flow-control change, were equal to or less than a particular amplitude was obtained from the cumulative distribution function (CDF) diagrams in Plate 19. The following tabulation summarizes the CDF diagrams for the acceleration amplitudes that correspond to a 95 percent probability of occurring prior to and during the flow-control change.

| | Peak Acceleration, g | | |
Transducer	Prior to Flow-Control (A) Change	During Flow-Control (B) Change	B/A Ratio
AVC	0.23	0.67	2.9
AVP	0.34	0.95	2.8

In general, the vibration amplitudes during the flow-control change are on the order of three times larger than those measured prior to the flow-control change.

63. Plates 20-23 present the power spectral density and cross-spectral density plots for acceleration and pressure intensity at valve openings between 81 and 83 percent (S/D equal to 0.397 and 0.406, respectively) for the FC&I valve, A significant peak in the cross-spectral plot would indicate that a strong correlation existed at a particular frequency (Bendat and Piersol 1968). Plates 20 and 21 are concerned with data prior to the control shift. There seems to be no significant peak associated with any frequency in the cross-spectral density plot indicating that the relationship between valve acceleration (AVC) and valve reducer pressure fluctuations (PC1) or valve acceleration (AVP) and vane pressure fluctuations (PUB) during this period prior to the flow-control change was not very strong. During the flow-control change, accelerometer AVC and pressure transducer PC1 still did not indicate that any correlation existed as shown in Plate 22. However, a stronger relationship between the acceleration and pressure

48

responses was most evident in Plate 23 where the prominent peak of the cross-spectral density plot coincides with approximately the same frequency (96 Hz) as the valve acceleration (AVP) and vane pressure (PUB) frequencies of the power spectral density plots. Also, note the ordinate scale increase from Plate 21 to Plate 23.

Strain

64. The point measurement of strain on the test vanes at the calculated point of maximum stress concentration required two sets of strain gages as discussed in paragraphs 18 and 19. Due to the variation of loadings to which the vane would be subjected, it was necessary to arrange the gages such that one form of strain (either axial or bending) be measured and at the same time eliminate any accompanying opposite strain signals. For example, one gage arrangement was such that only axial strain was measured while the accompanying bending strain signal was eliminated. Likewise, for monitoring bending strain, the arrangement of gages was such that the accompanying axial strain signal was eliminated.

65. Strain gages were located on the 10:30 o'clock vane of the LL valve and the 6:00 o'clock vane of the FC&I valve (Plates 2 and 3). The strain data were obtained from the magnetic tape analogs, digitized, and listed in Table 14 in the same manner as the pressure and acceleration data. A 1-sec digital time-history and FFT plot were made for each valve opening in the three series of tests.

66. Table 14 shows that in most cases the test vane experienced larger peak-to-peak fluctuations of axial strain during the second series of LL valve dynamic measurements than during the first. Peak-to-peak fluctuations of bending strain were also larger during almost all of the Series II, LL valve tests. This is assumed to be due to the 50-ft increase in head at the time of the tests. The increase in head also affected the valve opening at which a reversal of axial strain, compression to tension, occurred. The bending strain for the FC&I test vane could not be obtained during the dynamic measurements because the gages

49

became inoperative during the stepped valve opening test. The limited time that was available for testing prevented replacement of the gages.

67. The FFT plots of the strain gage recordings were reviewed to obtain the data presented in Table 15. The predominant frequency (f_D) for strain fluctuation (axial and bending) was found to be generally less than 20 Hz for both the LL and FC&I valve test vanes. As in Table 13, the FFT data contained several significant peaks at higher frequencies, but the highest peaks occurred in the less than 20-Hz range. The significant peaks at the higher frequencies were examined to determine if a consistent peak was present during each of the series of tests that could be identified as an apparent natural frequency of vibration for the test vane. The most frequently occurring frequencies for the Series I and Series II, LL valve tests were 160 Hz and 180 Hz, respectively. The slightly higher frequency of the Series II tests is as expected since the valve cone, to which the vane is connected, is subjected to higher loadings due to the increased velocity head. The most consistent frequency found to occur during the FC&I valve tests was 180 Hz. Further testing of the FC&I valve at higher heads would be required to determine what effect, if any, this would have on vane vibration frequencies.

68. The data presented in Table 15 compared with vibration and pressure FFT results indicate that the frequencies of strain fluctuations do not coincide with any natural frequency of the LL valve. Therefore, based on these results, the implications are that conditions of resonance or near resonance do not exist.

69. For the purposes of determining how strain measurements relate to possible fatigue failure (Crandal, Dahl, and Lardner 1972), it is necessary to refer to bending and axial strain in terms of alternating and mean stress components. Stress, σ, and strain, ε, are related by Hooke's Law, $\sigma = E(\varepsilon)$, where E is Young's modulus of elasticity (Roark 1965). From this equation, the measured peak-to-peak bending and axial strains may be converted to peak-to-peak stress, σ_f, at the vane surface as follows (the subscript f defines type of stress):

50

$$\sigma_f = E(\varepsilon) \qquad\qquad (11)$$

in which, for σ_f in psi and the peak-to-peak strain, ε , in μin./in. (Table 14), E equals 29×10^6 psi.

70. The measured peak-to-peak fluctuations of strain presented in Table 14 were converted into stress fluctuations by means of the preceding σ_f equation and are listed in the following tabulation.

Maximum Peak-to-Peak Stress Fluctuations, psi

Stress	Test Series	Test No. - Valve Opening in percent						
		5-25	7-40	12-50	8-60	9-70	11-85	10-100
σ_1	LL I	360	319	420	354	476	362	725
σ_2	LL I	319	362	--	406	--	522	792
		15-25	16-40	17-50	18-60	19-70	20-85	21-100
σ_1	LL II	444	528	342	1,366	365	624	1,137
σ_2	LL II	945	824	394	725	316	1,317	757
		24-25	25-40	26-50	27-60	28-70	29-85	30-100
σ_1	FC&I	380	461	667	1,151	423	58	52

Note: -- = data not recoverable.
σ_1 = axial stress; σ_2 = bending stress.

71. Some materials have an endurance limit; for stresses below this limit, they can tolerate an indefinite number of cycles without failure, corresponding to essentially infinite life (Crandal, Dahl, and Lardner 1972). An approximate value of endurance limit from the reference is:

Endurance limit stress = 0.4 (ultimate strength)

where the ultimate strength is defined as the point where the material strength no longer compensates for the decrease in cross-sectional area and the load required to cause further elongation begins to decrease. The yield stress (the stress required to produce a certain arbitrary plastic deformation) can be used if the ultimate strength is not known. This will give a conservative result. The endurance limit stress,

51

using the equation described above and estimating the yield stress as
100,000 psi (from specifications for the New Melones valves), is
40,000 psi. The fluctuating stresses listed in the preceding table
indicate a stress level at the calculated point of maximum stress concen-
tration to be well below the endurance limit stress of the vane material.
This would imply that a potential for failure due to fatigue at this
location on the vane is very low under the tested head conditions. How-
ever, it should be noted that these results do not relate to other
structural components of the valve. A complete structural analysis
would be required to accomplish this and is beyond the scope of this
report.

Summary of Results

72. The following determinations and conclusions result from
analyses of the data reduction of the New Melones prototype tests. The
recommendations are applicable only when the project is operated in the
same manner as during the subject tests.

73. Discharge characteristics determinations:

a. Flow rates through the low level (LL) and flood control
and irrigation (FC&I) valves were

$$Q = 84\sqrt{\Delta h_4} \quad \text{and} \quad Q = 313\sqrt{\Delta h_4} \text{ , respectively}$$

b. Discharge coefficients computed from the prototype data
agree well with the design curve and model data.

c. The flow entering the LL valve appears essentially uni-
form at all discharges while the flow in the FC&I valve
is nearly uniform only at higher discharges.

Flow conditions in the
fixed-cone valves and hoods

74. The following conditions pertain to flow within the valves
and resulting pressures:

a. Vane pressure loading. As observed in the model tests,
an average-pressure loading on the vanes exists probably
as a result of a slight misalignment of the vanes rela-
tive to the direction of the flow.

52

b. Cavitation. Some level of form cavitation is likely to be occurring at the vanes in both the LL and FC&I valves as indicated by the negative average pressures at transducer PUB during test Series II and III.

c. Flow control. Observations concerning the occurrences of flow-control shifts in the prototype are:

   (1) The lowest head conditions tested (el 750.5) for the LL valve did not indicate a defined range of intense vibration which would suggest a flow-control shift.

   (2) At all other tested head conditions, the LL Series II and FC&I Series III tests indicated a flow-control shift similar to that found in the model tests.

   (3) Geometric characteristics that affect the flow-control response in the model and prototype are as noted in paragraphs 34 and 35.

d. Pressure fluctuation frequency. The dominant frequencies of the fluctuating pressures are as follows:

   (1) The valve reducer (PC1 and PC3) peak frequencies are commonly between 0 and 15 Hz, with several peaks at higher frequencies probably caused by mechanical vibration.

   (2) The vane transducers (PLB, PLD, PUB, and PUD) contain frequencies between 0 and 15 Hz, with the exception of PLD as noted in paragraphs 40 and 41.

   (3) The hood transducer (PHB, PHC, and PH6-13) frequencies are dominated by isolated high frequencies caused by mechanical vibration of the hood.

e. Pressure fluctuation peak-to-peak amplitude. The amplitudes of the fluctuations at the valve reducer and vanes reveal that:

   (1) The pressure fluctuation magnitudes are not measurably different at any location on the vanes.

   (2) The amplitudes in the LL valve reducer and in the FC&I valve reducer are not measurably different.

   (3) The pressure fluctuations along the vanes of the LL valve are substantially greater than those in the FC&I valve, indicating that buffeting, due to the upstream bifurcations in the FC&I conduit, is less than occurs in the fully developed turbulent flow in the LL conduit.

53

(4) The differential vane pressures observed for the head conditions tested were well below the design pressures of 134 ft and 129 ft for the LL valve and FC&I valve, respectively.

(5) The hood and backsplash pressures were inconclusive in the determination of the impingement point of the issuing jet. Mean pressure changes for different valve openings are probably due to flow curvature at the hood surface and not to jet impingement.

Acceleration
amplitudes and frequencies

75. The following conditions pertain to vibrations resulting from flow through the valves and hoods:

a. LL valve. Under the conditions tested, the maximum peak-to-peak valve acceleration was 0.47 g occurring at AVC at an opening of 100 percent; the frequencies rf vibration were generally lower than the assumed natural frequency of 55 Hz.

b. LL hood. The maximum peak-to-peak acceleration of the hood was 0.70 g at AHA for an opening of 40 percent; the frequencies of vibration were significantly high ranging from a low value of 67 Hz to a maxiumum of 492 Hz.

c. FC&I valve. The acceleration amplitudes were generally higher than those of the LL valve with the maximum peak-to-peak acceleration of 12.73 g occurring at AVP for an opening of 70 percent; the vibration frequencies of the valve averaged 70 Hz which is slightly higher than the assumed natural frequency of the valve.

d. FC&I hood. The maximum peak-to-peak acceleration was 17.0 g occurring at openings of 40 and 50 percent; the frequencies of vibration ranged from 145 to 159 Hz.

e. Torsional vibration. The torsional vibration, computed using the differential acceleration of accelerometers AVP and AVC, did not reveal a general direction of torque existing on either the LL or FC&I valve.

f. Valve failure criteria. Parametric values computed for both the LL and FC&I valves, using Mercer's (1970) valve failure studies, are well below the limit (0.115) generally used to indicate a potential for failure.

g. Acceleration response to the flow control shift. Amplitudes of acceleration, during the flow control shift at the FC&I valve, were found to increase by a factor of 3.0 when compared with amplitudes occurring before the flow-control shift. The LL valve also experienced an

54

increase in acceleration amplitudes but of a much smaller magnitude.

Strain measurements on the vane

76. The following pertain to measurements of strain at the calculated point of maximum strain concentration:

    <u>a</u>. The predominant frequency of strain fluctuation is less than 20 Hz for both the LL and FC&I vanes.

    <u>b</u>. The fluctuating stresses, when compared with the endurance limit stress of the vane material, imply that fatigue failure at the point of maximum strain concentration is not likely to occur for the tested conditions.

Recommendations

77. Since the fluctuating pressures and stresses that were measured in the valves are well below any resonant frequencies of the structures, no major modification to the valves is deemed necessary. However, careful periodic inspections of the valve should be performed. Some structural modification to the FC&I hood may be necessary due to the large amplitudes and frequencies of acceleration found during operation of the valves. These values may be well above the tolerance limit of the hood materials.

78. The prototype test results indicate that a dynamic flow-control shift does occur and results in excessive vibration of the valve. This condition will probably occur at a pool elevation near 805 and greater and may exist to a lesser degree at lower pool elevations. Limiting the sleeve travel for the FC&I valve to 28.1 in. (73 percent open) should be adequate to avoid the problem area. A recommendation for the limiting sleeve travel of the LL valve, based on available information, is 25 in. (76 percent open). Limiting the sleeve travel to these proposed values is recommended until testing at higher pool elevations has been performed.

REFERENCES

Bendat, J. A., and Piersol, A. G. 1968. Measurement and Analysis of Random Data, 4th ed., Wiley, New York.

Campbell, F. B. 1961 (Mar). "Vibration Problems in Hydraulic Structures," Journal, Hydraulics Division, American Society of Civil Engineers, Vol 87, No. HY2, Paper No. 2772, pp 61-77.

Crandal, S. H., Dahl, N. C., and Lardner, T. J. 1972. An Introduction to the Mechanics of Solids, 2nd ed., McGraw-Hill, New York, pp 329-335.

Elder, R. A., and Dougherty, G. B. 1953. "Characteristics of Fixed-Dispersion Cone Valves," Transactions, American Society of Civil Engineers, Vol 118, Paper No. 2567, pp 907-945.

Maynord, S. T., and Grace, J. L., Jr. 1981 (Apr). "Fixed-Cone Valves, New Melones Dam, California; Hydraulic Model Investigation," Technical Report HL-81-4, U. S. Army Engineer Waterways Experiment Station, CE, Vicksburg, Miss.

Mercer, A. G. 1970. "Vane Failures of Hollow-Cone Valves," IAHR-AIRH Symposium, Stockholm.

Neilson, F. M. 1971 (Sep). "Howell-Bunger Valve Vibration, Summersville Dam Prototype Tests," Technical Report H-71-6, U. S. Army Engineer Waterways Experiment Station, CE, Vicksburg, Miss.

Neilson, F. M., and Pickett, E. B. 1980 (Feb). "Corps of Engineers Experiences with Flow-Induced Vibrations," Miscellaneous Paper HL-80-2, U. S. Army Engineer Waterways Experiment Station, CE, Vicksburg, Miss.

Roark, R. J. 1965. Formulas for Stress and Strain, 4th ed., McGraw-Hill, New York.

Wang, Chung-su. 1973 (Dec). "Analysis of Vibration of Hollow-Cone Valves," Journal, Engineering Mechanics Division, American Society of Civil Engineers, Vol 99, No. EM6, Paper No. 10215, pp 1147-1163.

Table 1

Valve Test Conditions, Apr-Jun 79

Valve Open %/in.	Test No.	$\frac{S^*}{\bar{D}}$	Date mo/day	Valve	Pool El ft NGVD	Calculated Discharge** cfs	Air Temp °F	Water Temp °F
†	4	--	4/16	LL	750.1	--	59	40
25/9.8	5	0.148			750.3	550	46	
40/14.3	6	0.217			750.4	780		
40/14.3	7	0.217			750.4	780		
50/17.3	12	0.262			750.6	870		
60/20.3	8	0.308			750.5	960		
70/23.3	9	0.353			750.5	970		
85/27.8	11	0.421			750.6	1,070		
100/29.7	10	0.450			750.5	1,090		
†	13	--	6/1		805.5	--	75	53
†	14	--				--		
25/9.8	15	0.148				740		
40/14.3	16	0.217				970		
50/17.3	17	0.262				1,060		
60/20.3	18	0.308				1,140	74	
70/23.3	19	0.353				1,180		
85/27.8	20	0.421				1,260		
100/29.7	21	0.450				1,280		
†	22	--	6/28	FC&I	804.1	--	93	63
†	23	--	6/29			--	88	65
25/11.3	24	0.145				1,170	76	64
40/16.6	25	0.213				1,880	74	
50/20.1	26	0.258				2,210		
60/23.6	27	0.303				2,500		
70/27.2	28	0.349				2,900		
85/32.4	29	0.415				3,340	71	
100/35.0	30	0.449				3,340	71	

* Ratio of the sleeve travel (S) to the valve diameter (D).
** One valve; assumes maximum losses.
† Continuous valve opening and closing.

Table 2

Test Instrumentation

Measurement	Location	Station*		Elevation*		Transducer	Code**	Range		
		LL	FC&I	LL	FC&I			LL(I) Apr 79	LL(II) Jun 79	FC&I Jun 79
Pressure	Conduit	60+08.3	3+98.5	534.8	521.3	Unbonded press gage	PC1	100 psia	150 psia	150 psia
			→	532.0	518.0		PC2	--	--	--
				529.3	514.8		PC3	--	--	--
				532.0	518.0		PC4	100 psia	150 psia	
	Vane →	60+14.7	4+05.7	534.4	515.3		PUD			
		60+14.7	4+05.7	533.4	→		PLD			
		60+18.2	4+09.2	533.4			PUB			
		60+18.2	4+09.2	533.4			PLB			100 psia
	Hood →	60+19.4	--	537.6	--		PHB	--	--	--
		60+23.9	--	537.7	--		PHC	--	--	--
		--	4+15.3	--	522.5		PH6	--	--	
		--	4+16.2	--	523.4		PH7	--	--	
		--	4+17.1	--	524.3		PH8	--	--	
		--	4+18.0	--	525.1		PH9	--	--	
		--	4+18.9	--	526.0		PH10	--	--	
		--	4+20.8	--	527.0		PH11	--	--	
		--	4+21.8	--	527.0		PH12	--	--	--
		--	4+22.8	--	527.0		PH13	--	--	--
Strain	Vane	60+19.0	4+10.0	533.9	514.8	Foil type bonded strain gage	EA	--	--	--
Strain	Vane	60+19.0	4+10.0	533.9	514.8	Foil type bonded strain gage	EB	--	--	--
Vibration →	Valve	60+18.9	4+11.5	532.0	518.0	Accelerometer	AVC	+5g	+5g	+5g
	Valve	60+18.9	4+11.5	532.0	518.0		ATC	+5g		+5g
	Valve	60+21.5	4+14.5	532.0	518.0		AVP		→	+5g
	Hood	60+19.4	4+13.5	537.6	524.0		AHA			+25g

* Rounded to nearest 0.1 ft.

** See Plates 2 and 3.

Table 3

Prototype Tests, Static Pressures

Pressure Transducer	Test Valve	Test No.-Valve Opening in Percent						
		5-25	7-40	12-50	8-60	9-70	11-85	10-100
PC1	LL	104.0	86.7	69.3	60.7	52.0	28.9	23.1
PC4		108.1	89.7	78.2	64.4	50.6	34.5	29.9
PUB		97.7	73.3	57.0	46.1	29.9	5.4	5.4
PUD		92.3	72.4	57.4	44.9	32.4	15.0	5.0
PLB		97.(	74.1	58.7	48.5	35.8	15.3	10.2
PLD		97.0	78.5	64.7	53.1	41.6	23.1	18.5
		15-25	16-40	17-50	18-60	19-70	20-85	21-100
PC1	LL	192.4	139.5	112.0	93.0	74.0	48.6	40.2
PC4		195.3	139.2	114.8	90.4	75.7	48.8	42.8
PUB		181.4	77.7	47.9	27.2	5.2	-18.1	-24.6
PUD		180.8	122.9	94.8	72.0	50.9	26.3	19.3
PLB		186.6	124.4	73.9	54.5	35.0	7.8	0.0
PLD		185.8	132.7	79.6	59.7	39.8	13.3	13.3
		24-25	25-40	26-50	27-60	28-70	29-85	30-100
PC1	FC&I*	260.3	237.9	219.9	213.2	193.0	159.3	159.3
PC3		273.8	248.7	232.7	225.9	203.1	175.7	175.7
PC4		271.8	249.6	236.5	221.9	199.7	172.0	172.0
PUB		257.7	209.5	188.6	163.4	125.7	-31.4	-31.4
PLB		256.9	218.9	197.0	168.5	146.6	26.3	26.3
PLD		262.2	227.9	207.7	187.6	157.3	110.9	110.9

Note: All pressures are in feet of water.
* Pressure transducer PUD was inoperative during these tests.

Table 4

LL Valve Pressures, Series I

Pressure Transducer	Item	Test No.-Valve Opening in Percent						
		5-25	7-40	12-50	8-60	9-70	11-85	10-100
PC1	H	105.0	88.3	70.6	62.8	53.1	30.4	25.5
	L	102.4	85.4	67.6	58.4	48.8	26.9	20.5
	P/P	2.4	2.1	1.7	1.2	2.7	2.9	2.9
	f_D	15.6	1.9	3.9	10.7	7.8	5.8	9.8
PC4	H	103.4	92.6	80.9	67.5	53.1	36.7	32.9
	L	101.1	88.4	76.1	63.1	49.0	32.5	27.4
	P/P	2.5	3.2	4.8	3.2	4.1	1.0	3.2
	f_D	60.5	180.7	180.7	180.7	180.7	180.7	180.7
PUB	H	100.1	75.6	58.9	48.4	32.2	7.6	9.6
	L	97.6	73.1	54.0	43.4	27.8	2.8	4.4
	P/P	2.0	2.0	2.9	2.3	3.1	3.5	3.5
	f_D	3.9	1.9	2.9	1.9	6.8	1.9	1.9
PUD	H	94.4	75.7	60.9	52.7	34.7	23.1	14.7
	L	91.0	71.7	54.3	43.0	28.5	12.4	3.3
	P/P	3.3	2.9	3.4	2.8	4.2	5.2	4.0
	f_D	11.7	2.0	2.0	2.0	2.0	2.0	2.0
PLB	H	99.1	75.0	60.9	51.4	38.0	18.3	15.1
	L	96.3	71.7	56.0	47.0	33.3	13.1	9.4
	P/P	2.3	2.9	3.7	1.6	4.7	2.1	3.2
	f_D	1.9	2.9	3.9	6.8	4.9	2.0	2.0
PLD	H	98.8	81.1	67.6	57.0	43.4	29.0	23.6
	L	96.4	76.1	62.2	49.7	36.6	19.8	12.6
	P/P	2.3	2.9	3.8	2.8	4.8	4.2	3.9
	f_D	2.9	2.9	3.9	2.0	2.0	2.9	1.9
PHC	H	27.9	29.1	8.4	21.0	8.8	19.4	29.1
	L	-13.3	-5.4	-26.6	-2.8	-19.6	-4.5	-3.0
	P/P	38.8	31.4	31.5	22.1	25.2	21.7	14.8
	f_D	4.8	2.0	8.8	3.9	8.8	4.9	5.8
PHB	H	0.2	0.1	0.3	0.4	0.3	0.1	0.2
	L	-0.6	-0.6	-2.9	-0.5	-5.0	-0.5	-0.4
	P/P	0.2	0.3	2.9	0.7	4.7	0.5	0.4
	f_D	1.9	4.8	2.9	2.0	2.0	2.0	2.0

Note: All pressures are in feet of water. H = highest instantaneous pressure; L = lowest instantaneous pressure; P/P = greatest instantaneous peak-peak pressure; f_D = dominant frequency, Hz.

Table 5

LL Valve Pressures, Series II

Pressure Transducer	Item	15-25	16-40	17-50	18-60	19-70	20-85	21-100
		Test No.-Valve Opening in Percent						
PC1	H	192.7	139.9	116.0	95.9	77.7	49.8	41.4
	L	191.9	139.1	111.5	91.6	72.8	43.2	37.8
	P/P	0.5	0.3	2.2	3.5	4.5	3.9	1.8
	f_D	11.3	5.7	8.5	11.4	10.2	6.8	6.8
PC4	H	201.2	145.4	116.8	92.4	78.1	52.5	43.2
	L	184.6	123.7	112.4	87.6	73.0	44.1	42.5
	P/P	11.4	19.9	2.4	2.7	3.1	5.2	0.5
	f_D	11.4	10.2	13.6	6.8	6.8	119.3	119.3
PUB	H	182.3	78.1	51.0	31.7	8.2	-16.8	-22.7
	L	179.8	75.6	42.3	21.2	-0.2	-25.2	-29.8
	P/P	2.5	1.6	8.5	8.4	7.7	6.8	6.0
	f_D	6.8	7.1	8.5	11.4	10.2	8.5	10.2
PUD	H	183.7	124.4	97.6	77.7	53.0	37.6	25.1
	L	180.4	120.8	90.7	70.4	43.9	9.0	6.0
	P/P	3.3	1.8	5.8	5.6	5.9	26.2	15.7
	f_D	11.4	2.8	6.8	11.4	6.8	6.8	5.7
PLB	H	186.7	126.4	74.3	55.8	36.6	9.4	2.8
	L	184.5	123.0	69.0	50.7	30.7	2.7	-5.6
	P/P	2.0	3.3	5.1	2.6	4.9	2.8	6.8
	f_D	10.7	8.5	5.7	5.7	5.7	5.7	10.2
PLD	H	189.0	136.1	82.0	62.4	42.4	17.5	16.9
	L	183.1	129.4	75.4	55.3	35.1	9.6	9.6
	P/P	5.9	2.9	5.8	6.6	5.7	5.7	5.0
	f_D	11.4	6.8	10.2	5.7	5.7	8.5	6.8
PHC	H	50.0	95.3	79.4	58.0	72.7	62.0	53.6
	L	2.3	34.0	-13.6	0.0	2.3	16.0	20.0
	P/P	36.3	61.3	59.0	53.4	70.4	31.6	30.0
	f_D	11.4	17.2	6.8	22.7	15.9	15.9	5.4
PHB	H	-6.3	-2.9	2.5	3.8	2.5	2.5	2.4
	L	-8.9	-9.5	-0.9	-2.2	0.1	-1.2	0.3
	P/P	2.5	6.3	2.7	6.1	1.9	3.7	2.0
	f_D	11.4	6.8	18.2	5.4	10.0	14.5	12.7

Note: All pressures are in feet of water. H = highest instantaneous pressure; L = lowest instantaneous pressure; P/P = greatest instantaneous peak-peak pressure; f_D = dominant frequency, Hz.

Table 6

FC&I Valve Pressures, Series III

Pressure Transducer	Item	Test No.-Valve Opening in Percent						
		24-25	25-40	26-50	27-60	28-70	29-85	30-100
PC1	H	261.4	239.9	221.7	215.4	195.3	163.0	162.5
	L	258.7	233.9	217.8	210.0	188.9	153.8	154.3
	P/P	2.4	5.9	3.3	5.0	6.3	5.0	6.6
	f_D	46.4	8.2	11.4	11.4	5.4	10.0	11.4
PC3	H	274.8	251.0	235.3	229.4	204.8	177.8	181.1
	L	272.3	247.4	230.6	223.6	197.9	168.9	166.6
	P/P	1.7	2.4	4.2	2.4	5.0	6.1	8.6
	f_D	25.0	45.4	10.9	8.2	8.2	10.0	11.4
PC4	H	275.7	254.2	241.9	226.9	205.1	--	177.2
	L	263.9	241.2	231.9	209.9	185.2	--	163.3
	P/P	10.9	11.0	6.2	14.6	10.2	--	6.8
	f_D	112.5	137.5	153.4	154.6	154.6	--	6.8
PLD	H	263.3	229.3	208.6	189.6	161.4	114.7	114.8
	L	260.6	226.4	204.5	184.8	155.4	105.9	107.2
	P/P	1.7	1.4	2.4	3.0	2.3	5.7	7.5
	f_D	45.5	10.2	5.7	5.7	14.2	5.7	8.5
PUB	H	258.6	210.4	191.2	164.2	128.6	-28.8*	-27.4*
	L	256.5	207.2	186.4	159.3	122.4	-36.3*	-36.9*
	P/P	1.5	2.4	4.8	3.5	4.2	4.4	7.7
	f_D	6.8	8.5	14.2	6.8	14.2	17.0	152.3
PLB	H	258.0	220.8	199.0	170.5	150.2	29.9	31.8
	L	255.6	217.6	194.2	165.4	143.7	21.2	16.6
	P/P	1.3	1.8	4.8	5.1	6.0	8.3	7.7
	f_D	6.8	10.2	8.5	11.4	12.5	11.4	166.5
PH6	H	0.6	0.4	0.6	0.6	1.0	1.4	1.8
	M	0.0	-0.1	-0.2	0.0	0.0	0.3	-0.2
	L	-0.4	-0.4	-0.6	-0.3	-0.2	-0.2	-0.7
	P/P	0.8	0.6	1.2	0.9	1.0	1.1	1.6
	f_D	145.4	150.0	156.8	155.4	78.6	20.7	5.4

(Continued)

Note: All pressures are in feet of water. H = highest instantaneous pressure; M = mean pressure; L = lowest instantaneous pressure; P/P = greatest peak-peak pressure; f_D = dominant frequency, Hz; -- = pressure not recoverable. Pressure transducer PUD was inoperative at time of testing.

* Pressure data questionable due to problems encountered during control shift phase.

Table 6 (Concluded)

Pressure Transducer	Item	Test No.-Valve Opening in Percent						
		24-25	25-40	26-50	27-60	28-70	29-85	30-100
PH7	H	0.4	0.2	0.6	1.1	1.0	23.2	17.7
	M	-0.6	-0.6	-0.4	-0.2	-0.1	1.7	0.0
	L	-1.1	-1.0	-0.8	-0.7	-0.5	-16.5	-7.6
	P/P	1.2	1.0	1.1	1.4	1.0	29.0	24.9
	f_D	149.1	44.6	58.2	97.7	64.6	17.3	15.9
PH8	H	1.5	2.4	5.0	11.0	29.6	45.4	34.1
	M	1.0	0.7	1.1	2.6	6.8	10.2	-5.7
	L	0.5	0.2	-1.4	-1.4	-17.0	-16.4	-33.0
	P/P	0.8	1.7	6.4	12.0	34.7	54.6	55.7
	f_D	59.1	12.7	9.1	10.0	11.4	15.9	11.4
PH9	H	55.7	93.2	93.2	67.0	38.6	28.4	19.8
	M	3.4	17.3	11.4	13.6	0.0	0.0	2.0
	L	-8.0	-31.8	-20.4	-13.6	-10/9	-16.8	-6.3
	P/P	63.6	65.9	100.0	76.1	46.6	39.2	18.4
	f_D	9.1	10.0	18.2	31.8	20.4	10.0	7.3
PH10	H	44.3	57.3	36.4	37.5	19.6	27.1	31.2
	M	1.1	20.9	10.0	0.0	0.0	0.0	24.8
	L	-12.5	5.0	-1.8	-9.6	-6.1	-10.7	5.0
	P/P	46.6	42.0	29.6	42.0	16.7	26.6	24.6
	f_D	64.6	17.3	19.1	6.8	35.9	99.1	20.4
PH11	H	45.0	56.8	46.6	23.0	0.8	0.6	20.0
	M	0.0	4.4	0.0	0.7	0.0	0.0	-2.7
	L	-20.4	-25.1	-22.0	0.0	-0.6	-0.5	-15.0
	P/P	52.7	63.6	64.8	21.9	0.9	1.0	31.8
	f_D	70.4	23.6	11.4	127.3	120.0	119.1	82.7
PH12	H	53.4	59.1	48.9	47.7	37.5	40.9	17.4
	M	4.1	0.0	-6.4	0.0	0.0	6.4	2.3
	L	-15.9	-25.0	-25.4	-22.7	-21.6	-14.1	-6.8
	P/P	48.2	73.9	59.1	59.1	48.9	42.7	20.9
	f_D	49.1	113.6	141.8	94.6	81.8	46.8	11.4
PH13	H	97.7	65.9	51.1	54.6	46.6	59.1	31.6
	M	6.8	0.0	-9.1	-8.0	0.0	3.9	0.0
	L	-11.4	-22.7	-27.3	-23.9	-19.3	-20.0	-9.3
	P/P	93.2	79.6	58.0	64.8	60.2	70.4	36.9
	f_D	35.4	54.6	32.7	40.9	88.6	19.1	47.7

Table 7

Overview of Pressure Transducer FFT Data

LL Valve - Series I

Pressure Transducer	Nature 5-25	Other Peaks, Hz 5-25	Nature 7-60	Other Peaks, Hz 7-60	Nature 12-50	Other Peaks, Hz 12-50	Nature 8-60	Other Peaks, Hz 8-60	Nature 9-70	Other Peaks, Hz 9-70	Nature 11-85	Other Peaks, Hz 11-85	Nature 10-100	Other Peaks, Hz 10-100
PC1	<20	--	<20	--	<20	--	<20	--	<20	--	<20	--	<20	60-100
PC4	Noise (e)	+	Noise (e)	+	Noise (e)	+		+	Noise (e)	+	Noise (e)	+	Noise (e)	+
PUB	<20	--	<20	--	<20	--	<20	--	<20	--	<20	--	<20	--
PUD	<20	--	<20	--	<20	--	<20	--	<20	--	<20	--	<20	60-100
PLB	<20	--	<20	--	<20	--	<20	--	<20	--	<20	--	<20	--
PLD	<20	--	<20	--	<20	--	<20	--	<20	--	<20	--	<20	--
PMC	Irr.	+	Irr.	+	Irr.	+	Irr.	+	Irr.	+	Irr.	+	Irr.	+
PMB	Irr.	160+	Irr.	180, 300+	Irr.	50, 100, 180+	Irr.	180, 240, 300+	Irr.	..	Irr.	180, 240, 275+	Irr.	+

LL Valve - Series II

Pressure Transducer	Nature 15-25	Other Peaks, Hz 15-25	Nature 16-40	Other Peaks, Hz 16-40	Nature 17-50	Other Peaks, Hz 17-50	Nature 18-60	Other Peaks, Hz 18-60	Nature 19-70	Other Peaks, Hz 19-70	Nature 20-85	Other Peaks, Hz 20-85	Nature 21-100	Other Peaks, Hz 21-100
PC1	Noise (u)	+	<20	155, 230	<20	--	<20	--	<20	25	<20	--	<20	--
PC4	<20	20, 155	<20	30	Irr.	25, 155, 230+	<20	25, 155, 230+	<20	+	Noise (e)	120	Noise (e)	120
PUB	<20	--	<20	20	<20	--	<20	--	<20	--	<20	55, 170	<20	40
PUD	<20	105	Irr.	130+	Irr.	--	<20	--	<20	25, 225	Irr.	+	<20	40
PLB	<20	20	Irr.	+	<20	25	<20	25	<20	25	<20	--	<20	40
PLD	<20	105, 250	<20	220	<20	195	<20	190	<20	25, 175	<20	170	<20	40, 160
PMC	Noise (u)	+	Noise (u)	+	Irr.	+	Noise (u)	+	Irr.	30+	Irr.	30+	Irr.	20+
PMB	Irr.	+	Irr.	+	Irr.	+	Irr.	90	Irr.	125+	Irr.	+	Irr.	70, 130+

FC&I Valve - Series III

Pressure Transducer	Nature 24-25	Other Peaks, Hz 24-25	Nature 25-40	Other Peaks, Hz 25-40	Nature 26-50	Other Peaks, Hz 26-50	Nature 27-60	Other Peaks, Hz 27-60	Nature 28-70	Other Peaks, Hz 28-70	Nature 29-85	Other Peaks, Hz 29-85	Nature 30-100	Other Peaks, Hz 30-100
PC1	Irr.	25, 45, 55	<20	45, 55+	<20	45, 85+	Irr.	+	Irr.	45+	Irr.	45+	Irr.	85+
PC3	25, 45,	25, 45, 55+	<20	25, 45+	<20	55, 85+	<20	25, 45, 85+	Irr.	30, 45, 85+	<20	25+	Irr.	35, 45, 110+
PC4	Noise (u)	115+	Noise (u)	25, 45	Noise (u)	+	Noise (u)	+	Noise (u)	+	--	--	Noise (u)	+
PUB	<20	55	<20	45, 80, 110	<20	--	<20	--	<20	90, 110	<20	30	<20	155, 170
PLB	<20	45, 80, 105	<20	45, 110+	<20	--	<20	--	<20	--	<20	185+	<20	150, 165
PLD	Noise (u)	45, 260+	<20	250	<20	245+	<20	230+	<20	220+	<20	210	<20	170
PM6	Noise (u)	145+	Noise (u)	45, 60, 150+	Noise (u)	35, 65, 155+	Noise (u)	155+	Noise (u)	80, 155+	Noise (u)	155+	Irr.	45, 155+
PM7	Noise (u)	150+	Noise (u)	45, 145+	Noise (u)	35, 60, 155+	Noise (u)	80+	Noise (u)	65+	Noise (u)	+	Irr.	+
PM8	Noise (u)	60, 155+	Noise (u)	85+	Irr.	+	Irr.	+	Irr.	+	Irr.	+	Irr.	45, 85+
PM9	Irr.	+	Noise (u)	+	Irr.	+	Noise (u)	+	Irr.	+	Irr.	+	Irr.	+
PM10	Noise (u)	+	Noise (u)	+	Noise (u)	+	Noise (u)	+	Noise (u)	+	Noise (u)	+	Irr.	+
PM11	Noise (u)	+	Noise (u)	+	Noise (u)	+	Noise (u)	130+	Noise (e)	+	Noise (e)	+	Noise (u)	+
PM12	Noise (u)	+	Noise (u)	+	Noise (u)	+	Noise (u)	+	Noise (u)	+	Noise (u)	+	Noise (u)	+
PM13	Noise (u)	+	Noise (u)	+	Noise (u)	+	Noise (u)	+	Noise (u)	+	Noise (u)	+	Noise (u)	+

Note: + = multiple peaks of significant amplitude; -- = no distinct peaks; Irr. = large variations in amplitude; Noise (u) = constant or increasing-with-amplitudes; and Noise (e) = apparent electrical noise.

Table 8

Nondimensional Valve Reducer Wall Pressure Fluctuations

Valve Opening, %	V fps	$\dfrac{V^2}{2g}$ ft	$(P_{max} - P_{min})\Big/\dfrac{V^2}{2g}$			
			PC1	PC4		
25	23.1	8.3	0.29	0.28		
40	32.8	16.7	0.17	0.14		
50	36.6	20.8	0.13	0.23		LL valve Series 1
60	40.4	25.3	0.17	0.17		
70	40.8	25.8	0.17	0.16		
85	45.0	31.4	0.11	0.13		
			PC1	PC4		
25	31.1	15.0	0.05	1.11		
40	40.8	25.8	0.03	0.84		
50	44.5	30.7	0.15	0.14		LL valve Series II
60	47.9	35.6	0.12	0.13		
70	49.6	38.2	0.13	0.13		
85	53.8	44.9	0.15	0.19		
			PC1	PC3	PC4	
25	35.2	19.2	0.14	0.13	0.61	
40	57.0	50.4	0.12	0.07	0.25	
50	66.6	68.8	0.06	0.07	0.15	FC&I valve Series III
60	75.3	88.0	0.06	0.07	0.19	
70	87.4	118.6	0.05	0.06	0.17	
85	100.6	157.2	0.06	0.06	*	

Note: LL valve area = 23.8 ft^2.
FC&I valve area = 33.2 ft^2.
See Table 1 for discharge; Tables 4-6 for pressures.
* Data not recoverable.

Table 9

Nondimensional Vane Pressure Fluctuations

Valve Open-ing, %	V fps	$\frac{V^2}{2g}$ ft	$(P_{max} - P_{min})$ / $\frac{V^2}{2g}$ PUB	PLB	PUD	PLD	
25	23.1	8.3	0.30	0.34	0.41	0.29	
40	32.8	16.7	0.15	0.20	0.24	0.30	
50	36.6	20.8	0.23	0.23	0.32	0.26	LL valve Series I
60	40.4	25.3	0.20	0.17	0.38	0.29	
70	40.8	25.8	0.17	0.18	0.24	0.27	
85	45.0	31.4	0.15	0.17	0.34	0.29	
25	31.1	15.0	0.16	0.14	0.21	0.38	
40	40.8	25.8	0.10	0.13	0.14	0.26	
50	44.5	30.7	0.28	0.17	0.22	0.21	LL valve Series II
60	47.9	35.6	0.29	0.14	0.21	0.20	
70	49.6	38.2	0.21	0.15	0.24	0.19	
85	53.8	44.9	0.19	0.15	0.64	0.18	
25	35.2	19.2	0.11	0.12	*	0.14	
40	57.0	50.4	0.06	0.06		0.06	
50	66.6	68.8	0.07	0.07		0.06	FC&I valve Series III
60	75.3	88.0	0.06	0.06		0.06	
70	87.4	118.6	0.05	0.05		0.05	
85	100.6	157.2	0.05	0.06		0.06	

Note: LL valve area = 23.8 ft^2.
       FC&I valve area = 33.2 ft^2.
       See Table 1 for discharge; Tables 4-6 for pressure.
    * Data not recoverable.

Table 10

Instantaneous Net Vane Pressures

Pressure Transducer	Test No.-Valve Opening in Percent						
	5-25	6-40	12-50	8-60	9-70	10-100	11-85

LL Valve Series I

	5-25	6-40	12-50	8-60	9-70	10-100	11-85
PUB-PLB							
Maximum	9.14	14.32	-4.36	2.89	3.94	7.94	-2.95
PUD-PLD							
Maximum	1.98	5.91	17.07	15.15	13.57	11.05	19.98

- = net pressure down

LL Valve Series II

	15-25	16-40	17-50	18-60	19-70	20-85	21-100
PUB-PLB							
Maximum	5.94	53.17	34.04	36.39	36.95	32.95	29.15
PUD-PLD							
Maximum	17.71	22.06	-7.40	-9.82	-9.72	-23.82	-19.78

- = net pressure down

FC&I Valve Series III

	24-25	25-40	26-50	27-60	28-70	29-85	30-100
PUB-PLB							
Maximum	4.58	-10.03	-10.81	-8.68	-25.16	15.06	-66.66

- = net pressure left

PUD-PLD*

Note: All pressures are in feet of water.
   * PUD was not functioning during the test period; therefore, no
      net pressures were obtained.

Table 11

Peak-to-Peak Valve and Hood Accelerations

Transducer	Units	Test No.-Valve Opening in Percent						
		5-25	7-40	12-50	8-60	9-70	11-85	10-100
		LL Valve Series I						
AHA	Accel, g	0.11	0.05	0.05	0.39	0.03	0.02	0.05
	f_D, Hz	456	492	68	75	67	411	458
	s, $\times 10^{-3}$ in.	*	*	0.10	0.70	0.06	*	*
ATC	Accel, g	0.08	0.07	0.08	0.05	0.06	0.13	0.40
	f_D, Hz	45	46	48	45	46	47	45
	s, $\times 10^{-3}$ in.	0.40	0.30	0.30	0.20	0.60	0.40	1.93
AVC	Accel, g	0.06	0.07	0.06	0.07	0.06	0.08	0.37
	f_D, Hz	44	43	47	43	46	47	48
	s, $\times 10^{-3}$ in.	0.30	0.40	0.30	0.40	0.30	0.40	1.60
AVP	Accel, g	0.11	0.18	0.14	0.15	0.16	0.16	0.45
	f_D, Hz	44	66	66	63	64	47	59
	s, $\times 10^{-3}$ in.	0.60	0.40	0.30	0.40	0.40	0.70	1.30
		LL Valve Test Series II						
		15-25	16-40	17-50	18-60	19-70	20-85	21-100
AHA	Accel, g	0.16	0.70	0.13	0.07	0.12	0.55	0.39
	f_D, Hz	110	111	102	111	102	89	426
	s, $\times 10^{-3}$ in.	0.10	0.60	0.10	0.05	0.10	0.68	0.02
ATC	Accel, g	0.21	0.14	0.18	0.18	0.27	0.23	0.26
	f_D, Hz	46	50	46	50	46	48	50
	s, $\times 10^{-3}$ in.	1.00	0.60	0.80	0.70	1.30	1.00	1.00
AVC	Accel, g	0.21	0.20	0.18	0.18	0.21	0.40	0.47
	f_D, Hz	43	44	45	47	45	45	52
	s, $\times 10^{-3}$ in.	1.30	1.00	0.80	0.80	1.80	1.90	1.70
AVP	Accel, g	0.26	0.25	0.37	0.38	0.39	0.32	0.35
	f_D, Hz	41	45	60	47	45	58	58
	s, $\times 10^{-3}$ in.	1.50	1.10	1.00	1.80	1.80	0.90	1.00
		FC&I Valve Test Series III						
		24-25	25-40	26-50	27-60	28-70	29-85	30-100
AHA	Accel, g	16.00	17.00	17.00	16.00	10.00	12.00	3.00
	f_D, Hz	145	145	159	148	148	148	150
	s, $\times 10^{-3}$ in.	7.20	7.70	6.50	7.40	4.40	5.40	1.30
ATC	Accel, g	0.18	0.30	1.70	2.40	2.70	2.00	4.00
	f_D, Hz	42	43	44	65	45	45	46
	s, $\times 10^{-3}$ in.	1.00	1.60	8.50	5.60	13.00	9.75	18.50
AVC	Accel, g	0.52	0.81	3.40	2.90	4.80	2.50	7.00
	f_D, Hz	66	66	75	74	80	75	71
	s, $\times 10^{-3}$ in.	1.20	1.80	5.90	5.20	7.30	4.30	13.60
AVP	Accel, g	0.70	0.45	2.66	7.43	12.73	6.36	5.80
	f_D, Hz	70	69	67	135	135	188	169
	s, $\times 10^{-3}$ in.	1.40	0.90	5.80	4.00	7.00	1.80	2.00

Note: f_D = dominant frequency, Hz; s = displacement. $s = \dfrac{(386 \text{ in./sec}^2/g)(\text{Accel, g})}{(2\pi f_D)}$

* Values are less than 0.01×10^{-3} in.

Table 12

Overview of Acceleration FFT Data

Test No.-Valve Opening in Percent

LL Valve Series I

Trans-ducer	5-25 Nature	Other Peaks, Hz	7-40 Nature	Other Peaks, Hz	12-50 Nature	Other Peaks, Hz	8-60 Nature	Other Peaks, Hz	9-70 Nature	Peaks, Hz	11-85 Nature	Peaks, Hz	10-100 Nature	Peaks, Hz
ATC	45+	355	46+	155, 330	48+	155, 330	45+	155, 235, 335	46+	--	47+	405	Noise (u)	45, 155, 440
AVC	44+	--	43+	--	47+	155	43+	155	46+	--	47+	160	Noise (u)	48, 235, 400
AVP	44+	65	66+	155, 370	66+	45, 155, 325	63+	45, 335	63+	45, 360	47+	160, 330	59+	335
AMA	Noise (u)	465	Noise (u)	300, 495	Noise (u)	70, 470	Noise (u)	70, 500	Noise (u)	70, 395	Noise (u)	65, 410	Noise (u)	520

LL Valve Series II

Trans-ducer	15-25 Nature	Other Peaks, Hz	16-40 Nature	Other Peaks, Hz	17-50 Nature	Other Peaks, Hz	18-60 Nature	Other Peaks, Hz	19-70 Nature	Peaks, Hz	20-85 Nature	Peaks, Hz	21-100 Nature	Peaks, Hz
ATC	46+	150,320	50+	150	45+	150	Irr.	50, 150		145, 340	48+	415	50+	455
AVC	43+	--	43+	--	44+	150	47+	--	45+	--	45+	150, 385	Noise (u)	52, 285
AVP	Irr.	61	45+	370	60+	45, 150, 375	47+	65, 370	45+	330	58+	150, 330	58+	155, 330
AMA	Noise (u)	110, 460	Noise (u)	110, 455	Noise (u)	105, 445	Noise (u)	110, 430	Noise (u)	100, 400	Noise (u)	90, 420	Noise (u)	120, 430

FG&I Valve Series III

Trans-ducer	24-25 Nature	Other Peaks, Hz	25-40 Nature	Other Peaks, Hz	26-50 Nature	Other Peaks, Hz	27-60 Nature	Other Peaks, Hz	28-70 Nature	Peaks, Hz	29-85 Nature	Peaks, Hz	30-100 Nature	Peaks, Hz
ATC	Noise (u)	40, 310	Noise (u)	43, 140	Noise (u)	44, 64, 310	Noise (u)	45, 65, 314	Noise (u)	45, 310	Noise (u)	45, 190, 340	Noise (u)	46, 165
AVC	66+	45	66+	45	Irr.	75	Irr.	74, 180	80+	42, 165	75+	45	Noise (u)	45, 71, 190
AVP	Irr.	41, 70, 190	Irr.	44, 69	Irr.	42, 67, 130	Irr.	135	Irr.	135	Irr.	60, 115, 185	Irr.	45, 169
AMA	Irr.	145, 190, 495	Irr.	145, 485	Irr.	144, 160, 475	Irr.	148, 185	Irr.	148, 485	Irr.	148, 255	Irr.	155

Note: + = distinct frequency at a large amplitude of FFT component.
-- = no other distinct peaks present.
Noise (u) = constant or increasing-with-frequency amplitudes.
Irr. = large variations in amplitude.

Table 13
Instantaneous Net Torsional Acceleration
AVP-AVC

	Test No.-Valve Opening in Percent			
	LL Valve Series I			
	5-25	7-40	8-60	11-85
Max. torsional accel, g	0.414	0.690	-0.712	-0.744
f_D, Hz	44	66	63	47
s, $\times 10^{-3}$ in.	2.10	1.50	-1.80	-3.30
	LL Valve Series II			
	15-25	16-40	18-60	20-85
Max. accel, g	0.063	0.052	0.872	0.217
f_D, Hz	41	45	47	58
s, $\times 10^{-3}$ in.	0.40	0.20	3.90	0.60
	FC&I Valve Series III			
	24-25	25-40	27-60	29-85
Max. accel, g	-2.118	-1.530	-1.142	-1.006
f_D, Hz	70	69	56	188
s, $\times 10^{-3}$ in.	-4.20	-3.10	-0.60	-0.30

Note: + = net acceleration acting in a counterclockwise direction (looking at the valve in a downstream direction); - = net acceleration acting in a clockwise direction.

Table 14

Strain Measurements

Strain	Item	5-25	7-40	12-50	8-60	9-70	11-85	10-100
				Test No.-Valve Opening in Percent				

LL Valve Series I

Strain	Item	5-25	7-40	12-50	8-60	9-70	11-85	10-100
ε_1	P/P	12.4	11.0	14.5	12.2	16.4	12.5	25.0
(axial)	f_D	2.0	3.9	7.8	2.0	10.7	5.8	5.9
ε_2	P/P	11.0	12.5	--	14.0	--	18.0	27.3
(bending)	f_D	2.0	2.0	--	7.8	--	2.0	2.0

LL Valve Series II

Strain	Item	15-25	16-40	17-50	18-60	19-70	20-85	21-100
ε_1	P/P	15.3	18.2	11.8	47.1	12.6	21.5	39.2
(axial)	f_D	2.8	5.0	1.0	1.0	1.0	2.8	1.0
ε_2	P/P	32.6	28.4	13.6	25.0	10.9	45.4	26.1
(bending)	f_D	6.2	17.0	6.2	12.5	9.7	10.2	6.2

FC&I Valve Series III

Strain	Item	24-25	25-40	26-50	27-60	28-70	29-85	90-100
ε_1	P/P	13.1	15.9	23.0	39.7	14.6	2.0	1.8
(axial)	f_D	<20	<20	<20	<20	<20	120.0	120.0
ε_2 (bending)		Gage destroyed; no data obtained						

Note: All strain measurements are in microinches/inch. P/P = greatest peak-peak strain; f_D = dominant frequency, Hz; -- = data not recoverable.

Table 15

Strain Gage FFT Data Summary

Strain	Test No.-Valve Opening in Percent													
	5-25		7-40		6-50		8-60		9-70		11-85		10-100	
	f_D	Peaks, Hz	f_D	Peaks, Hz	f_D	Peaks, Hz	f_D	Peaks, Hz	f_D	Peaks, Hz	f_D	Peaks, Hz	f_D	Peaks, Hz
LL Valve Series I														
ε_1 (axial)	<20	160, 240, 270	<20	160	<20	77, 155	<20	160, 235, 270	<20	80, 155, 270	<20	78, 270, 460	<20	105, 155, 270, 340
ε_2 (bending)	<20	150, 240, 275, 450	<20	65, 160, 435	<20	160	<20	155, 230, 260, 445	<20	80	<20	--	<20	60, 105
	15-25		16-40		17-50		18-60		19-70		20-85		21-100	
	f_D	Peaks, Hz	f_D	Peaks, Hz	f_D	Peaks, Hz	f_D	Peaks, Hz	f_D	Peaks, Hz	f_D	Peaks, Hz	f_D	Peaks, Hz
LL Valve Series II														
ε_1 (axial)	<20	--	<20	160, 180	<20	180, 230	<20	210	<20	180, 230	<20	160, 180	<20	180, 230, 460
ε_1 (bending)	<20	160, 180	<20	180	<20	--	<20	180	<20	180	<20	160, 180	<20	60, 180
	24-25		25-40		26-50		27-60		28-70		29-85		30-100	
	f_D	Peaks, Hz	f_D	Peaks, Hz	f_D	Peaks, Hz	f_D	Peaks, Hz	f_D	Peaks, Hz	f_D	Peaks, Hz	f_D	Peaks, Hz
FC&I Valve Series III														
ε_1 (axial)	<15	155, 180, 230, 460	<15	180, 300	<15	60, 180, 300	<15	160, 180, 230, 300	<15	180, 300	Electrical noise		Electrical noise	

Note: f_D = predominant frequency, Hz; -- = no other distinct peaks present.
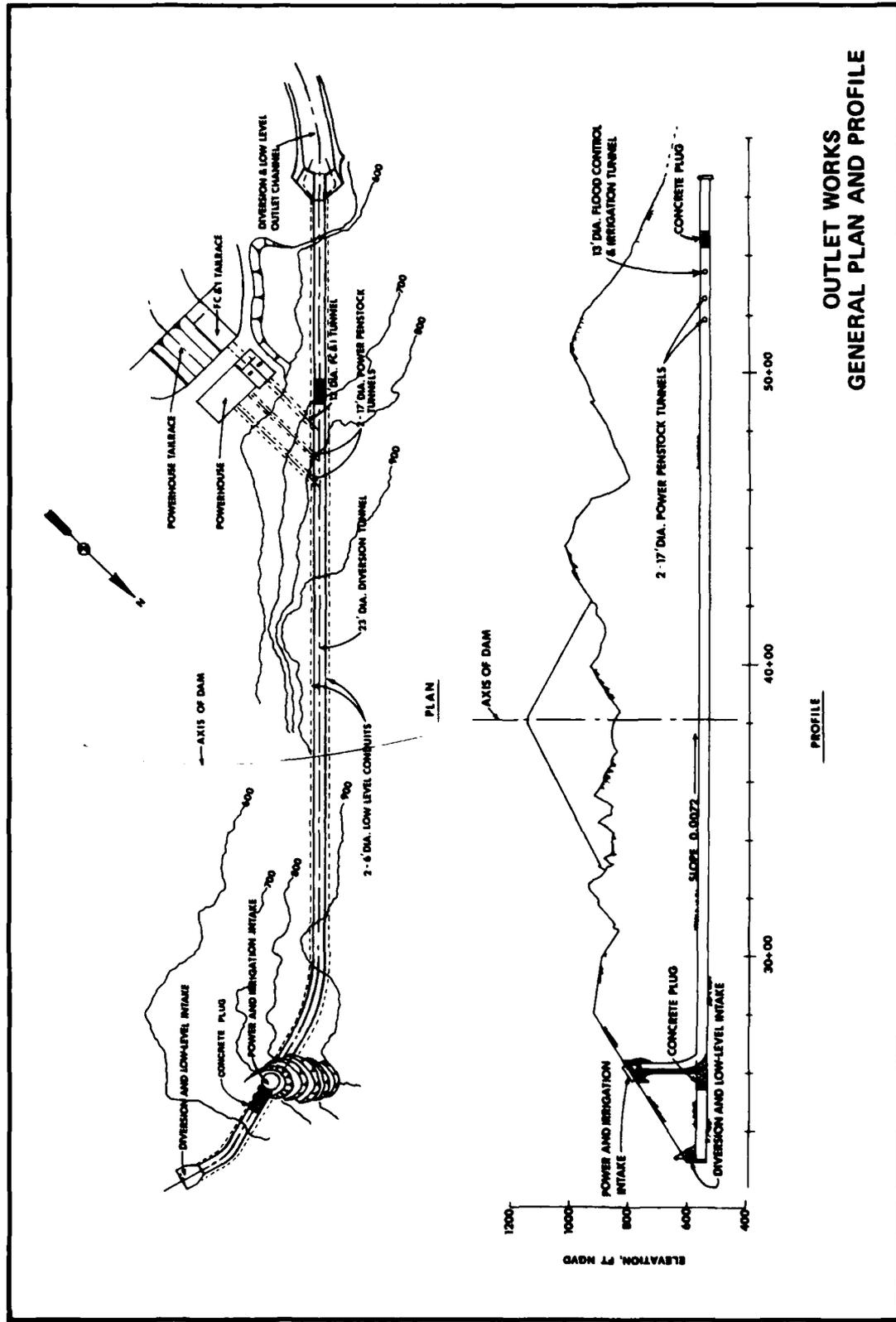
OUTLET WORKS
GENERAL PLAN AND PROFILE

PLATE 1

VALVE AND HOOD
INSTRUMENTATION
66-IN. LOW-LEVEL VALVE

PHC

HOOD

4' 6"

2' 3/4"

PHB
AHA

NO SCALE

STA 60 + 21.50

AVP

ATC
AVC

ACCELEROMETER
CABLE HOLE

€A, €B
PLB
PUB
CONE

PUD PLD
10 30 VANE

PC1 (12 00)

FLOW

O PC4 (9 00)
O PC2 (3 00)

PC3 (6 00)

€ EL 532.0

LEGEND

PC1 - PC4 - CONDUIT PRESSURE TRANSDUCERS
PUB, PLB - PUD, PLD - VANE PRESSURE TRANSDUCERS (10 30 VANE)
€A-€B - VANE STRAIN GAGES (10 30 VANE)
ATC - AVC - AVP - VALVE ACCELEROMETERS
PHB - HOOD PRESSURE TRANSDUCER
PHC - HOOD JET PRESSURE TRANSDUCER
AHA - HOOD ACCELEROMETER

PLATE 2

VALVE AND HOOD
INSTRUMENTATION
78-IN. FLOOD CONTROL AND
IRRIGATION VALVE
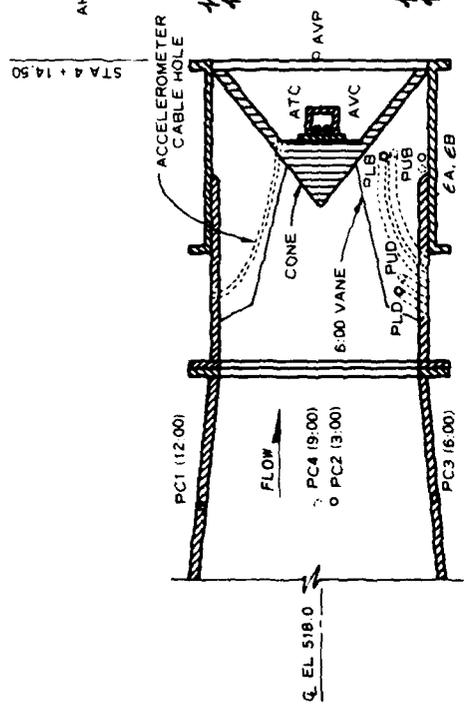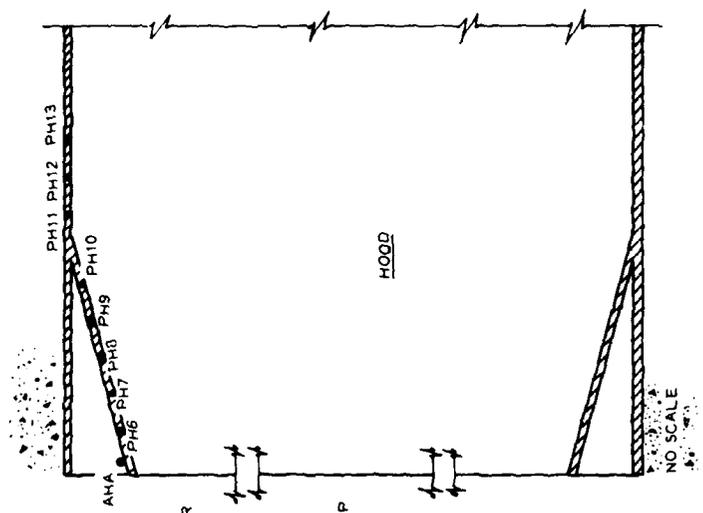
LEGEND

PC1-PC4 - CONDUIT PRESSURE TRANSDUCERS
PUD, PLD-PUB, PLB - VANE PRESSURE TRANSDUCERS (6:00 VANE)
ЄA, ЄB - VANE STRAIN GAGES (6:00 VANE)
ATC, AVC, AVP - VALVE ACCELEROMETERS
PH6 - PH13 - HOOD JET PRESSURE TRANSDUCERS
AHA - HOOD ACCELEROMETER
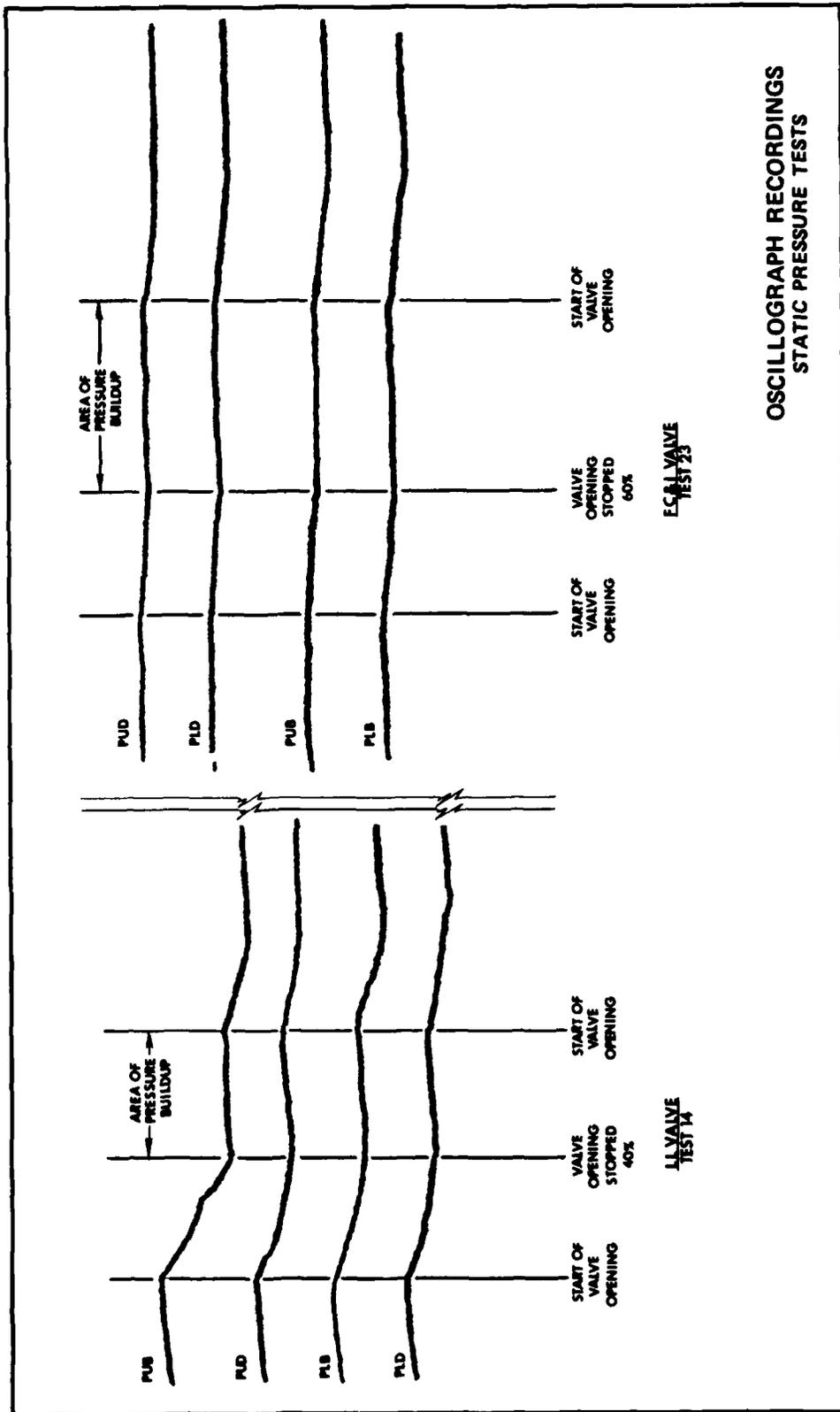
PLATE 3

OSCILLOGRAPH RECORDINGS
STATIC PRESSURE TESTS

PLATE 4
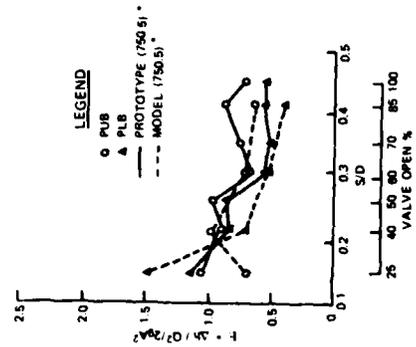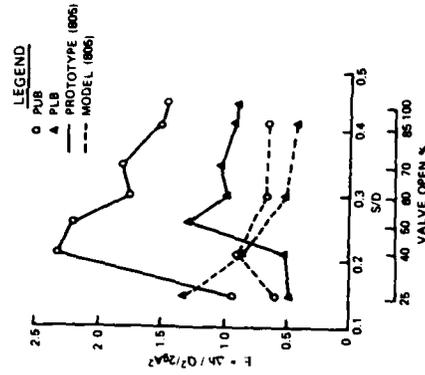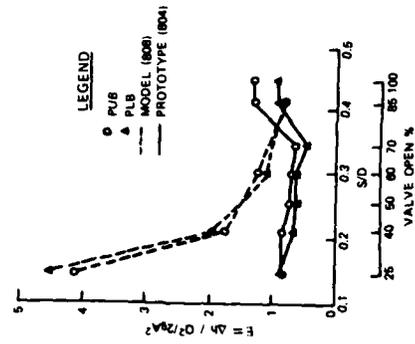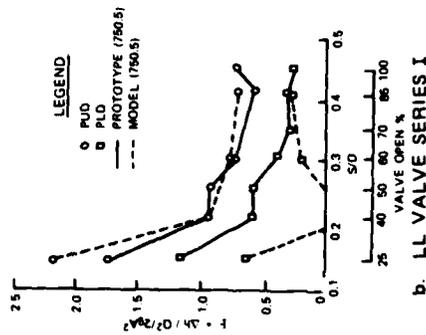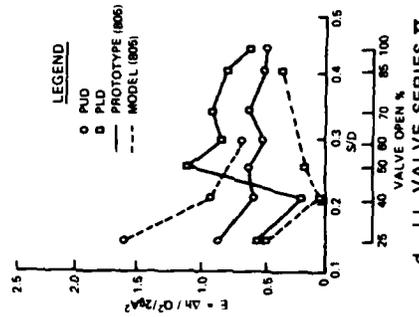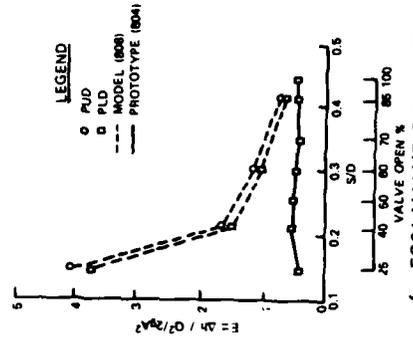
MODEL-PROTOTYPE
EULER NUMBER COMPARISON

PLATE 5
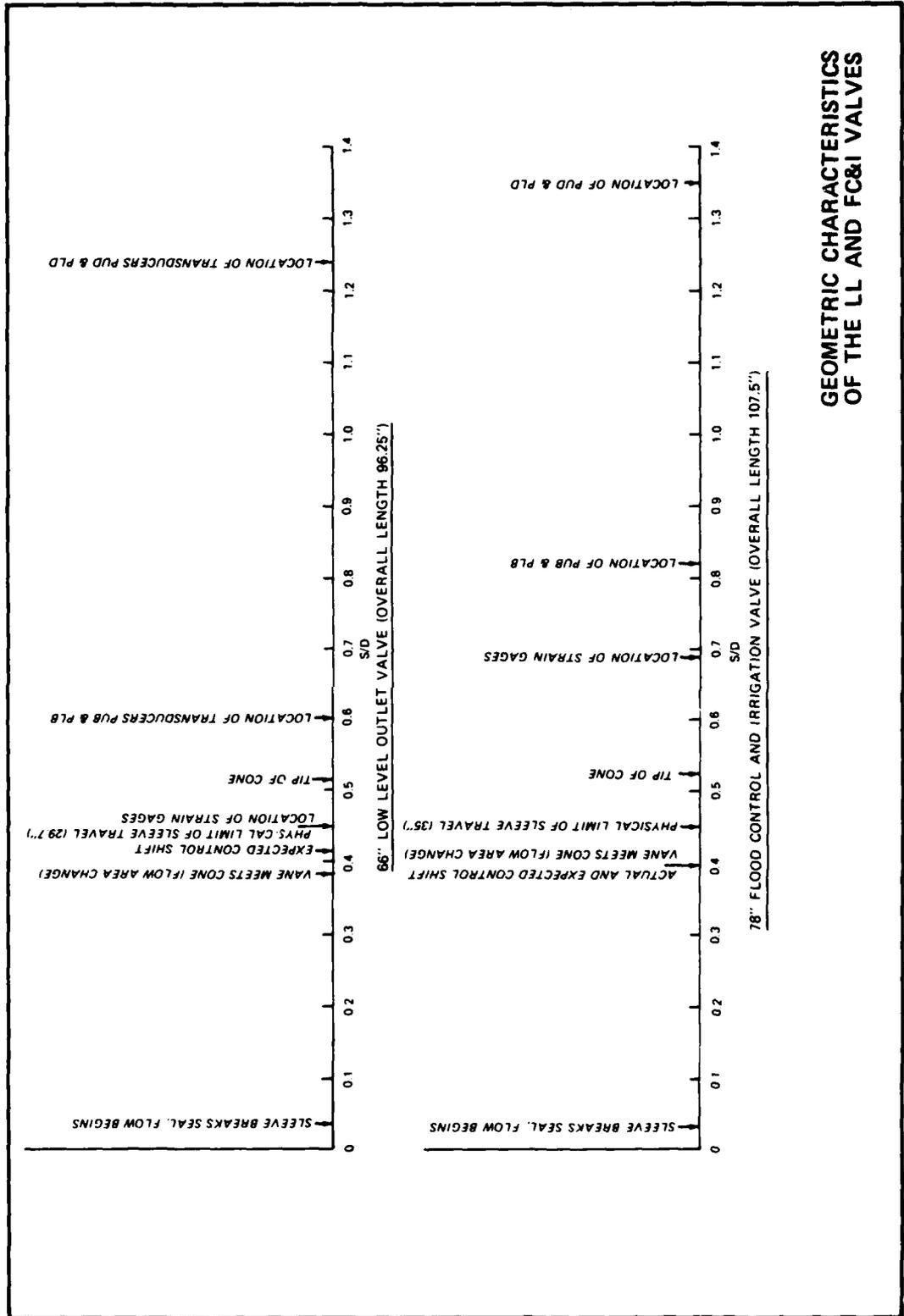
GEOMETRIC CHARACTERISTICS OF THE LL AND FC&I VALVES
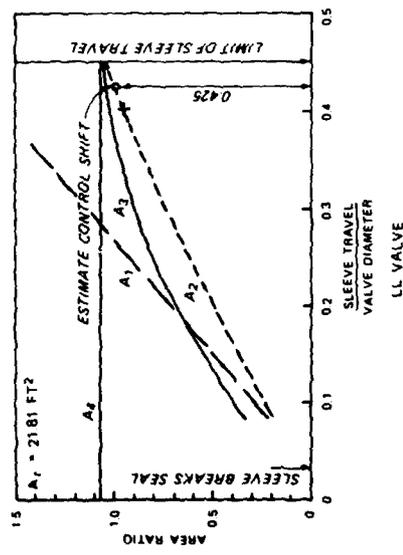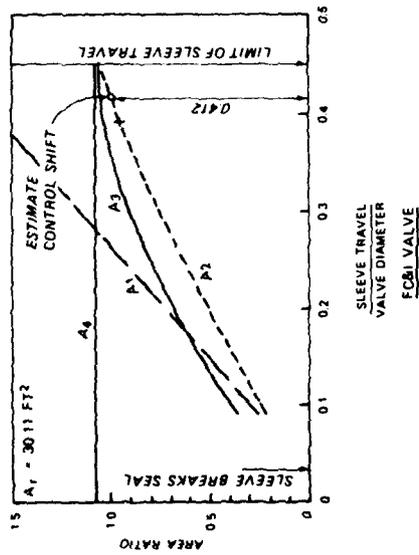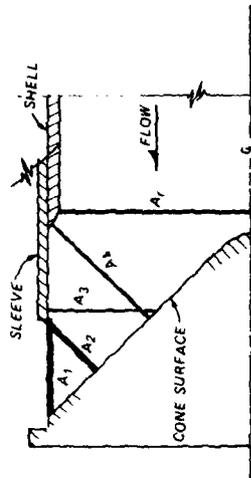
66" LOW LEVEL OUTLET VALVE (OVERALL LENGTH 96.25")

SLEEVE BREAKS SEAL. FLOW BEGINS
VANE MEETS CONE (FLOW AREA CHANGE)
EXPECTED CONTROL SHIFT
PHYSICAL LIMIT OF SLEEVE TRAVEL (29.7")
LOCATION OF STRAIN GAGES
TIP OF CONE
LOCATION OF TRANSDUCERS PUB & PLB
LOCATION OF TRANSDUCERS PUD & PLD
S/D

78" FLOOD CONTROL AND IRRIGATION VALVE (OVERALL LENGTH 107.5")

SLEEVE BREAKS SEAL. FLOW BEGINS
ACTUAL AND EXPECTED CONTROL SHIFT
VANE MEETS CONE (FLOW AREA CHANGE)
PHYSICAL LIMIT OF SLEEVE TRAVEL (35")
TIP OF CONE
LOCATION OF STRAIN GAGES
LOCATION OF PUB & PLB
LOCATION OF PUD & PLD
S/D

PLATE 6
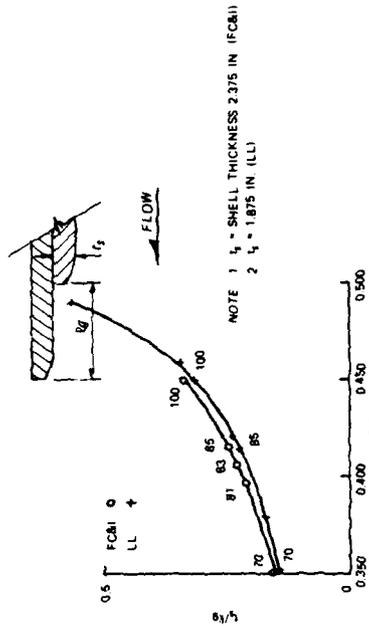
FLOW PASSAGE AREAS
OF LL AND FC&I VALVES

PLATE 7
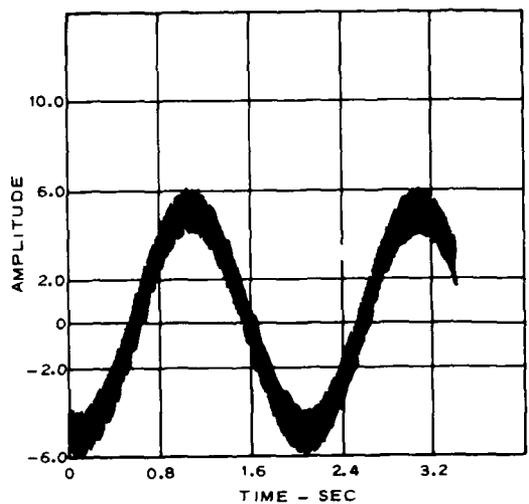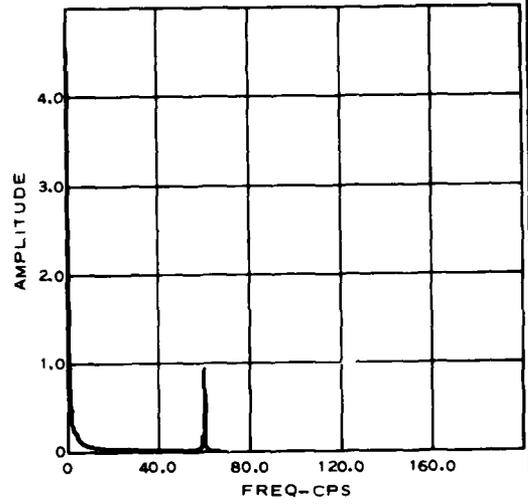
Time-History Plot   FFT Plot

UNFILTERED DATA
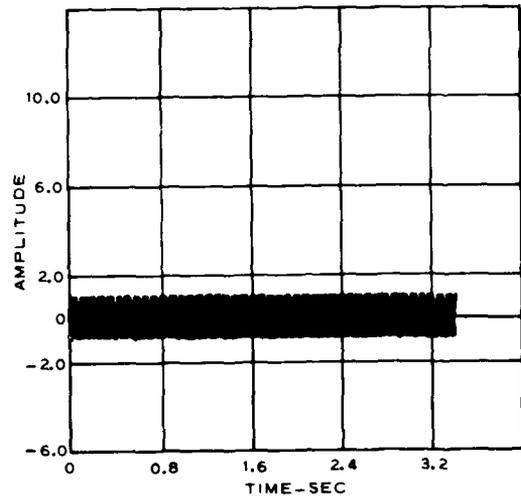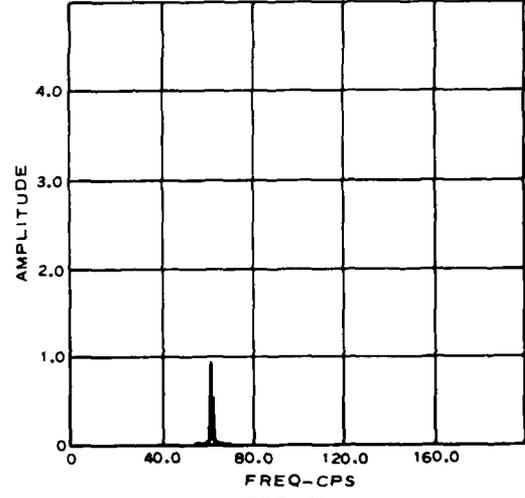
Time-History Plot   FFT Plot

FILTERED DATA

REMOVAL OF LOW FREQUENCY
BY FILTERING TECHNIQUES

PLATE 8

VALVE REDUCER WALL
PRESSURE FLUCTUATIONS

PLATE 9

VANE PRESSURE FLUCTUATIONS

PLATE 10
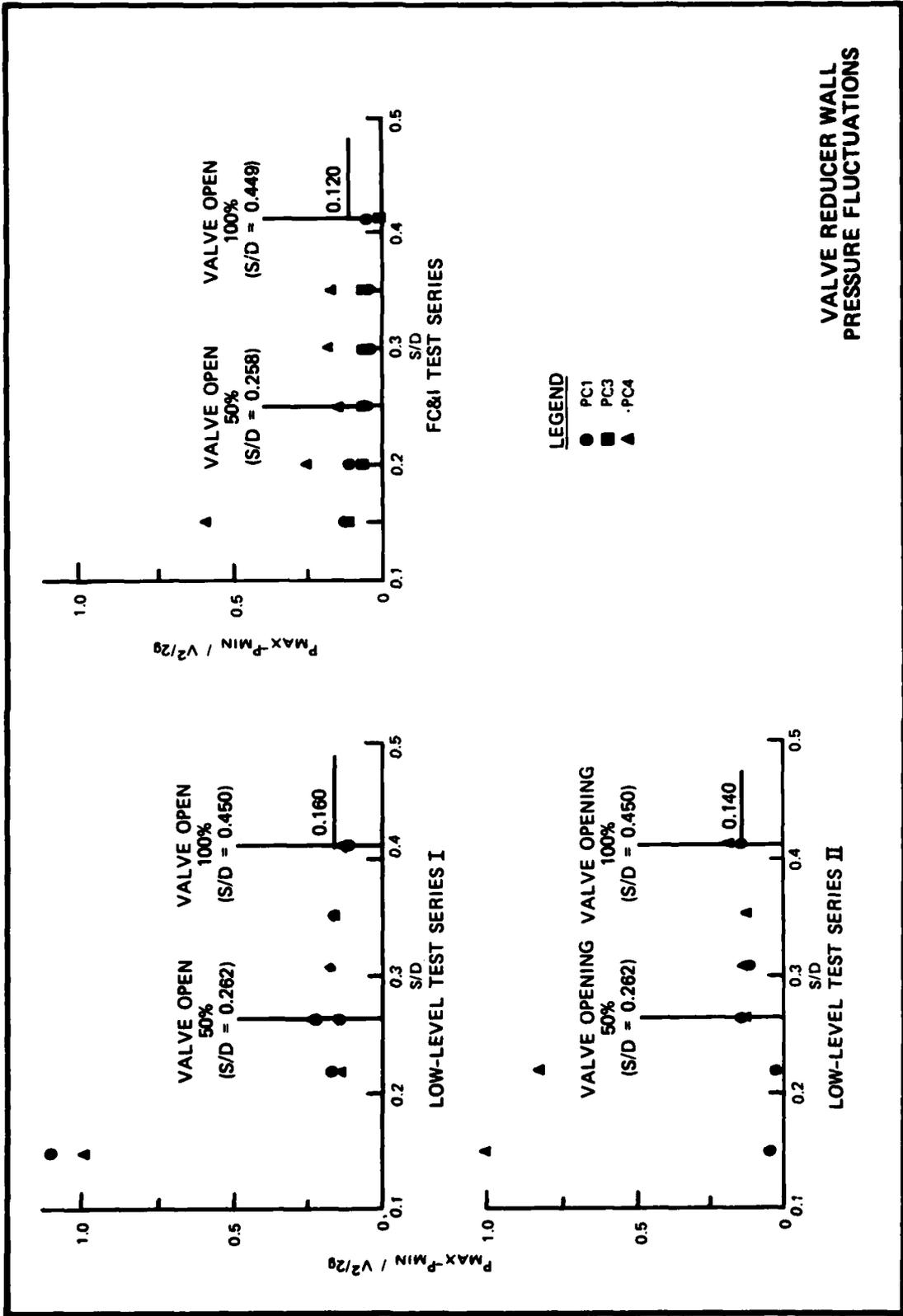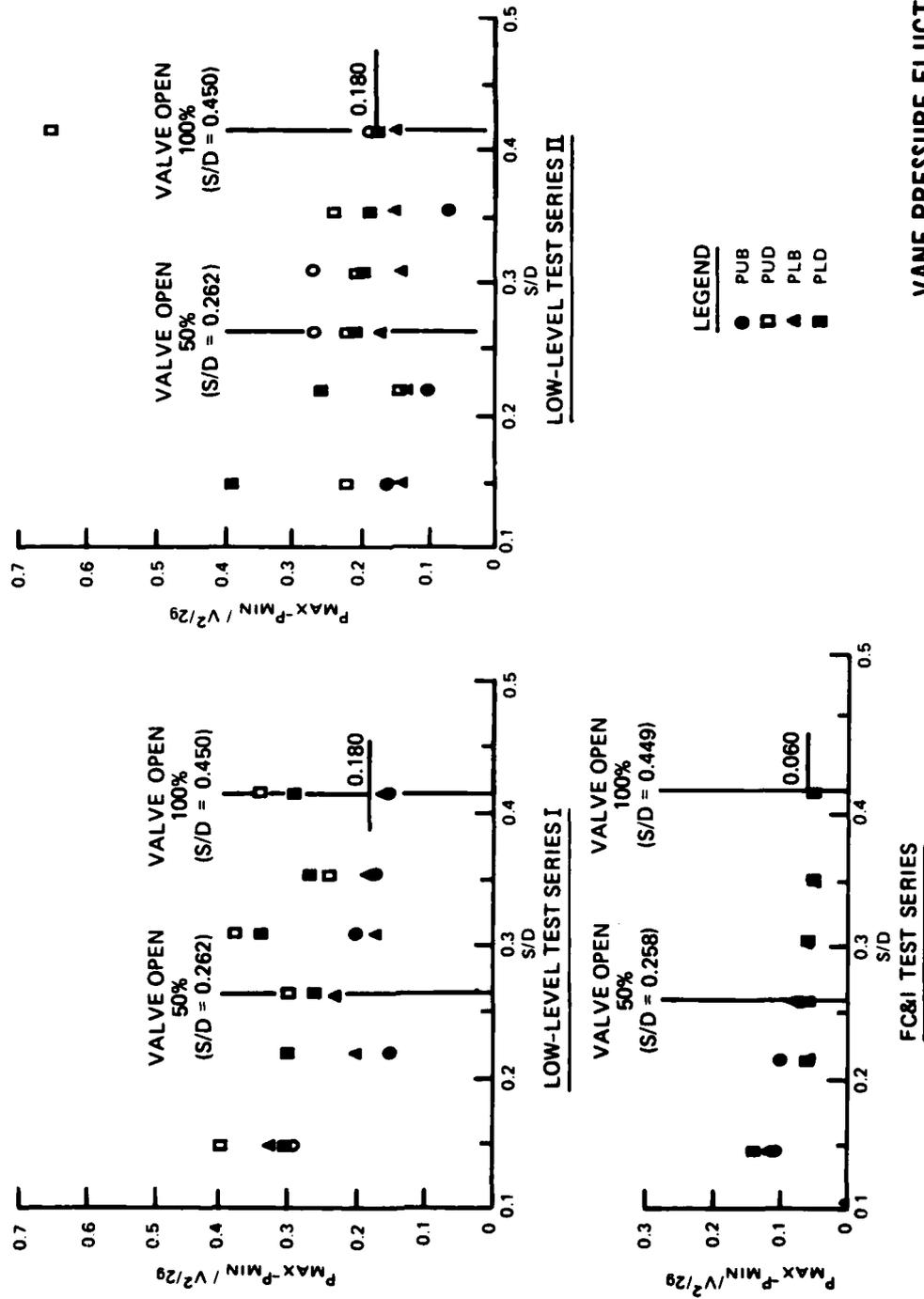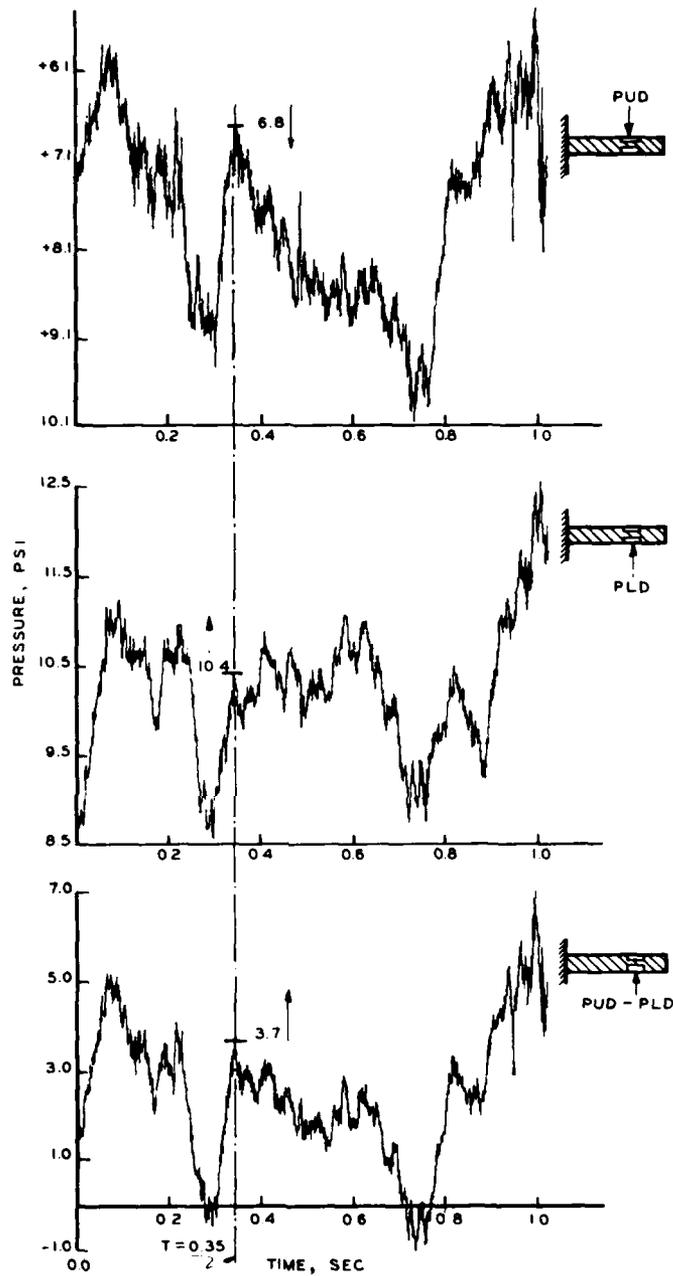
10:30 TEST VANE PRESSURES
LOW-LEVEL SERIES I
TEST 2, 85 PERCENT VALVE OPENING
S/D 0.421
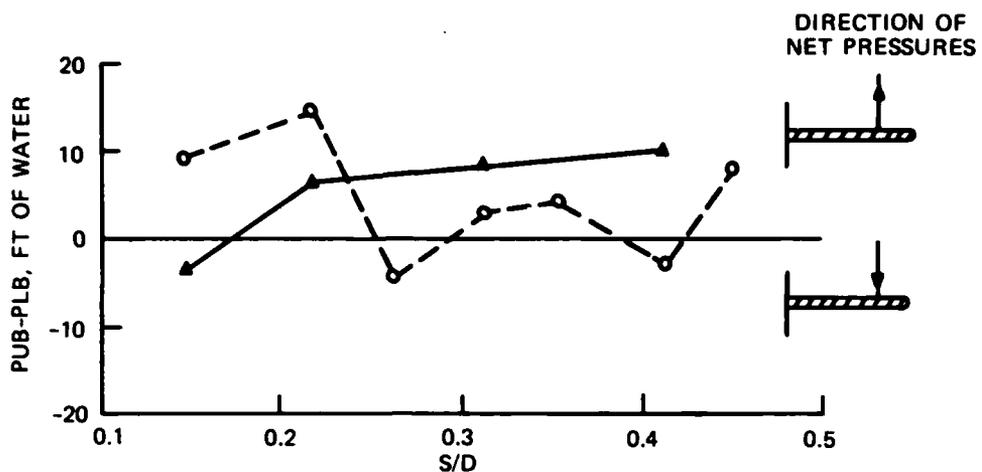
PLATE 11

DIFFERENTIAL VANE PRESSURES
MODEL VS PROTOTYPE
LL VALVE SERIES I AND II
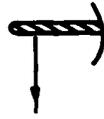
PLATE 12

DIFFERENTIAL VANE PRESSURES
MODEL VS PROTOTYPE
FC&I VALVE SERIES III

PLATE 13

ACCELEROMETERS AVP AND AVC
TEST NO. 18
60 PERCENT VALVE OPENING (S/D = 0.308)
LL VALVE TEST SERIES II

* NOTE DIFFERENCE IN VERTICAL SCALES
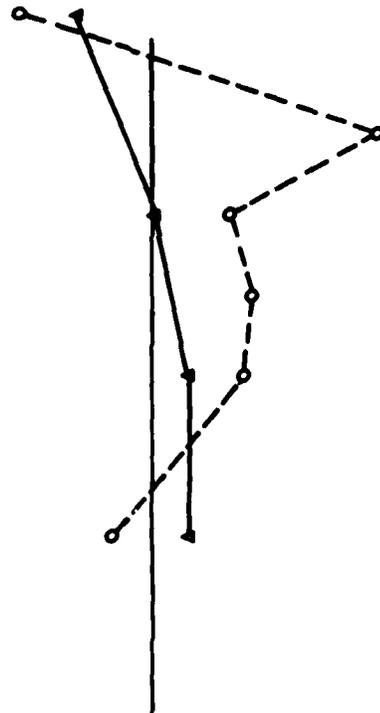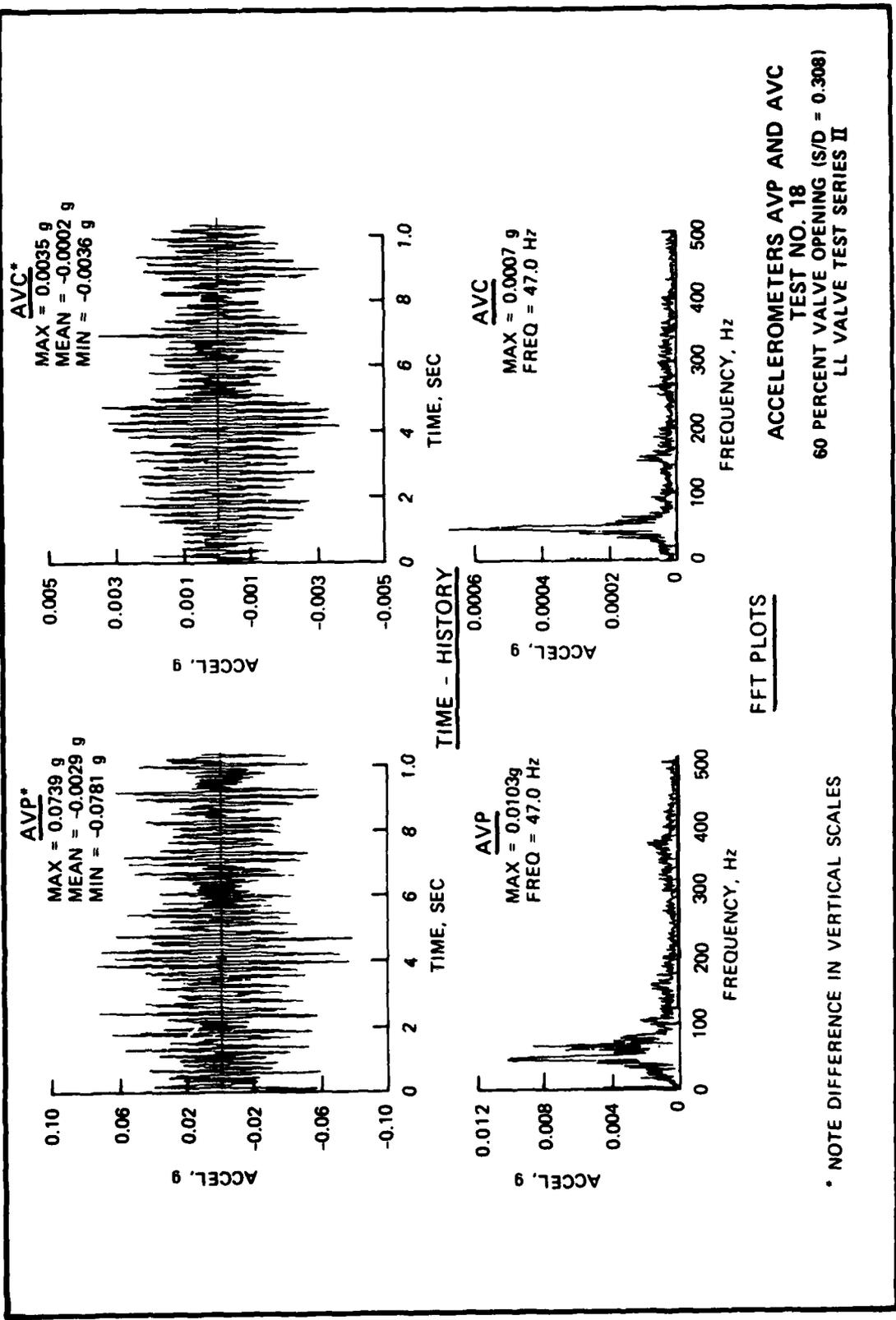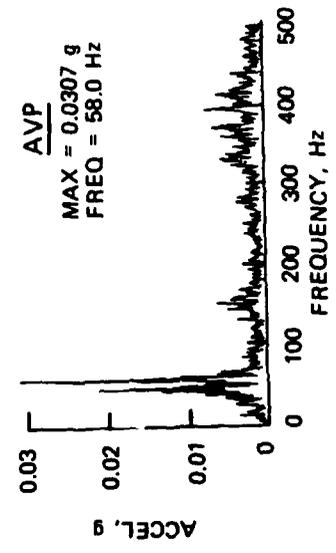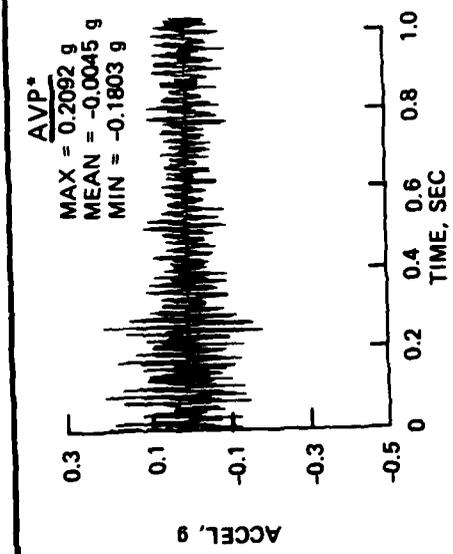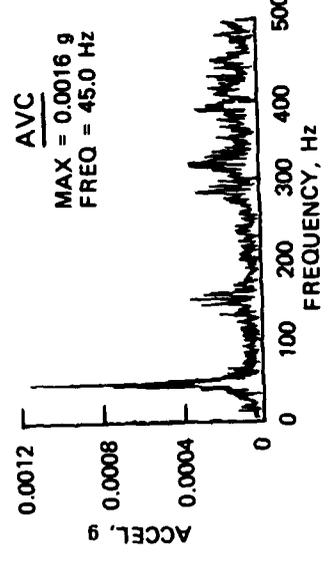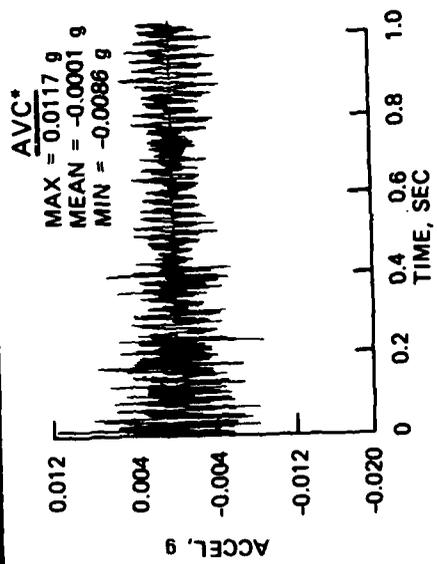
PLATE 14

ACCELEROMETERS AVP AND AVC
TEST NO. 20
85 PERCENT VALVE OPENING (S/D = 0.421)
LL VALVE TEST SERIES II

*NOTE DIFFERENCE IN VERTICAL SCALES

PLATE 15

SAMPLE OSCILLOGRAM
DURING CONTROL SHIFT
TEST NO. 22
FC&I VALVE
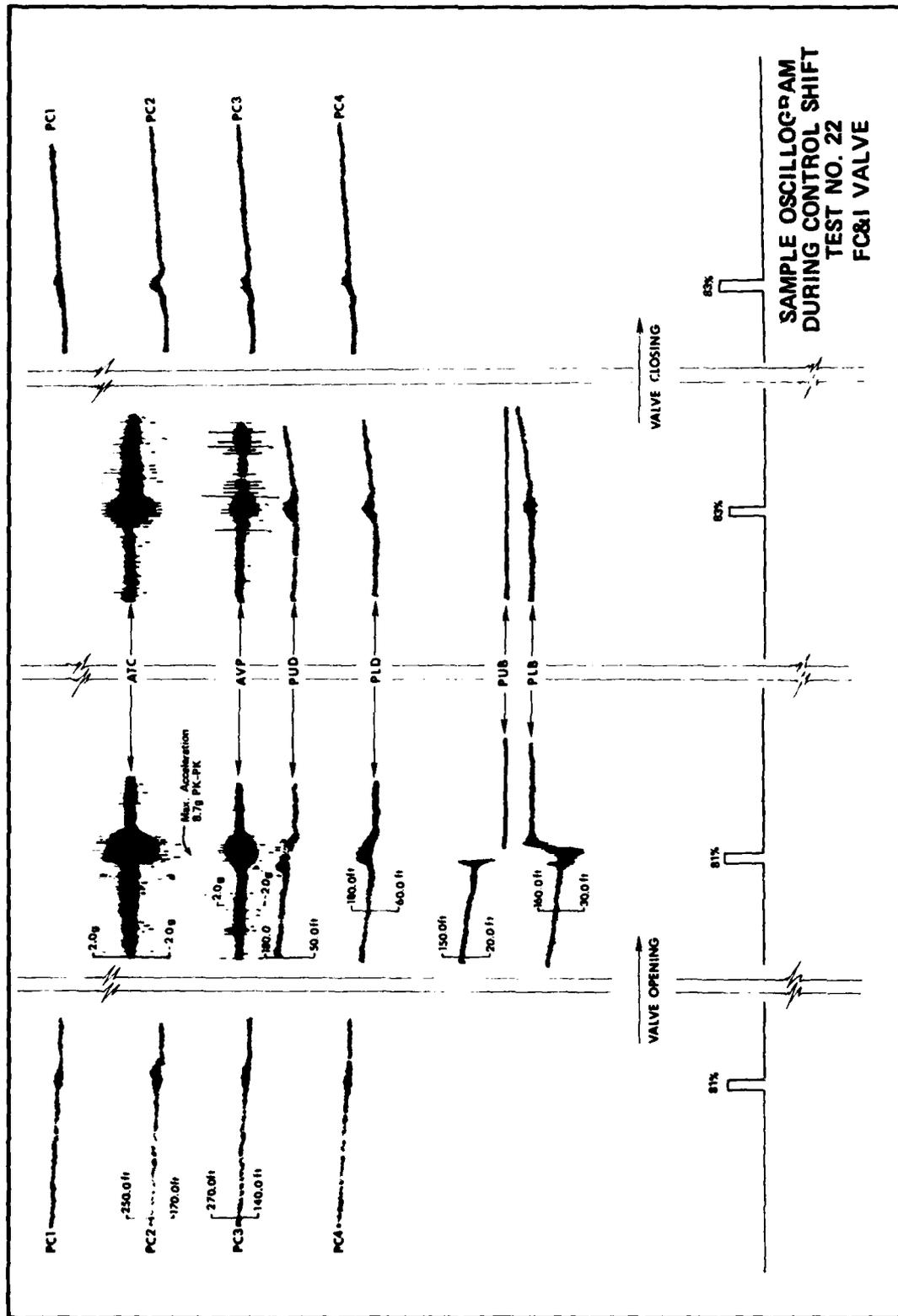
PLATE 16
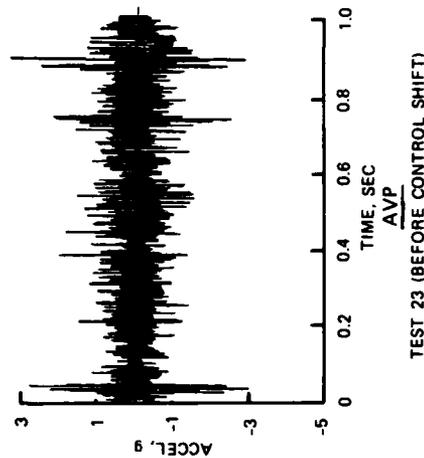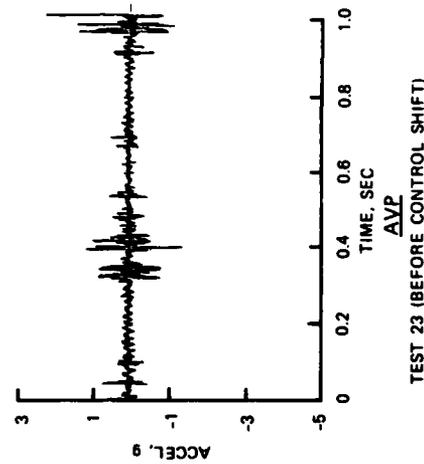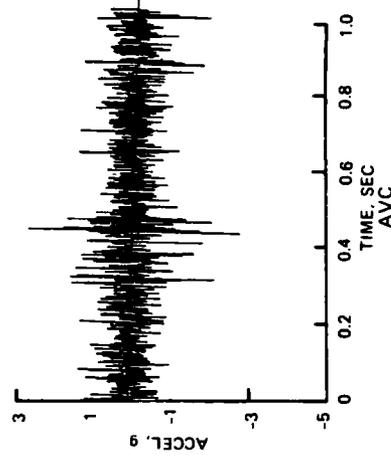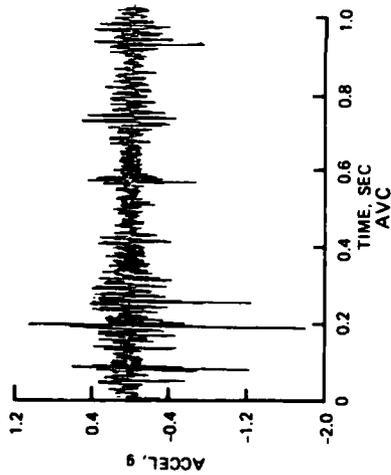
FC&I VALVE ACCELERATIONS
TIME-HISTORY PLOTS
ACCELEROMETERS AVC AND AVP
BEFORE AND DURING CONTROL SHIFT
81-83 PERCENT VALVE OPENING
SERIES III

PLATE 17
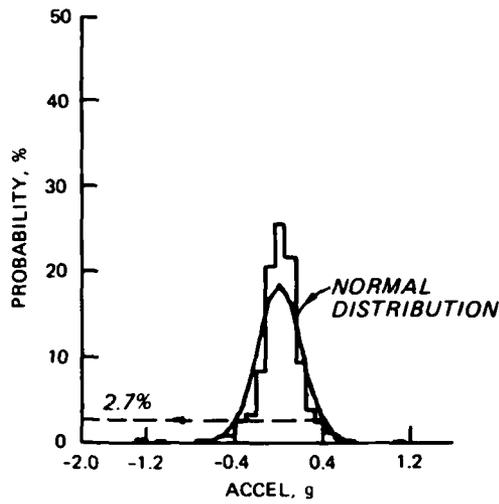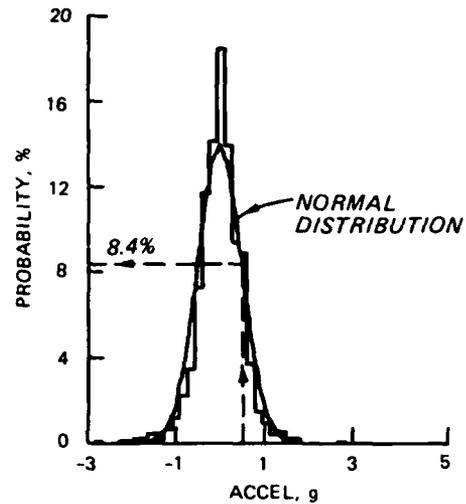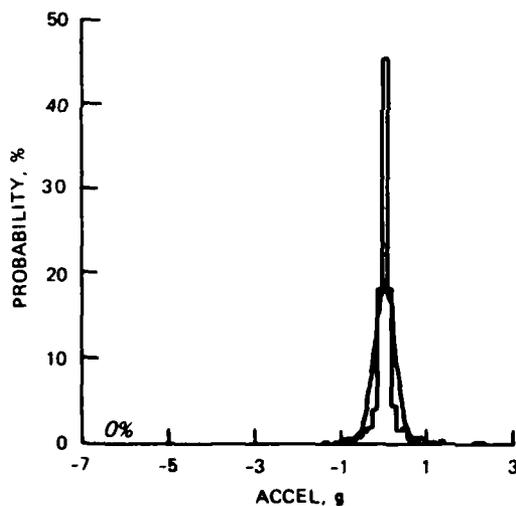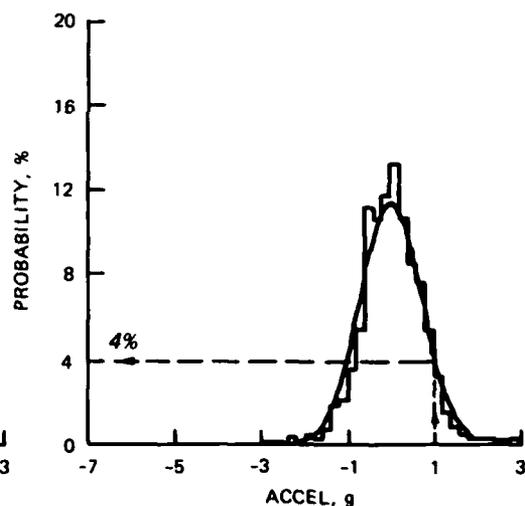
FC&I VALVE ACCELERATION
PROBABILITY DISTRIBUTION
TRANSDUCERS AVC AND AVP
BEFORE AND DURING CONTROL SHIFT
81–83 PERCENT VALVE OPENING
SERIES III

PLATE 18
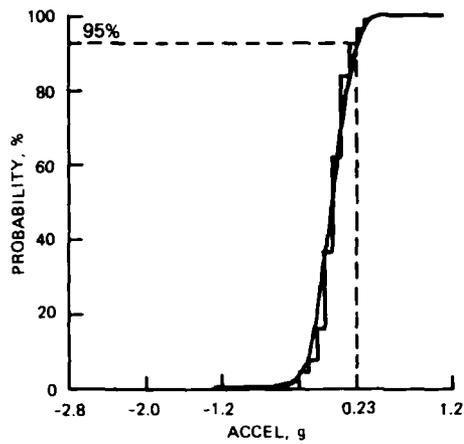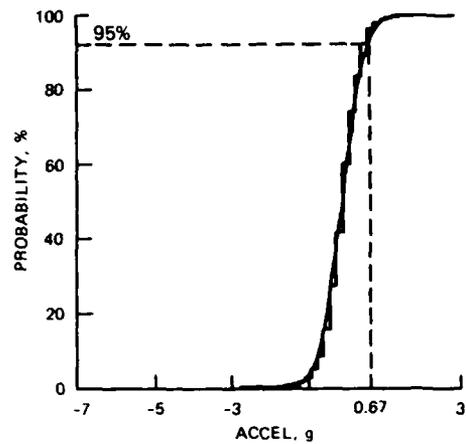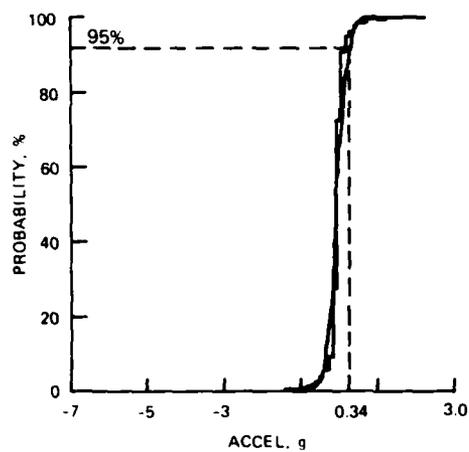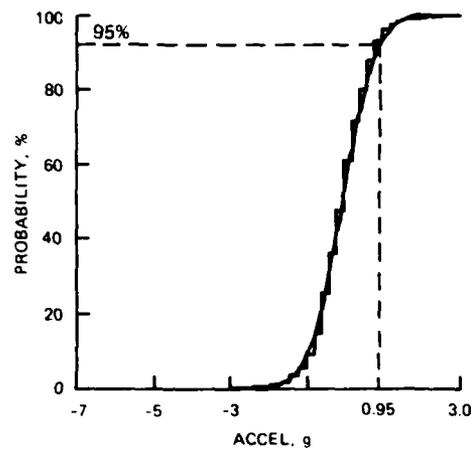
AMPLITUDE CUMULATIVE
DISTRIBUTION FUNCTIONS
ACCELEROMETERS AVC AND AVP
BEFORE AND DURING
FLOW-CONTROL SHIFT
SERIES III

PLATE 19

POWER SPECTRUM

TEST NO. 23	MAX = 0.0047821	RATE = 1000
CH NO 1		POINTS = 103
PC1	FREQ = 8.78906	RMS = 0.55508

POWER SPECTRUM

TEST NO. 23	MAX = 0.0008642	RATE = 1000
CH NO 10	DOF = 9	POINTS = 103
AVC	FREQ = 67.38281	RMS = 0.19178

CROSS SPECTRUM

TEST NO. 23	MAX = 0.0006318	RATE = 1000
CH NO 1 & 10	DOF = 9	POINTS = 103
PC1 x AVC	FREQ = 78.12500	RMS = 0.55508

SPECTRAL DENSITY PLOTS
PRESSURE AND ACCELERATION
FC&I VALVE
PRIOR TO CONTROL SHIFT
TRANSDUCERS PC1 AND AVC

PLATE 20

MICROCOPY RESOLUTION TEST CHART
NATIONAL BUREAU OF STANDARDS-1963-A

POWER SPECTRUM

TEST NO 23   MAX = 0.0022623   RATE = 1000
CH NO 6   DOF = 9   POINTS = 103
PUB   FREQ = 156.25000   RMS = 0.55677

POWER SPECTRUM

TEST NO 23   MAX = 0.0010648   RATE = 1000
CH NO 12   DOF = 9   POINTS = 103
AVP   FREQ = 100.42968   RMS = 0.23294

CROSS SPECTRUM

TEST NO 23   MAX = 0.0007178   RATE = 1000
CH NO 6 & 12   DOF = 9   POINTS = 103
PUB AVP   FREQ = 156.25000   RMS = 0.55677

SPECTRAL DENSITY PLOTS
PRESSURE AND ACCELERATION
FC&I VALVE
PRIOR TO CONTROL SHIFT
TRANSDUCERS PUB AND AVP

PLATE 21

POWER SPECTRUM

TEST NO. 23   MAX = 0.0014002   RATE = 1000
CH NO 1   DOF = 9   POINTS = 103
PC1   FREQ = 86.91406   RMS = 1.74571

POWER SPECTRUM

TEST NO. 23   MAX = 0.0021861   RATE = 1000
CH NO 10   DOF = 9   POINTS = 103
AVC   FREQ = 226.56250   RMS = 0.43770

CROSS SPECTRUM

TEST NO. 23   MAX = 0.0052991   RATE = 1000
CH NO 1 & 10   DOF = 9   POINTS = 103
PC1 & AVC   FREQ = 84.95093   RMS = 1.74571

**SPECTRAL DENSITY PLOTS
PRESSURE AND ACCELERATION
FC&I VALVE
DURING CONTROL SHIFT
TRANSDUCERS PC1 AND AVC**

PLATE 22

POWER SPECTRUM

TEST NO. 23	MAX = 0.4645805	RATE = 1000
CH NO 6	DOF = 9	POINTS = 103
PUB	FREQ = 95.70312	RMS = 7.68935

POWER SPECTRUM

TEST NO. 23	MAX = 0.0162704	RATE = 1000
CH NO 12	DOF = 9	POINTS = 103
AVP	FREQ = 97.65625	RMS = 0.68928

CROSS SPECTRUM

TEST NO. 23	MAX = 0.0475902	RATE = 1000
CH NO 6 & 12	DOF = 9	POINTS = 103
PUB AVP	FREQ = 96.67968	RMS = 7.68935

SPECTRAL DENSITY PLOTS
PRESSURE AND ACCELERATION
FC&I VALVE
DURING CONTROL SHIFT
TRANSDUCERS PUB AND AVP

PLATE 23

APPENDIX A: NOTATION

A	Cross-sectional area of flow passage at valve intake, ft^2
A_r	Minimum area in the valve body, ft^2
A_R	Flow passage cross-sectional area at station corresponding to h_R , ft^2
A_1	Transverse area of a cylinder, ft^2
A_2	Transverse area of a truncated cone and the minimum flow passage area at the sleeve lip, ft^2
A_3	Surface area of an annular ring, ft^2
A_4	Transverse area of a truncated cone, ft^2
c	Flow width of jet, ft
C	Valve discharge coefficient
C_v	Dimensionless valve coefficient
C_{ED}	Flow coefficient for flow passage downstream of PC4, $ft^{5/2}/sec$
C_{EU}	Flow coefficient for the flow passage upstream of PC4, $ft^{5/2}/sec$
D	Valve diameter, in.
E	Young's modulus of elasticity, psi
f	Strouhal number frequency, Hz
f_D	Predominant frequency, Hz
FC&I	Flood control and irrigation valve
g	Acceleration due to gravity, ft/sec^2
h_R	Piezometric head in the conduit, ft
h_4	Piezometric head at transducer PC4, ft
H_{net}	Net total head at valve intake, ft
H_L	Head loss, ft
H_T	Total head at conduit intake, ft
k	Upstream conduit loss coefficient
LL	Low-level valve
ℓ_g	Sleeve extension past end of shell, ft
P_{max}	Maximum peak pressure amplitude above the mean value, psi
P_{min}	Minimum peak pressure amplitude below the mean value, psi
Q	Discharge through one valve, cfs

r	Distance from the center line of the valve to the jet impingement point on the hood, ft
R	Radius of the fixed-cone valve, ft
s	Displacement
S	Sleeve travel, in.
S_t	Strouhal number
S/D	Dimensionless distance traveled by the sleeve
t_s	Thickness of the shell, ft
t_v	Thickness of the vane, ft
V	Velocity, fps
w	Thickness of the three-dimensional jet, ft
β	Angle of deflection of the flow jet, deg
Δ	Distance sleeve moves before flow from valve begins, in.
Δh	Piezometric head differential, ft
Δh_4	Piezometric head drop between pool and transducer PC4, ft
ε	Strain, μin./in.
ε_1	Axial strain, μin./in.
ε_2	Bending strain, μin./in.
ρ	Mass per unit volume, lb-sec^2/ft^4
σ	Mean stress value, psi
σ_f	Mean stress in regard to type of strain, psi
σ_1	Mean axial stress, psi
σ_2	Mean bending stress, psi
$\mathbb{E}$	Euler number

Fagerburg, Timothy L.
  Fixed-cone valve prototype tests New Melones Dam,
California / by Timothy L. Fagerburg (Hydraulics
Laboratory, U.S. Army Engineer Waterways Experiment
Station). -- Vicksburg, Miss. : The Station ; Springfield,
Va. : available from NTIS, 1983.
  74 p. in various pagings, 23 p. of plates : ill. ;
27 cm. -- (Technical report ; HL-83-2)
  Cover title.
  "February 1983."
  Final report.
  "Prepared for U.S. Army Engineer District, Sacramento."
  Bibliography: p. 56.

  1. Hydraulics. 2. New Melones Dam (Calif.)
3. Pressure. 4. Valves. I. United States. Army. Corps
of Engineers. Sacramento District. II. U.S. Army

Fagerburg, Timothy L.
  Fixed-cone valve prototype tests New Melones : ... 1983.
                                               (Card 2)

Engineer Waterways Experiment Station. Hydraulics
Laboratory. III. Title IV. Series: Technical report
(U.S. Army Engineer Waterways Experiment Station) ;
HL-83-2.
TA7.W34 no.HL-83-2